Institut für Physik und Astronomie
Theoretische Quantenoptik

Resonance Fluorescence in a Photonic Crystal

Dissertation zur Erlangung des akademischen Grades *doctor rerum naturalium* (Dr. rer. nat.) in der Wissenschaftsdisziplin *Physik*. Eingereicht am 28. März 2013 an der Mathematisch-Naturwissenschaftlichen Fakultät der Universität Potsdam von

Geesche Boedecker

Betreuer:
PD Dr. Carsten Henkel

Published online at the
Institutional Repository of the University of Potsdam:
URL http://opus.kobv.de/ubp/volltexte/2014/6959/
URN urn:nbn:de:kobv:517-opus-69591
http://nbn-resolving.de/urn:nbn:de:kobv:517-opus-69591

Acknowledgements

First and foremost I would like to thank my supervisor Dr. Carsten Henkel for his kind assistance, advice and valuable suggestions.

Thanks also to the Quantum Optics group.

Special thanks to my mother for constant support and care.

I would like to acknowledge financial support to Deutsche Forschungsgemeinschaft, DFG-Schwerpunktprogramm “Photonische Kristalle”

Contents

Chapter 1

Introduction

The field of quantum optics [1, 2] lies at the crossing point of atomic physics and quantum field theory, where atoms, the electromagnetic field and their interaction are investigated. It provides a setting to explore fundamental quantum problems like quantum measurement, hidden variables and entanglement. On the other hand, many practical applications and devices stem from quantum optics, like the laser, atomic clocks or a randomness generator [3]. Typical problems of quantum optics that are relevant in the context of this work are the spontaneous decay of the electronic state of an atom under the emission of a photon, the atom driven by a laser, and cavity QED, a problem dealing with an atom interacting with an electromagnetic field whose modes are modified by a cavity. In a similar way, photonic crystals can modify electromagnetic modes.

Photonic crystals are periodic structures of materials with different refractive index. From the viewpoint of classical optics, the multiple reflections and refractions of light at the interfaces and their interference alters the transmission of light, depending on angle and frequency. In the quantum framework, periodicity allows to treat photonic crystals with similar mathematical tools like crystals in solid state physics. Like the electrons in a solid state crystal form a bandstructure of allowed and forbidden bands, in a photonic crystal there is a bandstructure with band gaps. Therefore photonic crystals are also called photonic band gap materials. The role of the electronic modes is played by the photonic modes. An atom that is placed in a photonic crystal will be inhibited strongly to emit a photon in the band gap, i.e. the spontaneous decay is modified [4]. If the atom is pumped by a laser, the resulting emission spectrum will be altered as well.

In contrast to solid state crystals, photonic crystals are in general artificially manufactured materials. Due to the technological progress in nanofabrication, the experimental possibilities has grown substantially in the recent years. In the rapidly evolving field of photonics, photonic crystals appear as waveguides, photonic crystal fibers or cavities. Modified spontaneous emission of semiconductor quantum dots in photonic crystals have been observed experimentally [5].

The system focused on in this work, the pumped two level atom in a photonic crystal environment, is an example of an open quantum system. Open quantum systems [6] are systems with few relevant variables and an environment, also called bath, that interacts with the system. The objective is to determine the behaviour of the system while the environment variables are 'traced out', i.e. they are taken into account only in a compact way like a response function. Open quantum systems appear in many fields of physics like solid state physics, chemical physics or nuclear physics. Many approaches have been developed.

In a closed quantum system the unitary evolution ensures the conservation of probability. In an open quantum system the evolution is not unitary any more, but is required to preserve the trace of the system's reduced density operator. Many authors also add the requirement of a completely positive evolution [7, 8]. However, in the derivation of the equations of motion approximations have to be made that spoil the theoretical requirements. Actually, even the assumption of an entangled initial state may destroy the completely positive evolution [9].

In the Heisenberg picture, the reduced dynamics leads to generalized quantum Langevin equations, where the noise originates from the environment. In our case, these equations are the Bloch equations. In the Schrödinger picture, the resulting system density matrix obeys a quantum master equation. Both approaches are equivalent.

If the characteristic time scales of the environment correlation functions are much smaller than the system evolution, one can neglect memory effects for the reduced system. The dynamics can be described by a Markovian quantum master equation in Lindblad form [8, 6].

With the usual Wigner-Weisskopf-approximations, Photons that are emitted by a pumped atom in free space disappear from the system. Therefore the system has no memory. In contrast to that, if the atom is located inside a photonic crystal,the former approximations cannot be applied. One can image, that the photons may be reflected and thereby the crystal provides a

memory for the system, where the history has to be taken into account.

In the present case, the two level system represents the relevant degrees of freedom, whereas the photonic modes are considered as irrelevant. In the general case, the question, which degrees of freedom belong to the system and which to the environment, is not fixed a priori. In cases where only few environment variables are coupled to the system, it may be appropriate to include them into the system. If the environment spectral function can be approximated by Lorentzians, then the non-Markovian open system can be treated like a Markovian system by including additional degrees of freedom [10].

Open quantum systems in solid state physics have to deal with a finite temperature of the environment. In our case the photonic cristal is assumed to be free of excitations, apart from those emitted by the atom. That corresponds to zero temperature of the environment and a vacuum initial state. The vacuum initial state for the environment together with an arbitrary atomic initial state is a product initial state. The product initial state is already a Markov approximation but seems to be justified in the zero temperature case. For the calculation of the spectra, we use the stationary system state.

Many methods for open quantum systems have been developed; also for the driven and non-Markovian case, but they are not always applicable. A quantum jump approach can be used to solve non-Markovian master equations [11]. The time evolution is calculated numerically with a quantum Monte Carlo wave function method. The method was not appropriate with the photonic crystal correlation function. Furthermore, the driving caused a strongly growing computing time with system time, such that the statistical limit cannot alway be reached.

Path integrals [12, 13] provide another approach to open quantum systems. When the bath is integrated out and the system coordinates are fixed, the relevant degrees of freedom are described by the influence functional, that gives the weights for the paths of the system. This approach was developed in the context of the spin boson model. The difficulty of arriving at practical results was partially overcome by approximation techniques like NIBA (non-interacting blip approximation). The conditions for the NIBA are not always met and hard to verify, so this approach did not turn out useful for the present work.

In this work, mostly the Heisenberg appoach is used with the Liouville approximation and a projection operator technique.

Outline

In chapter 2, we discuss some aspects of a one-dimensional photonic crystal, like the band structure and reflectance as well as the local density of states. We use transfer matrices that connect Bloch eigenstates to develop a effective medium theory. Defect modes and negative refraction is also adressed. In chapter 3 we explain the Hamilton operator and its variations as well as the density of states for the present problem. In chapter 4, related problems like the dephasing model, the driven atom and resonance fluorescence in free space are discussed. Chapter 5 shows a analytical solution for the time evolution of a pumped two-level atom in a photonic crystal. The calculation of correlation functions and spectra is the topic of chapter 6. The results of two different methods using the quantum regression theorem on the one hand and the fluctuation dissipation theorem on the other hand are compared. We also give some examples for squeezing. In chapter 7, we use projection methods to calculate time evolution and spectra.

Publications that do not appear in this thesis

[14] G. Boedecker, C. Henkel, Ch. Hermann, O. Hess, 'Spontaneous emission in photonic structures: Theory and simulation' in *Photonic Crystals*, (edited by K. Busch, S. Lölkes, R. Wehrspohn, H. Föll), John Wiley & Sons (2006). Basic concepts (Fermi's Golden Rule, local density of states) are reviewed and possibilities of optically tuning an optical transition frequency across a band edge are discussed. We give a review of quantum electrodynamic approaches to radiative decay close to a photonic gap. In the second section, simulation techniques are described that permit the determination of the local density of photon states in arbitrary photonic structures.

[15] C. Henkel, G. Boedecker, M. Wilkens, 'Local fields in a soft matter bubble', *Appl. Phys. B* **93**, 217 (2008).
The electric field created by a point dipole located in a dielectric void ("bubble") is calculated. We consider a continuous profile of the medium permittivity and find that, at large distances, the effective dipole field depends on the model chosen for the bubble walls, in particular their thickness. A boundary layer model is analyzed that gives good agreement with numerical calculations.

Chapter 2

Aspects of a one-dimensional photonic crystal

This chapter was published in [16]. We consider light propagation in a finite photonic crystal with a transfer matrix approach. The Bloch modes inside and the vacuum modes outside the photonic crystal are linked with a transformation matrix that is interpreted as a transfer matrix. So the transmission and reflection from a one-dimensional system are described in an effective medium theory, which reproduces exactly the results of transfer matrix calculations. We derive simple formulas for the reflection from a semi-infinite crystal, the local density of states in absorbing crystals, and discuss defect modes and negative refraction.

2.1 Introduction

Periodic crystals do not exist in the real world, they are all finite. It turns out that in a finite crystal one has to consider the reflection of the Bloch waves at the endfaces. This leads to the formation of standing waves, as mentioned e.g. by [17]. Reflection amplitudes are easy to find in the long wavelength limit using effective medium theory. We construct here an effective medium theory that describes at all frequencies the light propagation through a finite crystal. Its key ingredients are the reflection and transmission coefficients for a half-space crystal, calculated using an expansion in Bloch waves. With our approach, standard formulas for a homogeneous layer can be used for a finite crystal. We consider a few important applications: the local density of

states for finite or infinite systems, even with absorption, and frequencies of defect modes. We discuss negative refraction. Our results are illustrated by exact formulas for a 1D Kronig-Penney (planar scatterer) model.

2.2 Transfer matrix approach

We start by recalling the transfer matrix method for a one-dimensional system made of a finite number N of unit cells. We use units with $c = 1$ and denote ω the wavevector in the background medium with permittivity $\varepsilon = 1$. The transfer matrix T connects the field E_n at the left edge of the nth unit cell to the field E_{n+1} at the next cell. Expanding the fields in plane waves propagating to the left and right

$$E_n(x) = a_n\, e^{i\omega(x-na)} + b_n\, e^{-i\omega(x-na)}, \tag{2.1}$$

where a is the crystal period, we have (see chap. 6 of [18])

$$\begin{pmatrix} a_{n+1} \\ b_{n+1} \end{pmatrix} = T \begin{pmatrix} a_n \\ b_n \end{pmatrix}. \tag{2.2}$$

Since $\det T = 1$, its eigenvalues $\lambda_\pm$ can be written in the form $\lambda_\pm = e^{\pm ika}$ where k is the Bloch quasimomentum. An eigenvalue on the unit circle (real k) corresponds to a propagating (extended) Bloch mode whereas real eigenvalues (k imaginary) are found in the band gaps. An example is shown in Fig. 2.1 for the Kronig-Penney model detailed below.

The reflection and transmission amplitudes from a finite crystal are given by the Nth power of the primitive transfer matrix, e.g. $r_N = -T_{21}^N/T_{22}^N$. T^N is particularly simple to compute in the Bloch basis:

$$T^N = M \begin{pmatrix} e^{ikaN} & 0 \\ 0 & e^{-ikaN} \end{pmatrix} M^{-1}, \qquad M = \begin{pmatrix} N_+ & N_- \\ N_+c_+ & N_-c_- \end{pmatrix}. \tag{2.3}$$

The ratios of the plane wave amplitudes for the Bloch states $\pm k$ are

$$c_\pm = \frac{e^{\pm ika} - T_{11}}{T_{12}} = \frac{T_{21}}{e^{\pm ika} - T_{22}}. \tag{2.4}$$

Independent of the normalization factors $N_\pm$ chosen for the Bloch eigenstates, the reflection coefficient is given by (in agreement with [17, 19])

$$r_N = \frac{c_+c_-(e^{ikaN} - e^{-ikaN})}{c_+e^{ikaN} - c_-e^{-ikaN}}. \tag{2.5}$$

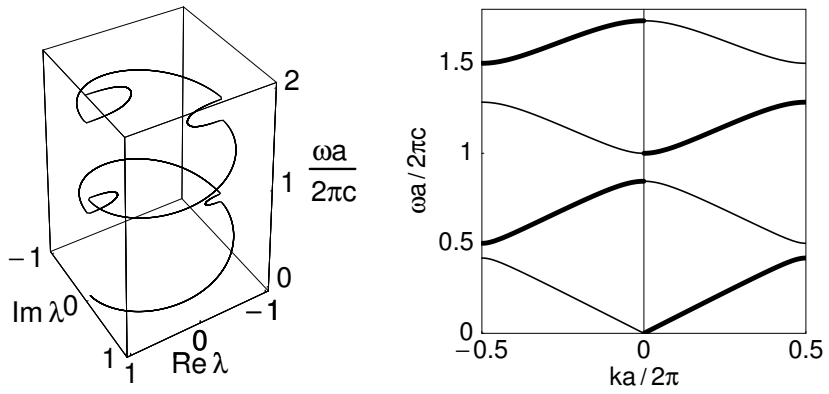

Figure 2.1: Left panel: complex eigenvalue $\lambda_+ = e^{ika}$ vs. frequency for the Kronig-Penney model, Eq. (2.9), with point scatterers of polarizability $\alpha = (0.2 + 0i)\, a$. Right panel: band structure $\omega(k)$ of the infinite crystal. The thick dispersion curves correspond to the physical Bloch momentum fixed by the requirements of causality and energy conservation. Even bands exhibit negative refraction ($k < 0$).

For a finite number of periods N, the reflectance $|r_N|$ shows oscillations as a function of frequency due to the formation of standing waves between the end faces of the crystal, with a fringe spacing scalingwith $1/N$. If these are not resolved due to some finite frequency resolution (or fluctuations in the crystal thickness), the envelope of the reflectance is a useful generalization. Maximizing $|r_N|$ with respect to N for each fringe period, we find from Eq. (2.5) in allowed bands (see Fig. 2.2)

$$0 \le |r_N| \le \left| \frac{2c_+c_-}{c_+ + c_-} \right|, \tag{2.6}$$

provided energy conservation holds. This envelope function is consistent with [17] and overestimates the reflectance in the band gap.

In the preceding plots, a Kronig-Penney type model has been used for definiteness. We consider a wave equation with point scatterers (see [21] for a 3D generalization)

$$\frac{d^2E(x)}{dx^2} + \omega^2\Big(1 + \sum_{n=1}^{N} \alpha_n \delta(x - (n - \tfrac{1}{2})a)\Big) E(x) = 0 \tag{2.7}$$

where the polarizability α_n characterizes the strength of the nth scatterer. We focus on $\alpha_n = \alpha$ to get a periodic crystal. The continuity of the electric

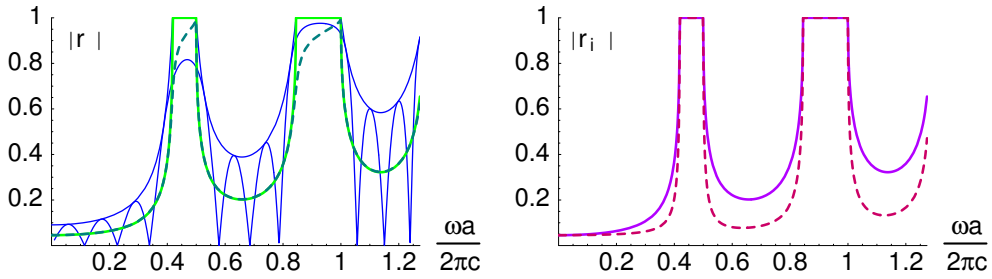

Figure 2.2: Left: reflectance $|r_N|$ for the Kronig-Penney model with $\alpha = (0.2+0i)\,a$, $N = 4$ (blue line). The envelope, Eq. (2.6), is shown as well. Solid green line: half-space approximation $|r|$, Eq. (2.11). Dashed dark green line: $|r|$ for absorbing scatterers ($\alpha = (0.2 + 0.02i)\,a$). Right: reflection coefficient $|r_\mathrm{i}|$ for Bloch waves reflected from the end face of a semi-infinite crystal. Solid line: our result, Eq. (2.13); dashed line: proposed by Sakoda [20]. Kronig-Penney model with $\alpha = (0.2 + 0i)\,a$.

field E and its first derivative on the scatterers leads to the transfer matrix

$$T = \begin{pmatrix} (1 + \frac{i}{2}\omega\alpha)e^{i\omega a} & \frac{i}{2}\omega\alpha \\ -\frac{i}{2}\omega\alpha & (1 - \frac{i}{2}\omega\alpha)e^{-i\omega a} \end{pmatrix} \tag{2.8}$$

whose eigenvalues are given by

$$\lambda_\pm = \cos(\omega a) - \frac{\omega\alpha}{2}\sin(\omega a) \pm i\sin(\omega a)\sqrt{1 + \omega\alpha\cot(\omega a) - \tfrac{1}{4}\omega^2\alpha^2} \tag{2.9}$$

We have chosen the sign of the square root such that λ_+ is located on or inside the unit circle (provided α has an infinitesimally positive imaginary part).

2.3 Half-space-approximation

We show here that the Bloch modes for the infinite crystal can be used to define a reflection coefficient r for a semi-infinite crystal. The key idea is to use the transformation matrices M and M^{-1} occurring in Eq. (2.3) as transfer matrices, linking plane waves in the vacuum outside the crystal to Bloch modes inside the crystal. For a unit incident amplitude from the left,

transmission and reflection amplitudes are thus given by

$$\begin{pmatrix} t \\ 0 \end{pmatrix} = M^{-1} \begin{pmatrix} 1 \\ r \end{pmatrix}. \tag{2.10}$$

Independent of the eigenmode normalizations, this yields

$$r = c_+ = \frac{e^{i\omega a} - e^{ika}}{e^{i\omega a} e^{ika} - 1}, \tag{2.11}$$

where the second equation is valid for the Kronig-Penney model. At low frequency, we recover the standard effective medium result $r \approx (1-n_{\text{eff}})/(1+n_{\text{eff}})$ with the effective index $n_{\text{eff}} = (1+\alpha/a)^{1/2} = \lim_{\omega\to 0} k(\omega)/\omega$. Fig. 2.2 shows that Eq. (2.11) gives, for all frequencies, a good approximation to the reflectance from a finite crystal, when $|r_N|$ is averaged over the standing wave fringes. In the band gaps, we recover the intuitively expected perfect reflector, $|r| = 1$.

In a similar manner, we define a coefficient r_{i} for the 'interior' reflection of a Bloch wave from a crystal end face, say the left one:

$$\begin{pmatrix} r_{\text{i}} \\ 1 \end{pmatrix} = M^{-1} \begin{pmatrix} 0 \\ t' \end{pmatrix} \tag{2.12}$$

Reflection from both end faces can be described by the same coefficient. This fixes the normalization of the Bloch eigenmodes:

$$r_{\text{i}} = -\frac{N_-}{N_+} = -\frac{N_+ c_+}{N_- c_-} = -c_+. \tag{2.13}$$

For the last equality, we have used the relation $c_+ c_- = 1$ which follows from the symmetry relation $T_{12} = -T_{21}$ of the transfer matrix for an even scatterer. Note the π phase shift between 'exterior' and 'interior' reflection amplitudes.

Our expression for the interior reflection can be compared to a conjecture by Sakoda, $r_{\text{i}}(\text{Sakoda}) = (n_{\text{g}}-1)/(n_{\text{g}}+1)$ where the group index $n_{\text{g}} = dk/d\omega$. When the standing waves inside a finite crystal are used for lasing, $|r_{\text{i}}|$ determines the quality factor of this cavity [20]. Sakoda's result qualitatively agrees with ours (see Fig. 2.2), but underestimates $|r_{\text{i}}|$, except very close to the band edges.

2.4 Applications and discussion

Effective medium theory. In the preceding section, we have seen that physically reasonable reflection and transmission amplitudes can be introduced for the endfaces of a photonic crystal, when the field inside the crystal is expanded in Bloch modes. This immediately suggests an effective medium description of a finite length crystal. The reflectance r_N, e.g. would be given by the well-known Fabry-Pérot expression [22]

$$r_{N,\mathrm{FP}} = r + \frac{t r_\mathrm{i} t' e^{2ikaN}}{1 - r_\mathrm{i}^2 e^{2ikaN}}, \tag{2.14}$$

where the standing wave oscillations arise by summing a multiple scattering series.

It is easy to check that $r_{N,\mathrm{FP}}$ coincides with the transfer matrix result r_N, Eq. (2.5), by substituting the reflection amplitudes, Eqs. (2.11, 2.13), and the corresponding transmissions. In fact, this is not surprising because according to the definitions Eqs. (2.10, 2.12) of these amplitudes, the transformation matrices M and M^{-1} can play the role of transfer matrices at the crystal endfaces. If we express them in terms of the r, r_i, t, t', the expression Eq. (2.3) for T^N becomes precisely the product of transfer matrices one would write down for a homogeneous layer, and leads to Eq. (2.14).

It has been previously noted that the Bloch momentum k is a useful quantity to describe the propagation inside a finite-size crystal [19, 21, 23]. In particular, Jeong et al. [23] interpret the phase of the transmission amplitude in terms of a frequency-dependent effective index, but find differences with respect to the conventional expression $n_\mathrm{eff} = k/\omega$ close to the band edges. Our analysis indicates that this is due to the contribution of the Fabry-Pérot denominator in the expression $t_N = tt' e^{ikaN}/(1 - r_\mathrm{i}^2 e^{2ikaN})$.

Local density of states. The LDOS $\rho(x, \omega)$ is the key quantity for the radiative decay of a two-level system in the crystal [24], and it is well known that it is obtained from the imaginary part of the Green function $G(x, x; \omega)$ (the field radiated by a pointlike test source). If we put two (finite or semi-infinite) crystals at distances $d_{L,R}$ from a test source, the Green function is easily obtained from the corresponding reflection coefficients $r_{L,R}$. Normal-

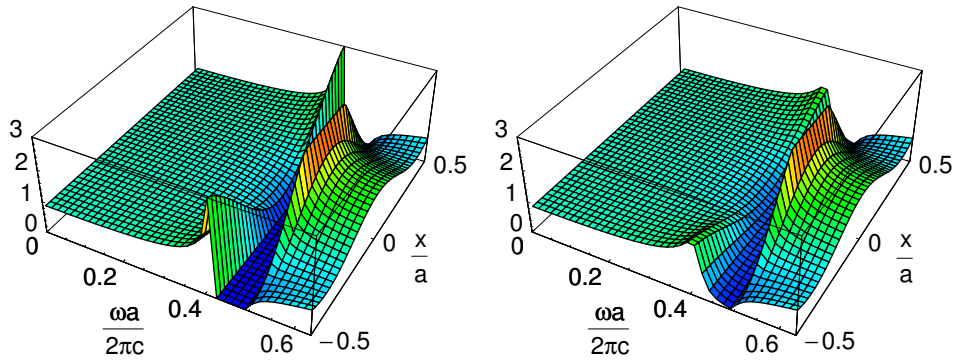

Figure 2.3: LDOS, Eq. (2.15), in an infinite crystal with scatterers at $x = \ldots, -a/2, a/2, \ldots$ Left: no absorption ($\alpha = 0.2\,a$). Right: nonzero absorption ($\alpha = (0.2 + 0.05i)\,a$).

izing to the free space LDOS, we get in this way

$$\rho(x,\omega) = \mathrm{Re}\Big(\frac{r_L(\omega)e^{2id_L\omega} + r_R(\omega)e^{2id_R\omega} + 2}{1 - r_L(\omega)r_R(\omega)e^{2i(d_L+d_R)\omega}} - 1\Big), \qquad d_L = -d_R = x. \tag{2.15}$$

Note that the distances $d_{L,R}$ are defined relative to the reference planes implicit in the reflection coefficients $r_{L,R}$ (located $a/2$ in front of the first scatterer in our example). This simple formula reproduces more involved expressions given, e.g. in [25]. For an infinite crystal with point scatterers, the LDOS is plotted in Fig. 2.3 and shows the characteristic inverse square root singularities close to the band edges [19]. One also recovers the well-known dielectric and air bands at the gap edges.

Our approach immediately allows for a nonzero absorption in the sample where, at least for an infinite crystal, standard band theory breaks down because all Bloch vectors become complex (extended states do not exist any more; see [26] for a detailed discussion). For finite absorbing systems, it is well-known that transfer matrix techniques still provide the required reflection and transmission spectra (see, e.g. [27]). To define consistently a half-space reflection amplitude Eq. (2.11), we require that $r(\omega)$ be nonsingular as a function of complex frequency in the upper half plane (as dictated by causality). For the Kronig-Penney model, we can show that it suffices to choose the eigenvalue e^{ika} located inside the unit circle. (This condition is

consistent with the limit $N \to \infty$ of Eq. (2.5) for finite absorption.) The reflection coefficient for finite absorption is shown in Fig. 2.2: it drops below unity in the band gaps. The LDOS (Fig. 2.3) exhibits a smoothing out of the dielectric band edge while the singularity at the upper gap edge persists. This is due to the approximation of point-like scatterers in our Kronig-Penney model, which makes the mode functions at the air band edge insensitive to the scattering strength α.

Defect modes. As a final application, we investigate the situation that two crystals surround a defect scatterer with $\alpha_d \neq \alpha$. Expanding the field in plane waves around the defect, we find that the defect mode frequency is determined by

$$-i\omega\alpha_{\rm d} = \frac{r_R(\omega)e^{2i\omega d_R}-1}{r_R(\omega)e^{2i\omega d_R}+1} + \frac{r_L(\omega)e^{2i\omega d_L}-1}{r_L(\omega)e^{2i\omega d_L}+1}, \tag{2.16}$$

where $d_{R,L}$ are again the distances between the crystals and the defect. For given real ω, $\alpha_{\rm d}$ is in general complex and can be absorbing or even active. In the latter case, the crystal backscatters more light than is incident when the defect resonance is hit (see Fig. 2.4). By varying $\alpha_{\rm d}$, the defect mode frequency can be tuned across the band gap.

Negative refraction. To conclude, we point out that the simple one-dimensional Kronig-Penney model provides an exactly soluble example of a photonic crystal with negative refraction. For a non-absorbing, semi-infinite crystal, the requirement that $|r|^2 \leq 1$ leads to the condition $\sin(\omega a)\sin(ka) \geq 0$ for the 'physical' Bloch momentum k. This is fulfilled when an incident plane wave in an even frequency band injects a Bloch wave with negative k into the crystal. Note that this choice of k is consistent with the well-known rule that the Bloch wave should have a positive group velocity $v_{\rm g} = d\omega/dk$ (see, e.g. [28]), as is manifest from the thick lines in Fig. 2.1.

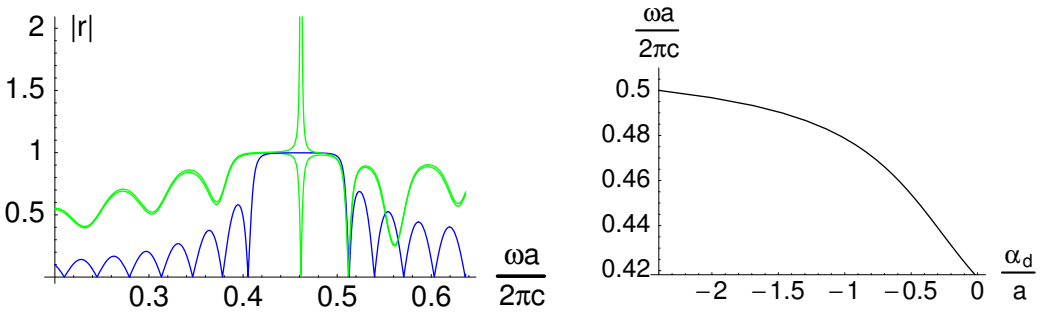

Figure 2.4: Left: reflectance from two $N = 6$ layer crystals ($\alpha = 0.2\,a$) with a defect in between ($d_R = d_L = a/2$). Green line with peak: active defect with scattering strength $\alpha_{\rm d}/a \approx -0.62 - 0.04i$, given by Eq. (2.16) for $\omega a/2\pi c \approx 0.462$. The same structure with a passive defect ($\alpha_{\rm d} \approx -0.62\,a$) gives the green line with the transmission dip. Blue line: reflectance for $\alpha_{\rm d} = \alpha$.
Right: defect frequency in the first band gap vs. real part of scattering strength $\alpha_{\rm d}$.

Chapter 3

Quantum optics in a photonic crystal

3.1 Atom-field quantized interaction in a PhC

In a photonic crystal, the dielectric constant ϵ is position-dependent and periodic. It is assumed to be real. We use the gauge condition ([29]) $\nabla \cdot (\epsilon A) = 0$, $B(r,t) = \nabla \times A(r,t)$, $E(r,t) = -\frac{\partial}{\partial t} A(r,t)$. The wave equation

$$\frac{1}{\epsilon(\vec{r})} \nabla \times (\nabla \times \vec{E}(\vec{r},t)) = -\frac{1}{c^2} \frac{\partial^2}{\partial t^2} \vec{E}(\vec{r},t) \tag{3.1}$$

has to be solved with a periodic $\epsilon(\vec{r} + \vec{a}_i) = \epsilon(\vec{r})$, $\vec{a}_i$ being an elementary lattice vector. The solution is of the form

$$\vec{E}(\vec{r},t) = \vec{E}(\vec{r}) e^{-i\omega t} \tag{3.2}$$

Because of the periodic ϵ, Bloch's theorem applies and the solution is of the form

$$\vec{E}(\vec{r}) = \vec{E}_{\vec{k}n}(\vec{r}) = \vec{u}_{\vec{k}n}(\vec{r}) e^{i\vec{k}\cdot\vec{r}} \tag{3.3}$$

with a periodic function $\vec{u}_{\vec{k}n}(\vec{r} + \vec{a}_i) = \vec{u}_{\vec{k}n}(\vec{r})$ and a band index n. $\vec{k}$ is a wave vector in the first Brilouin zone.
The electric field is expanded into eigenmodes $\vec{E}_{\vec{k}n}(r)$. The amplitudes describe a harmonic oscillation. So the field can be quantized by replacing the amplitude by annihilation and creation operators.

The electric field operator is then

$$\hat{E}(r,t) = \sum_{\vec{k}n} i\sqrt{\frac{\hbar\omega_{\vec{k}n}}{2\epsilon_0 V}}[\hat{a}_{\vec{k}n}(t)\vec{E}_{\vec{k}n}(r) - \hat{a}^\dagger_{\vec{k}n}(t)\vec{E}_{\vec{k}n}(r)] \tag{3.4}$$

V is the the volume of the photonic crystal and the normalization factor is chosen such that the eigenmodes of the electric field in the crystal are the states of a harmonic oscillator with the elctromagnetic energy per mode $\hbar\omega$ times the photon number operator (not including the zero-point energy).
The interaction Hamiltonian for $A \cdot p$-coupling is (discarding the term $\propto A^2$ is allowed for not too intense light beams)

$$\begin{aligned} H_{int} &= -\frac{e}{m_e} A \cdot p & (3.5)\\ &= -\frac{e}{m_e}\sum_{\vec{k}n}\sqrt{\frac{\hbar}{2\epsilon_0 V\omega_{\vec{k}n}}}[\hat{a}_{\vec{k}n}(t)E_{\vec{k}n}(r) - \hat{a}^\dagger_{\vec{k}n}(t)E^*_{\vec{k}n}(r)]\cdot p & (3.6)\\ &= -i\sum_{\vec{k}n} g_{\vec{k}n}[\hat{a}_{\vec{k}n}(t) - \hat{a}^\dagger_{\vec{k}n}(t)]\sigma_x & (3.7) \end{aligned}$$

We take the electric field at the position of the nucleus r (dipole approximation). Furthermore we used $p = m_e\dot{d}/e = i\omega_A m_e d/e$ and defined

$$g_{\vec{k}n} = \omega_A\sqrt{\frac{2\hbar}{\epsilon_0 V\omega_{\vec{k}n}}}E_{\vec{k}n}\cdot d_{ge} \tag{3.8}$$

If d is real (only m=0 transitions) then $d = 2\langle g|d|e\rangle\sigma_x = 2d_{ge}\sigma_x$

3.2 The Hamilton operator

The full system Hamilton operator describes a two level atom with frequency ω_A that is driven by a laser characterized by the Rabi frequency $\epsilon = d_{ge}$ $\cdot\mathbf{E}/\hbar$. and the laser frequency ω_L. The environment Hamiltonian describes the photonic modes where $a^\dagger_\lambda, a_\lambda$ are the photon creation and annihilation operators. The summation over λ includes the wave vector as well as the band index. The last term is the coupling of the atom and the electric field.

$$H = \frac{1}{2}\hbar\omega_A\sigma_z + \hbar\epsilon\cos\omega_L t\ \sigma_x + \sum_\lambda \hbar\omega_\lambda a_\lambda^\dagger a_\lambda + i\hbar\sum_\lambda g_\lambda(a_\lambda^\dagger - a_\lambda)\sigma_x \quad (3.9)$$

In the rotating wave approximation rapidly oscillating terms are discarded.

$$H = \frac{1}{2}\hbar\omega_A\sigma_3 + \hbar\epsilon(\sigma_+ e^{-i\omega_L t} + \sigma_- e^{i\omega_L t}) + \sum_\lambda \hbar\omega_\lambda a_\lambda^\dagger a_\lambda + i\hbar\sum_\lambda g_\lambda(a_\lambda^\dagger\sigma_- - a_\lambda\sigma_+) \quad (3.10)$$

$\sigma_\pm = \sigma_x \pm i\sigma_y$ describes the excitation/deexcitation of the two-level atom. For certain methods it is appropriate to use a transformed Hamilton operator.

3.2.1 Hamiltonian in the frame rotating with laser frequency

This transformation delivers a Hamilton operator without explicit time dependence. A unitary transformation with $U = \exp(-i\omega_L\sigma_z t/2)\exp(-i\omega_L t\sum_\lambda a_\lambda^\dagger a_\lambda/2)$ leads to

$$H = \frac{1}{2}\hbar\Delta_{AL}\sigma_3 + \hbar\epsilon(\sigma_+ + \sigma_-) + \sum_\lambda \hbar\Delta_{\lambda_L} a_\lambda^\dagger a_\lambda + i\hbar\sum_\lambda g_\lambda(a_\lambda^\dagger\sigma_- - a_\lambda\sigma_+) \quad (3.11)$$

with $\Delta_{AL} = \omega_A - \omega_L$, $\Delta_{\lambda L} = \omega_\lambda - \omega_L$. Due to the rotating wave approximation, the summation is over near-resonant frequencies.

3.2.2 Frame rotating with atom frequency ω_A

In this frame the term for the free atom Hamiltonian disappears.

$$H = \hbar\epsilon(\sigma_+ e^{i\omega_{AL}t} + \sigma_- e^{-i\omega_{AL}t}) + \sum_\lambda \hbar\Delta_{\lambda A} a_\lambda^\dagger a_\lambda + i\hbar\sum_\lambda g_\lambda(a_\lambda^\dagger\sigma_- - a_\lambda\sigma_+) \quad (3.12)$$

with $\Delta_{\lambda A} = \omega_\lambda - \omega_A$

3.2.3 Dressed basis interaction Hamiltonian

The dressed basis states are the eigenstates of the system consisting of atom and driving laser. After the transformation to the dressed basis the laser

part of the Hamilton operator disappears.

$$\begin{aligned} |\tilde{1}\rangle &= c|1\rangle + s|2\rangle \\ |\tilde{2}\rangle &= -s|1\rangle + c|2\rangle \end{aligned}$$

where $c = \cos\phi$, $s = \sin\phi$, $\sin^2\phi = \frac{1}{2}[1 - 1/(4\epsilon^2/\Delta_{AL}^2 + 1)^{\frac{1}{2}}]$, and $\Omega = [\epsilon^2 + \Delta_{AL}^2/4]^{\frac{1}{2}}$, the new spin matrices are $R_3 = |\tilde{2}\rangle\langle\tilde{2}| - |\tilde{1}\rangle\langle\tilde{1}|$ etc.
The non-interacting part of the Hamiltonian is then

$$H_0 = \hbar\Omega R_3 + \hbar\sum_\lambda \Delta_\lambda a_\lambda^\dagger a_\lambda$$

On resonance $\Delta_{AL} = 0$ both coefficients are equal, $c = s$ and $\Omega = \epsilon$. For weak driving, H_0 describes approximately the whole system. The interaction Hamiltonian in the interaction picture

$$\begin{aligned} H_I(t) &= i\hbar[(csR_3 + c^2R_+e^{-i2\Omega t} - s^2R_-e^{i2\Omega t})]\sum_\lambda g_\lambda a_\lambda^\dagger e^{i\Delta_\lambda t} \\ &\quad + h.c. \end{aligned} \tag{3.13}$$

This interaction Hamiltonian includes resonant as well as antiresonant terms. The R_3 terms produce dephasing.

3.2.4 Spin-Boson-Hamiltonian

A frequently discussed system is the spin-boson model, see e.g.[13]. It is a double-well potential, where the detuning of the ground states is denoted by ϵ, the quantity $\frac{1}{2}\hbar\Delta$ is the matrix element for tunneling between the wells, the "tunnel splitting". It can be compared easier to our system, if we rotate the spin coordinates around the y axis by $\pi/2$, thereby exchanging σ_x and σ_y.

$$H_{SB} = -\frac{1}{2}\hbar\Delta\sigma_x - \frac{1}{2}\hbar\epsilon\sigma_z + \frac{1}{2}\sigma_z\hbar\sum_\alpha \gamma_\alpha(a_\alpha + a_\alpha^+) + \hbar\sum_\alpha \omega_\alpha a_\alpha^+ a_\alpha \tag{3.14}$$

The rotating wave approximation is usually not performed in this context. A model with time-dependent potential $\epsilon(t)$ was discussed in [12].

3.3 Environment

The photonic crystal provides an environment of the atom that changes the photonic modes by multiple Bragg scattering at the interfaces. Since the dispersion relation is in general complicated, we consider an effective mass approximation at the band edge [30]. In the isotropic model, the dispersion relation is given by $\omega(\vec{k}) = \omega_e \pm A(k-k_0)^2$. ω_e is the band edge frequency, k_0 is the radius of the sphere in $\vec{k}$ space, about which the expansion is performed and $A = \frac{1}{2}\partial^2\omega/\partial k^2|_{k=k_0}$ is a constant characteristic for the material. A better approximation to a realistic photonic crystal is the anisotropic model with a dispersion relation

$$\omega(\vec{k}) = \omega_e + A(\vec{k} - \vec{k}_0)^2 \tag{3.15}$$

$\vec{k}_0$ is a point in the boundary of the Brillouin zone and the dispersion relation approximates the "air band" above the bandgap. We will use the anisotropic dispersion relation in this work. The density of states describes the number of modes present for a certain frequency. A definition of the density of states is

$$\rho_0(\omega) = \sum_{\vec{k}} \delta(\omega(\vec{k}) - \omega) \tag{3.16}$$

In the following, we use the projected local density of states:

$$\rho(\omega) = \sum_{\vec{k}} |g_{\vec{k}}|^2 \delta(\omega(\vec{k}) - \omega) \tag{3.17}$$

$g_{\vec{k}}$ characterizes the coupling of the Bloch modes at the position of the atom.

$$g_{\vec{k}} = \omega_A \sqrt{\frac{2\hbar}{\epsilon_0 V \omega_{\vec{k}}}} E_{\vec{k}} \cdot d_{ge} \tag{3.18}$$

$$\begin{aligned}
\rho(\omega) &= \sum_{\vec{k}} |g_{\vec{k}}|^2 \delta(\omega(\vec{k}) - \omega) \\
&= \frac{2\hbar\omega_A^2 d_{ge}}{\epsilon_0 (2\pi)^3} \int_{\vec{k}_0}^{\infty} d^3\vec{k} \frac{1}{\omega_{\vec{k}}} \delta(\omega(\vec{k}) - \omega) \\
&= \frac{2\hbar\omega_A^2 d_{ge}}{\epsilon_0 (2\pi)^3} \int_0^{\infty} dk \frac{k^2}{\omega_e + Ak^2} \delta(\omega_e + Ak^2 - \omega) \\
&\quad \int_0^{\pi} d\theta \sin\theta \cos^2\theta \int_0^{2\pi} d\phi \\
&= \frac{4\hbar\omega_A^2 d_{ge}}{3\epsilon_0 (2\pi)^2} \frac{2}{A^{\frac{3}{2}}} \frac{\sqrt{\omega - \omega_e}}{\omega} \Theta(\omega - \omega_e) \\
&\approx \alpha \sqrt{\omega - \omega_e} \Theta(\omega - \omega_e) \qquad (3.19)
\end{aligned}$$

with $\alpha = \frac{8\hbar\omega_A^2 d_{ge}}{3\epsilon_0 (2\pi)^2 A^{\frac{3}{2}} \omega_e}$. We have taken into account that the dispersion relation is only valid for ω near the band-edge. Therefore we keep only the differences $\omega - \omega_e$ and approximate $\omega \approx \omega_e$.

Environment correlation function The correlation function is in the interaction picture

$$\begin{aligned}
G_{IP}(t - t') &= \langle 0| \sum_{\vec{k}} a_{\vec{k}} e^{i(\omega - \omega_A)t} \sum_{\vec{k}} a_{\vec{k}}^+ e^{-i(\omega - \omega_A)t'} |0\rangle \qquad (3.20) \\
&= \sum_k g_k^2 e^{i(\omega_k - \omega_A)(t - t')} \qquad (3.21) \\
&= \int d\omega e^{i(\omega - \omega_A)(t - t')} \sum_{\vec{k}} g_k^2 \delta(\omega - \omega_k) \qquad (3.22) \\
&= \int d\omega e^{i(\omega - \omega_A)(t - t')} \rho(\omega) \qquad (3.23)
\end{aligned}$$

In the Heisenberg picture the expression differs only in a factor $e^{i\omega_A(t-t')}$

$$G_H(t - t') = \int d\omega e^{i\omega(t - t')} \rho(\omega) \qquad (3.24)$$

For the anisotropic DOS ($\omega \approx \omega_e$):

$$\begin{aligned}
G(t - t') &= \alpha \int d\omega e^{i(\omega - \omega_A)(t - t')} \sqrt{\omega - \omega_e} \theta(\omega - \omega_e) \qquad (3.25) \\
&= \frac{e^{-i(t - t')(\omega_A - \omega_e)} \alpha \sqrt{\pi/2}(-1 + i)}{2(t - t')^{3/2}} \qquad (3.26)
\end{aligned}$$

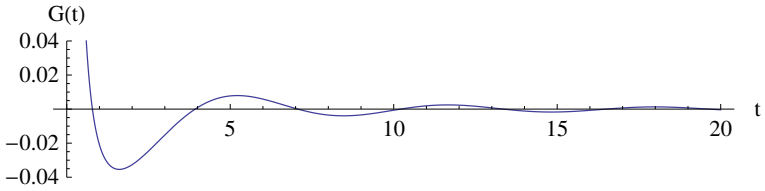

In contrast to the free space correlation function $\propto \delta(t-t')$, the photonic crystal correlation function provides a memory for the system. Earlier times have to be taken into account.

Since the root function $\sqrt{\omega-\omega_e}$ in the density of states is infinitely growing, we may want to use a cutoff in later chapters $\sqrt{\omega-\omega_e}e^{-\lambda(\omega-\omega_e)^2}$. A realistic density of states will look much more complicated and the square root approximation is only valid at the band edge. The cutoff parameter should be chosen such that the nonrelativistic approximation is valid.

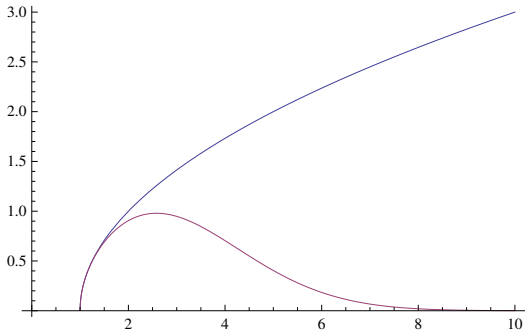

Figure 3.1: Density of states
Blue: $\rho(\omega)=\sqrt{\omega-\omega_e}$, $\omega_e=1$;
Red:$\rho(\omega) = \sqrt{\omega-\omega_e}e^{-\lambda(\omega-\omega_e)^2}$,
$\lambda=1/10$, $\omega_e=1$

spin boson bath In the spin-boson model eq.(3.14) the bath spectrum (spectral function) is defined as follows:

$$J(\omega)=\sum_\alpha \gamma_\alpha^2\delta(\omega-\omega_\alpha)=\frac{q_0^2}{2\hbar}\sum_\alpha\frac{c_\alpha^2}{m_\alpha\omega_\alpha}\delta(\omega-\omega_\alpha) \tag{3.27}$$

The spectral function is of the form

$$J(\omega)=B\omega^s e^{-\omega/\omega_c} \tag{3.28}$$

For $s=1$, this is called ohmic dissipation, $0<s<1$ subohmic, $s>1$ superohmic. The subohmic case for $s=\frac{1}{2}$ is similar to the photonic crystal bath, but without the shift to the bandedge ω_e.

Chapter 4

Related problems

In this chapter we discuss several problems which illustrate some aspects of our problem and can be treated more easily than the full problem. The dephasing model arises from our full resonance fluorescence model by omitting the atom rotation. The driven atom only considers the self rotation of the atom and the driving laser. The resonance fluorescence in free space uses a flat density of states instead of the photonic crystal density of states.

4.1 Analytical solution of simplified Hamiltonian – the dephasing model

We consider the spin-boson Hamiltonian eq.(3.14) in the zero tunneling case $\Delta = 0$. This is treated by Palma et al. [31] by using the interaction picture evolution operator ($\hbar = 1$).

$$H = \epsilon\sigma_z + \sum_\lambda \Delta_\lambda a_\lambda^\dagger a_\lambda + \sum_\lambda g_\lambda \sigma_z (a_\lambda^\dagger + a_\lambda) \tag{4.1}$$

We use the interaction picture with $H_0 = \epsilon\sigma_z + \sum_\lambda \Delta_\lambda a_\lambda^\dagger a_\lambda$, $U_0 = e^{-iH_0 t}$. The state

$$|\Psi\rangle = c_0|0\rangle + c_1|1\rangle \tag{4.2}$$

is in interaction picture:

$$|\tilde{\Psi}\rangle = U_0^+|\Psi\rangle = e^{iH_0 t}(c_0|0\rangle + c_1|1\rangle) = e^{i\epsilon t}c_0|0\rangle + e^{-i\epsilon t}c_1|1\rangle \tag{4.3}$$

and the interaction Hamiltonian is

$$\tilde{H}_I(t) \;=\; e^{iH_0t}H_Ie^{-iH_0t} = \sum_k g_k\sigma_z(a_k^\dagger e^{i\Delta_k t} + a_k e^{-i\Delta_k t}) \tag{4.4}$$

The time evolution is then

$$U(t) \;=\; \mathrm{T}\; e^{-i\int_0^t \tilde{H}_I(t')dt'} \tag{4.5}$$

In order to simplify $U(t)$, we break up he integral into infinitesimal time intervals $\epsilon = \frac{t-t_0}{N}$, $N \to \infty$ and define

$$\tilde{H}_{I,n} := -i\int_{t_0+(n-1)\epsilon}^{t_0+n\epsilon} \tilde{H}_I(t')dt'. \tag{4.6}$$

$$\begin{aligned} U(t,t_0) &= U(t,t-\epsilon)U(t-\epsilon,t-2\epsilon)...U(t_0+2\epsilon,t_0+\epsilon)U(t_0+\epsilon,t_0) \\ &= \lim_{N\to\infty} e^{\tilde{H}_{I,N}}e^{\tilde{H}_{I,N-1}}...e^{\tilde{H}_{I,2}}e^{\tilde{H}_{I,1}} \end{aligned} \tag{4.7}$$

Since

$$[\tilde{H}_I(t'),\tilde{H}_I(t'')] = -2i\sum_k g_k^2\sin(\Delta_k(t'-t'')) \tag{4.8}$$

and

$$[\tilde{H}_I(t),[\tilde{H}_I(t'),\tilde{H}_I(t')]] = 0 \tag{4.9}$$

we can apply the Baker-Campbell-Haussdorff relation $e^Ae^B = e^{A+B+[A,B]/2}$. and get

$$\begin{aligned} U(t,t_0) &= \lim_{N\to\infty}\exp\left[\sum_{n=1}^N\left(\tilde{H}_{I,n} + \frac{1}{2}\left[\tilde{H}_{I,n},\sum_{k=1}^N\tilde{H}_{I,k}\right]\right)\right] \\ &= \exp\left[-i\int_0^t\tilde{H}_I(t')dt' + i\int_0^t dt'\int_0^{t'}dt''\sum_k g_k^2\sin(\Delta_k(t'-t''))\right] \\ &= A(t)\exp[-i\int_0^t\sum_k g_k\sigma_z(a_k^\dagger e^{i\Delta_k t'} + a_k e^{-i\Delta_k t'})dt'] \\ &= A(t)\exp[\sigma_z\frac{1}{2}\sum_k(a_k^\dagger\xi(t) - a_k\xi^*(t))] \end{aligned} \tag{4.10}$$

where we defined

$$\xi_k(t) = 2g_k\frac{1-e^{i\Delta_k t}}{\Delta_k} \tag{4.11}$$

and $A(t) = \exp\left[i\int_0^t dt' \int_0^{t'} dt'' \sum_k g_k^2 \sin(\Delta_k(t'-t''))\right]$. The phase factor $A(t)$ drops out in the calculation of expectation values and correlations.
$U(t)$ is a displacement operator for the field, depending on the system state

$$U(t)|0\rangle|\Psi\rangle_b = |0\rangle \prod_k D(-\frac{1}{2}\xi_k(t))|\Psi\rangle_b A(t) \tag{4.12}$$

$$U(t)|1\rangle|\Psi\rangle_b = |1\rangle \prod_k D(+\frac{1}{2}\xi_k(t))|\Psi\rangle_b A(t) \tag{4.13}$$

with

$$D(\xi_k(t)) = \exp\{a_k^\dagger \xi_k(t) - a_k \xi_k^*(t)\} \tag{4.14}$$

and

$$D(-\xi_k(t)) = D^+(\xi_k(t)) \tag{4.15}$$

4.1.1 Expectation values

Since the Hamilton operator commutes with σ_z:

$$\tilde{\sigma}_z = U(t)\sigma_z U^+(t) = \sigma_z \tag{4.16}$$

the expectation value is constant

$$\langle\sigma_z(t)\rangle = \langle\tilde{\Psi}|\tilde{\sigma}_z|\tilde{\Psi}\rangle = -|c_0|^2 + |c_1|^2 \tag{4.17}$$

The operator σ_x in interaction picture:

$$\tilde{\sigma}_x = \tilde{\sigma}_+ + \tilde{\sigma}_- = \sigma_+ e^{-2i\epsilon t} + \sigma_- e^{2i\epsilon t} \tag{4.18}$$

and

$$\tilde{\sigma}_y = -i(\tilde{\sigma}_+ - \tilde{\sigma}_-) = -i(\sigma_+ e^{-2i\epsilon t} - \sigma_- e^{2i\epsilon t}) \tag{4.19}$$

Now we can calculate the expectation value of σ_x:

$$\langle\sigma_x(t)\rangle = \langle\tilde{\Psi}|\tilde{\sigma}_x|\tilde{\Psi}\rangle \tag{4.20}$$

$$\begin{aligned} &= \prod_k \langle\Psi|_b \left(D^+(-\frac{1}{2}\xi_k(t))\langle 0|c_0^* + D^+(\frac{1}{2}\xi_k(t))\langle 1|c_1^* \right) \\ &\quad (\sigma_+ e^{-2i\epsilon t} + \sigma_- e^{2i\epsilon t}) \\ &\quad \prod_{k'} \left(c_0|0\rangle D(-\frac{1}{2}\xi_{k'}(t)) + c_1|1\rangle D(+\frac{1}{2}\xi_{k'}(t)) \right) |\Psi\rangle_b \\ &= \prod_k \left(c_0^* c_1 e^{-2i\epsilon t}\langle\Psi|_b D(+\xi_k(t))|\Psi\rangle_b + c_0 c_1^* e^{2i\epsilon t}\langle\Psi|_b D(-\xi_k(t))|\Psi\rangle_b \right) \\ &= e^{-\Gamma(t)}(c_0^* c_1 e^{-2i\epsilon t} + c_0 c_1^* e^{2i\epsilon t}) \end{aligned} \tag{4.21}$$

with the definition

$$\Gamma(t) = \sum_k \frac{1}{2}|\xi_k(t)|^2 \tag{4.22}$$

and we used

$$\prod_k \langle 0|_b D(\xi_k(t))|0\rangle_b = e^{-\sum_k \frac{|\xi_k(t)|^2}{2}} = e^{-\Gamma(t)} \tag{4.23}$$

With a similar calculation for $\langle\sigma_y\rangle$ we can write down the system density matrix

$$\rho(t) = \begin{pmatrix} |c_1|^2 & e^{-\Gamma(t)} c_0 c_1^* e^{-2i\epsilon t} \\ e^{-\Gamma(t)} c_0^* c_1 e^{2i\epsilon t} & |c_0|^2 \end{pmatrix} \tag{4.24}$$

Its eigenvalues are $\lambda_{1/2} = \frac{1}{2}(1 \pm \sqrt{1 - 4e^{-2\Gamma(t)}|c_0|^2|c_1|^2})$. Since $0 \leq |c_0|^2|c_1|^2 \leq \frac{1}{4}$, and if $\Gamma(t) > 0$, both eigenvalues are positive. We discuss the function $\Gamma(t)$ at the end of this section.

The purity is

$$\begin{aligned} p &= \rho_{11}^2 + \rho_{22}^2 + 2\rho_{12}\rho_{21} \\ &= 1 + 2|c_0|^2|c_1|^2(e^{-2\Gamma(t)} - 1) \end{aligned} \tag{4.25}$$

Since $p < 1$ for $\Gamma(t) > 0$, we have a mixed state.

4.1.2 Correlations

We calculate the correlations to be able to compare them to the solution of our original problem. We note that $U(t) = U_0^+(t)U_H(t)$

$$\begin{aligned}
\langle\sigma_+(t)\sigma_-(t')\rangle &= \langle\Psi(t)|\sigma_+U_H(t)U_H^+(t')\sigma_-|\Psi(t')\rangle \\
&= \langle\Psi(t)|U_0(t)U_0^+(t)\sigma_+U_0(t)U_0^+(t)U_H(t) \\
&\quad U_H^+(t')U_0(t')U_0^+(t')\sigma_-U_0(t')U_0^+(t')|\Psi(t')\rangle \\
&= \langle\tilde{\Psi}(t)|\tilde{\sigma}_+(t)U(t)U^+(t')\tilde{\sigma}_-(t')|\tilde{\Psi}(t')\rangle \\
&= \prod_k\langle\Psi|\left(D^+(-\frac{1}{2}\xi_k(t))\langle 0|c_0^* + D^+(\frac{1}{2}\xi_k(t))\langle 1|c_1^*\right) \\
&\quad \sigma_+e^{-2i\epsilon t}U(t)U^+(t')\sigma_-e^{2i\epsilon t'} \\
&\quad \prod_k\left(c_0|0\rangle D(-\frac{1}{2}\xi_k(t'))|\tilde{\Psi}\rangle_b + c_1|1\rangle D(+\frac{1}{2}\xi_k(t'))|\Psi\rangle_b\right) \\
&= \prod_k\langle\Psi|D^+(\frac{1}{2}\xi_k(t))\langle 0|c_1^*U(t)U^+(t')(c_1|0\rangle D(+\frac{1}{2}\xi_k(t'))|\Psi\rangle_b \\
&= \prod_k\langle\Psi|D^+(\xi_k(t))\langle 0|c_1^*c_1|0\rangle D(\xi_k(t'))|\Psi\rangle_b e^{-2i\epsilon(t-t')} \\
&= |c_1|^2e^{-\frac{1}{2}\sum_k|\xi_k(t)-\xi_k(t')|^2}e^{-2i\epsilon(t-t')} \qquad (4.26)
\end{aligned}$$

Other correlations:

$$\begin{aligned}
\langle\sigma_z(t)\sigma_z(t')\rangle &= \langle\tilde{\Psi}(t)|\tilde{\sigma}_z(t)U(t)U^+(t')\tilde{\sigma}_z|\tilde{\Psi}(t')\rangle \\
&= e^{-\frac{1}{2}\sum_k|\xi_k(t)-\xi_k(t')|^2} \qquad (4.27)
\end{aligned}$$

$$\langle\sigma_z(t)\sigma_y(t')\rangle = -i\left(c_0^*c_1e^{-\Gamma(t)}e^{-2i\epsilon t'} + c_1^*c_0e^{\Gamma(t)}e^{2i\epsilon t'}\right) \qquad (4.28)$$

$$\langle\sigma_y(t)\sigma_z(t')\rangle = \langle\sigma_z(t')\sigma_y(t)\rangle^+ \qquad (4.29)$$

$$\begin{aligned}
\langle\sigma_y(t)\sigma_y(t')\rangle &= \langle\tilde{\Psi}(t)|\tilde{\sigma}_y(t)U(t)U^+(t')\tilde{\sigma}_y|\tilde{\Psi}(t')\rangle \\
&= e^{-\Gamma(t)-\Gamma(t')}(|c_0|^2e^{-4i\epsilon t} + |c_1|^2e^{4i\epsilon t}) \qquad (4.30)
\end{aligned}$$

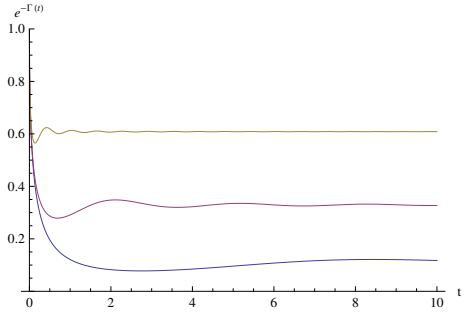

Figure 4.1: $e^{-\Gamma(t)}$ with $\delta = -0.5$ (blue), $\delta = -2$ (red), $\delta = -10$ (yellow)

$$\bar{\sigma}_+ = \sigma_z + i\sigma_y \tag{4.31}$$
$$\bar{\sigma}_- = \sigma_z - i\sigma_y \tag{4.32}$$

$$\begin{aligned}\langle\bar{\sigma}_-(t)\bar{\sigma}_+(t')\rangle &= \langle\sigma_z(t)\sigma_z(t')\rangle + i\langle\sigma_y(t)\sigma_z(t')\rangle - i\langle\sigma_z(t)\sigma_y(t')\rangle + \langle\sigma_y(t)\sigma_y(t')\rangle \\ &= 1 - 2c_0c_1^*e^{-\frac{1}{2}(\Gamma(t)+\Gamma(t'))}e^{-2i\epsilon t} - 2c_0^*c_1e^{-\frac{1}{2}(\Gamma(t)+\Gamma(t'))}e^{2i\epsilon t} \\ &\quad +|c_0|^2e^{-\Gamma(t)-\Gamma(t')}e^{-4i\epsilon t} + |c_1|^2e^{-\Gamma(t)-\Gamma(t')}e^{4i\epsilon t}\end{aligned} \tag{4.33}$$

The decay function $\Gamma(t)$ is for the photonic crystal density of states

$$\begin{aligned}\Gamma(t) &= \frac{1}{2}\sum_k |\xi_k(t)|^2 \\ &= 2\sum_k g_k^2\frac{1-\cos\omega_k t}{\omega_k^2} \\ &= \mathrm{Re}\int_0^\infty d\omega J(\omega)\frac{1-e^{-i((\omega-\omega_A)t}}{(\omega-\omega_A)^2} \\ &= \mathrm{Re}\int_0^\infty d\omega(\omega-\omega_e)^{\frac{1}{2}}e^{-(\omega-\omega_e)/\omega_c}\Theta(\omega-\omega_e)\frac{1-e^{-i((\omega-\omega_A)t}}{(\omega-\omega_A)^2} \\ &= \mathrm{Re}\int_0^\infty d\omega\omega^{\frac{1}{2}}e^{-\omega/\omega_c}\frac{1-e^{-i((\omega+\omega_e-\omega_A)t)}}{(\omega+\omega_e-\omega_A)^2}\end{aligned} \tag{4.34}$$

If the atom frequency is in the band, $\delta := \omega_A - \omega_e > 0$, the integral is diverging and the atom decays instantaneously.

In the gap $\delta < 0$ and

$$\Gamma(t) \xrightarrow{\omega_c\to\infty} \mathrm{Re}[\sqrt{it}e^{i\delta t} - i\pi\sqrt{-\delta}t - \frac{\pi}{2\sqrt{-\delta}}(1-2i\delta t)\mathrm{erf}\sqrt{-i\delta t}]$$

The error function for large arguments is to lowest order

$$\mathrm{erf}(z) = 1 - \frac{1}{\sqrt{\pi}z} e^{-z^2} \tag{4.35}$$

and therefore

$$\begin{aligned} \Gamma(t) &= \mathrm{Re}[\sqrt{it}e^{i\delta t} - i\pi\sqrt{\delta}t - \frac{\pi}{2\sqrt{-\delta}}(1-2i\delta t)\mathrm{erf}\sqrt{-i\delta t}] \\ &\xrightarrow{t\to\infty} \frac{\pi}{2\sqrt{-\delta}} \end{aligned} \tag{4.36}$$

Fermi's Golden Rule predicts zero decay, actually we find a partial decay, i.e. an initial decay at the beginning and a constant nonzero value for long times.

4.2 Driven atom

For a very weak coupling to the environment, the limiting case is the atom with only driving. This can be solved analytically. The dressed state Hamiltonian can be used, since the dressed states are its eigenstates.

$$H = \frac{1}{2}\Delta_{AL}\sigma_z + \epsilon(\sigma_+ + \sigma_-) \tag{4.37}$$

The equations of motion are

$$\begin{aligned} \dot{\sigma}_-(t) &= i[H,\sigma_-] = -i\Delta_{AL}\sigma_-(t) + i\epsilon\sigma_z \\ \dot{\sigma}_z(t) &= i[H,\sigma_z] = 2i\epsilon(-\sigma_+ + \sigma_-) \end{aligned} \tag{4.38}$$

The solution is with $\Omega = \sqrt{\Delta^2 + 4\epsilon^2}$, $\Delta = \Delta_{AL}$

$$\begin{aligned} \sigma_-(t) &= \frac{1}{\Omega^2}\Big[[2\epsilon^2 + \frac{1}{4}(\Delta-\Omega)^2 e^{i\Omega t} + \frac{1}{4}(\Delta+\Omega)^2 e^{-i\Omega t}]\sigma_-(0) \\ &\quad \epsilon^2[2 - e^{-i\Omega t} - e^{i\Omega t}]\sigma_+(0) + [\Delta\epsilon - \epsilon^2]\sigma_z(0)\Big] \\ \sigma_z(t) &= \frac{1}{\Omega^2}\Big[[\epsilon(2\Delta - (\Delta+\Omega)e^{-i\Omega t} - (\Delta-\Omega)e^{i\Omega t})]\sigma_-(0) \\ &\quad +[\epsilon(2\Delta - (\Delta+\Omega)e^{i\Omega t} - (\Delta-\Omega)e^{-i\Omega t})]\sigma_-(0) \\ &\quad +[\Delta^2 + 2\epsilon^2 e^{-i\Omega t} + 2\epsilon^2 e^{i\Omega t}]\sigma_z(0)\Big] \end{aligned} \tag{4.39}$$

The dipole correlation is $\langle\psi|\sigma_+(t)\sigma_-(t')|\psi\rangle$. The Fourier transformed correlation function with $\tau = t - t'$ and $t = 0$ is

$$\begin{aligned} S(\omega) &= \frac{1}{\Omega^4}\sqrt{2\pi}[\Delta^2(\Delta^2+2\epsilon^2)+4\epsilon^2(\Delta^2+2\epsilon^2)]\delta(\omega) \\ &+\frac{1}{\Omega^2}\sqrt{\frac{\pi}{2}}[(\Delta+\Omega)^2+4\epsilon^2]\delta(\omega-\Omega) \\ &+\frac{1}{\Omega^2}\sqrt{\frac{\pi}{2}}[(\Delta-\Omega)^2+4\epsilon^2]\delta(\omega+\Omega) \end{aligned} \tag{4.40}$$

it consists of three δ-peaks at $0, -\Omega, +\Omega$.

4.3 Resonance fluorescence in free space

The discussion of resonance fluorescence in free space can be found for example in [1].The resulting spectrum is the Mollow triplet. With the Hamilton operator eq.(3.10), where the g_k are the free space coupling constants in this section, the Heisenberg equations of motion are

$$\dot{\sigma}_-(t) = i[H,\sigma_-] = -i\omega_A\sigma_- + i\epsilon e^{-i\omega_L t}\sigma_z + \sum_\lambda g_\lambda a_\lambda \sigma_z \tag{4.41}$$

$$\dot{\sigma}_z(t) = i[H,\sigma_z] = 2i\epsilon(-\sigma_+ e^{-i\omega_L t} + \sigma_- e^{i\omega_L t}) - 2\sum_\lambda g_\lambda(a_\lambda^+\sigma_- + \sigma_+ a_\lambda) \tag{4.42}$$

$$\dot{a}_\lambda(t) = i[H,a_\lambda] = -i\omega_\lambda a_\lambda - g_\lambda\sigma_- \tag{4.43}$$

The last equation is formally solved by

$$a_\lambda(t) = a_\lambda(0)e^{-i\omega_\lambda t} - \int_0^t g_\lambda\sigma_-(t')e^{-i\omega_\lambda(t-t')}dt' \tag{4.44}$$

Then

$$\sum_\lambda g_\lambda a_\lambda(t) = \sum_\lambda g_\lambda a_\lambda(0)e^{-i\omega_\lambda t} - \sum_\lambda \int_0^t g_\lambda^2\sigma_-(t')e^{-i\omega_\lambda(t-t')}dt' \tag{4.45}$$

For the second term we change the sum into an integral

$$\sum_\lambda \to 2\frac{V}{(2\pi)^3}\int dk k^2 \int \sin\theta d\theta \int d\varphi \tag{4.46}$$

$$
\begin{aligned}
I &= \sum_{\lambda} \int_0^t g_\lambda^2 \sigma_-(t') e^{-i\omega_\lambda (t-t')} dt' \\
&= 2\frac{V}{(2\pi)^3} \int dk k^2 \int \sin\theta d\theta \int d\varphi \int_0^t g_\lambda^2 \sigma_-(t') e^{-i\omega_\lambda (t-t')} dt' \\
&= \frac{\hbar \omega_A^2 d_{ge}^2}{2\epsilon_0 c^3 \pi^3} \int d\omega \omega \int d\theta \sin\theta cos^2\theta \int d\varphi \int_0^t \sigma_-(t') e^{-i\omega (t-t')} dt' \\
&= \frac{2\hbar \omega_A^2 d_{ge}^2}{3\epsilon_0 c^3 \pi^2} \int d\omega \omega \int_0^t \sigma_-(t') e^{-i\omega (t-t')} dt' \\
&\approx \frac{2\hbar \omega_A^2 d_{ge}^2}{3\epsilon_0 c^3 \pi^2} \int d\omega \omega \int_0^t dt' \sigma_-(0) e^{-i\omega_A t'} e^{-i\omega (t-t')} \\
&= \frac{2\hbar \omega_A^2 d_{ge}^2}{3\epsilon_0 c^3 \pi^2} e^{-i\omega_A t} \sigma_-(0) \int d\omega \omega \int_0^t dt' e^{i(\omega-\omega_A)(t'-t)} \qquad (4.47)
\end{aligned}
$$

With the free space dispersion relation $k = \frac{\omega}{c}$, $\hat{e}_{\vec{k}} \cdot d_{ge} = \cos\theta d_{ge}$ and we used the lowest order (Liouville) approximation:

$$\sigma_-(t) = e^{-i\omega_A t} \sigma_-(0) \qquad (4.48)$$

In the integral

$$\int_0^\infty d\omega \omega \int_0^t dt' e^{i(\omega-\omega_A)(t'-t)} \qquad (4.49)$$

the quantity ω varies little around $\omega = \omega_A$ for which the time integral is not negligible. Therefore we replace ω by ω_A and the lower integration limit with $-\infty$.
We use

$$\int_{-\infty}^\infty d\omega e^{i(\omega-\omega_A)(t'-t)} = 2\pi\delta(t'-t) \qquad (4.50)$$

To get the result

$$
\begin{aligned}
I &= \frac{4\hbar \omega_A^3 d_{ge}^2}{3\epsilon_0 c^3 \pi} e^{-i\omega_A t} \sigma_-(0) \qquad (4.51) \\
&= \frac{4\hbar \omega_A^3 d_{ge}^2}{3\epsilon_0 c^3 \pi} \sigma_-(t) \qquad (4.52)
\end{aligned}
$$

The response function is

$$G(\tau) = \frac{4\hbar \omega_A^3 d_{ge}^2}{3\epsilon_0 c^3 \pi} \delta(\tau) =: \beta\delta(\tau) \qquad (4.53)$$

This is a delta-peaked response function that does not include the state of the system at earlier times. In a photonic crystal this approximation cannot be made and the equations of motion have a memory kernel.

$$\begin{aligned}\dot{\sigma}_-(t) &= -i\omega_A\sigma_-(t) + i\epsilon e^{-i\omega_L t}\sigma_z(t) - \beta\sigma_-(t) \\ &\quad + \sum_\lambda g_\lambda \sigma_z(t) a_\lambda(0) e^{-i\omega_\lambda t} \qquad (4.54)\\ \dot{\sigma}_z(t) &= 2i\epsilon(-\sigma_+ e^{-i\omega_L t} + \sigma_- e^{i\omega_L t}) - 2\beta(1+\sigma_z) \\ &\quad -2\sum_\lambda g_\lambda(\sigma_+ a_\lambda(0) e^{-i\omega_\lambda t} + \sigma_- a_\lambda^+(0) e^{i\omega_\lambda t}) \qquad (4.55)\end{aligned}$$

Taking the expectation value with a vacuum bath state ($\langle a_\lambda\rangle = \langle a_\lambda^+\rangle = 0$) and solving for $\langle\sigma_z + 1\rangle$:

$$\begin{aligned}\langle\sigma_z+1\rangle &= e^{-2\beta t}\langle\sigma_z(0)+1\rangle \\ &\quad + \frac{4\epsilon^2}{\beta^2+\Delta_{AL}^2}\int_{t_0}^t dt'[(-\Delta)e^{\beta(t'-t)}\sin\Delta_{AL}(t'-t)) \\ &\quad + (\beta\cos\Delta_{AL}(t'-t)e^{\beta(t'-t)} - \beta e^{2\beta(t'-t)})]\langle\sigma_z(t')\rangle \qquad (4.56)\end{aligned}$$

With the definition $\Delta_{AL} := \omega_A - \omega_L$
Resonant case $\Delta = 0$:

$$\begin{aligned}\langle\sigma_z(t)+1\rangle &= +\frac{4\epsilon^2}{\beta}\int_{t_0}^t dt'(e^{\beta(t'-t)} - e^{2\beta(t'-t)})\langle\sigma_z(t')\rangle \\ &\quad + e^{-2\beta t}\langle\sigma_z(0)+1\rangle \qquad (4.57)\end{aligned}$$

The convolution integral suggests a Laplace transformation

$$\langle\sigma_z(s)\rangle = -\frac{(s+\beta)(s+2\beta)(-2\beta + s\langle\sigma_z(0)\rangle}{s((s+\beta)(s+2\beta)+4\epsilon^2)(s+2\beta)} \qquad (4.58)$$

We assume an initial condition $\sigma_z(0) = -1$ and define $\Omega := \sqrt{16\epsilon^2 - \beta^2}$. The back transformation shows a constant term and damped oscillations.

$$\langle\sigma_z(t)\rangle = -\frac{2\beta^2}{2\beta^2+4\epsilon^2} - \frac{\epsilon^2(i\Omega+3\beta)}{(2\beta^2+4\epsilon^2)i\Omega}e^{-\frac{1}{2}(3\beta-i\Omega)t} - \frac{\epsilon^2(i\Omega-3\beta)}{(2\beta^2+4\epsilon^2)i\Omega}e^{-\frac{1}{2}(3\beta+i\Omega)t} \qquad (4.59)$$

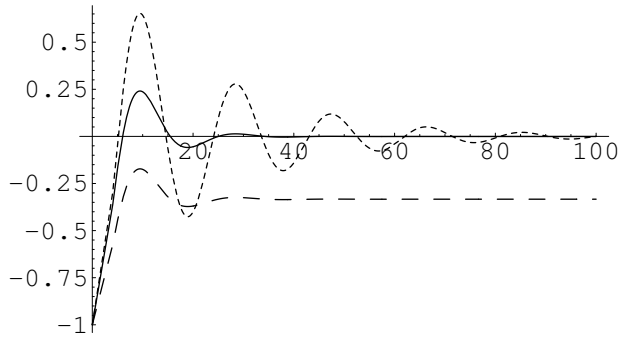

Figure 4.2: $\sigma_z(t)$
solid:$\epsilon = 3, \beta = 0.1$
dotted:$\epsilon = 3, \beta = 0.03$
dashed:$\epsilon = 0.1, \beta = 0.1$

In the long time limit the oscillating terms decay

$$\langle \sigma_z(t) \rangle \rightarrow -\frac{2\beta^2}{2\beta^2 + 4\epsilon^2} \tag{4.60}$$

$\langle \sigma_- \rangle$ and $\langle \sigma_+ \rangle$ oscillate with frequency ω_A

$$\langle \sigma_-(t) \rangle = i\epsilon e^{(-i\omega_A - \beta)t} \int dt' e^{\beta t'} \langle \sigma_z(t) \rangle \rightarrow -\frac{2i\epsilon\beta}{2\beta^2 + 4\epsilon^2} e^{-i\omega_A t} \tag{4.61}$$

$$\langle \sigma_+(t) \rangle \rightarrow \frac{2i\epsilon\beta}{2\beta^2 + 4\epsilon^2} e^{i\omega_A t} \tag{4.62}$$

This can be compared later with the solution in a photonic crystal.

Chapter 5

Driven two-level atom in a PhC

In this chapter we calulate analytically the expectation value of the population inversion $\langle\sigma_z(t)\rangle$ in the Liouville approximation of lowest order. The equations of motion are after adiabatic elimination of the photonic degrees of freedom:

$$\begin{aligned}
\dot{\sigma}_-(t) &= -i\omega_A\sigma_-(t) + i\epsilon e^{-i\omega_L t}\sigma_z(t) - \int_0^t G(t-t')\sigma_-(t') \\
&\quad + \sum_\lambda g_\lambda \sigma_z(t) a_\lambda(0) e^{-i\omega_\lambda t} \qquad (5.1) \\
\dot{\sigma}_z(t) &= 2i\epsilon(-\sigma_+(t)e^{-i\omega_L t} + \sigma_-(t)e^{i\omega_L t}) \\
&\quad - \int_0^t (G(t-t')e^{i\omega_A(t-t')} + G^*(t-t')e^{-i\omega_A(t-t')})(1+\sigma_z(t')) \\
&\quad -2\sum_\lambda g_\lambda(\sigma_+(t)a_\lambda(0)e^{-i\omega_\lambda t} + a_\lambda^+(0)\sigma_-(t)e^{i\omega_\lambda t}) \qquad (5.2)
\end{aligned}$$

The equation for $\sigma_+(t)$ is the hermitian conjugate of the $\sigma_-(t)$ equation. Taking the expectation values in vacuum state removes the last terms. The Laplace transformation is, with initial values $\langle\sigma_-(0)\rangle$, $\langle\sigma_z(0)\rangle$:

$$\begin{aligned}
(s + i\omega_A + G(s))\langle\sigma_-(s)\rangle &= \langle\sigma_-(0)\rangle + i\epsilon\langle\sigma_z(s+i\omega_L)\rangle \\
(s + G(s-i\omega_A) + G^*(s+i\omega_A))\langle\sigma_z(s)\rangle &= \langle\sigma_z(0)\rangle - 2i\epsilon\langle\sigma_+(s+i\omega_L)\rangle + 2i\epsilon\langle\sigma_-(s-i\omega_L)\rangle \\
&\quad -\frac{1}{s}(G(s-i\omega_A) + G^*(s+i\omega_A))
\end{aligned}$$

Where $G^*(s+i\omega_A)$ is the Laplace transformation of $G^*(t)e^{-i\omega_A t}$. The equations are solved for $\sigma_z(s)$. $\sigma_z(0)$ is σ_z for $t=0$ etc.

$$\sigma_z(s)\Big(s+G(s-i\omega_A)+G^*(s+i\omega_A)+\frac{2\epsilon^2}{s+i\delta+G^*(s+i\omega_L)}+\frac{2\epsilon^2}{s-i\delta+G(s-i\omega_L)}\Big)$$
$$=\sigma_z(0)-\frac{2i\epsilon\sigma_+(0)}{s+i\delta+G^*(s+i\omega_L)}+\frac{2i\epsilon\sigma_-(0)}{s-i\delta+G(s-i\omega_L)}-\frac{1}{s}(G(s-i\omega_A)+G^*(s+i\omega_A))$$

We consider the case $\sigma_-(0)=\sigma_+(0)=0$ and define $\delta=\omega_L-\omega_A$, $G_A(s):=G(s-i\omega_A)$, $G_A^*(s):=G^*(s+i\omega_A)$, $G_L(s):=G(s-i\omega_L)$, $G_L^*(s):=G(s+i\omega_L)$

$$\sigma_z(s)=\frac{[s\sigma_z(0)-(G_A(s)+G_A^*(s)](s+i\delta+G_L^*(s))(s-i\delta+G_L(s))}{s\{[s+G_A(s)+G_A^*(s)](s+i\delta+G_L^*(s))(s-i\delta+G_L(s))+2\epsilon^2(2s+G_L(s)+G_L^*(s))\}}$$

This has four poles like the free space solution eq.(4.58), but also four branch cuts stemming from the square root in $G(s)=\alpha\sqrt{i}\sqrt{s+i\omega_e}$. For the backtransformation we have to take into account the branch cuts.

$$\int_{\gamma-i\infty}^{\gamma+i\infty}\sigma_z(s)e^{st}+\int_{cuts}\sigma_z(s)e^{st}=2\pi i\sum_{zeroes}\mathrm{Res}[\sigma_z] \tag{5.3}$$

$\mathrm{Res}[\sigma_z]$ are the residues of σ_z and the sum is over the zeroes of the denominator of $\sigma_z(s)$. We use the following contour on the complex plane

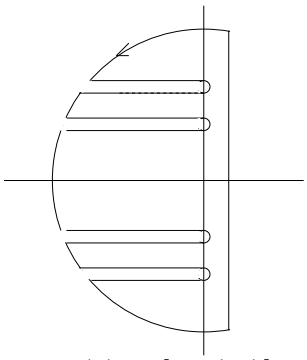

Since $G_A^*(s)=[G_A(s^*)]^*$ we see $\sigma_z(s)=[\sigma_z(s^*)]^*$. The poles appear in pairs, so the pole contributions are real, exponentially decaying functions.
Due to the direction of the line integral, the cut contribution is imaginary.
The backtransformation is done with Mathematica by numerically finding the zeroes of the denominator and consequently calculating the residues. The results depend on the distance to the band edge $\omega_A-\omega_e=\omega_L-\omega_e$ and

the Rabi frequency ϵ in units of the coupling α.
With small Rabi frequency and an atomic frequency slightly in the band, we see a fast and complete decay:

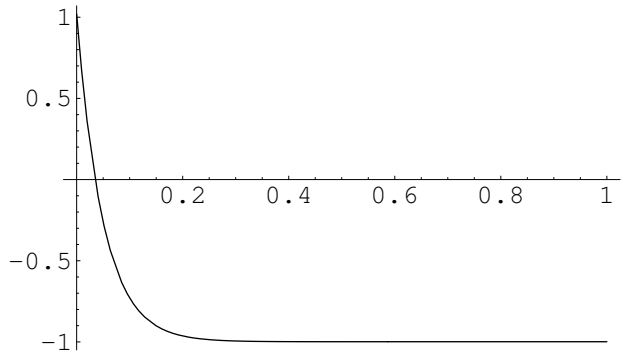

Figure 5.1: $\langle \sigma_z(t) \rangle$
$\omega_A = \omega_L$, $\omega_A - \omega_e = 0.27$,
$\epsilon = 0.25$, $\alpha = 1$

In the band, we get decaying oscillations for stronger Rabi frequency and stronger decay for weaker Rabi frequency.

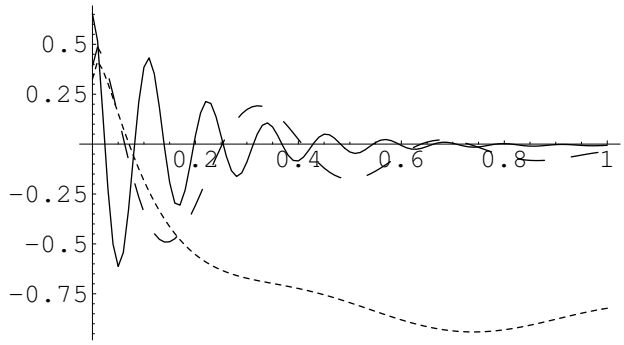

Figure 5.2: $\langle \sigma_z(t) \rangle$
$\omega_A = \omega_L$, $\omega_A - \omega_e = 10$,
$\alpha = 1$, solid: $\epsilon = 30$,
dashed: $\epsilon = 10$, dotted:
$\epsilon = 1$

A stronger coupling α causes faster decay and larger oscillation frequencies:

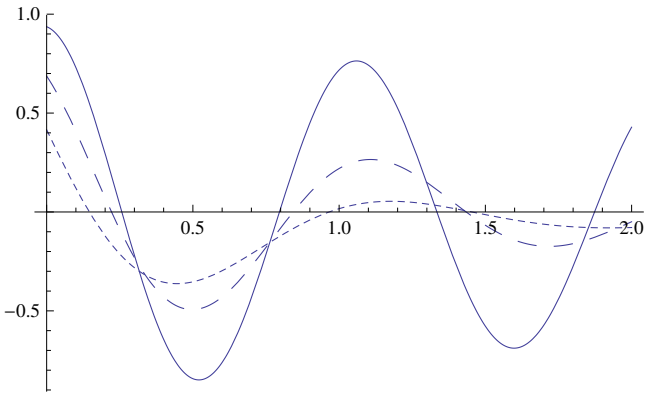

Figure 5.3: $\langle\sigma_z(t)\rangle$ $\omega_A = \omega_L$, $\omega_A - \omega_e = 1$, $\epsilon = 3$, solid: $\alpha = 0.1$, dashed: $\alpha = 0.5$, dotted: $\alpha = 1$

Three different band edge frequencies such that the oscillations in the gap decay more slowly.

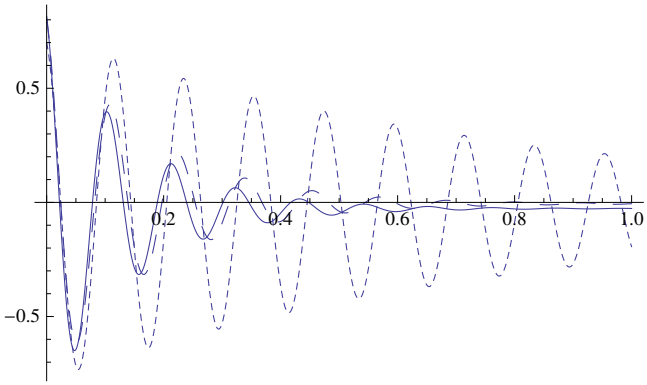

Figure 5.4: $\langle\sigma_z(t)\rangle$ $\omega_A = \omega_L = 100$, $\epsilon = 30$, solid: $\omega_e = 50$, dashed: $\omega_e = 90$, dotted: $\omega_e = 150$

These results may be compared to the decay given by Fermi's golden rule [32]. The expression for the decay rate of the excited state to the ground state

$$\begin{aligned}\Gamma &= 2\pi \sum_{\vec{k},n} |\langle 0, 1_{\vec{k},n}|\vec{d}\cdot\vec{E}|1, 0_{\vec{k},n}\rangle|^2 \delta(\omega_{\vec{k},n} - \omega_A) \\ &= 2\pi\rho(\omega_A) \\ &= 2\pi\alpha\sqrt{\Delta_{Ae}} \end{aligned} \tag{5.4}$$

And therefore $\sigma_z(t) = 2|e^{-\Gamma t}|^2 - 1 = 2|e^{-2\pi\alpha\sqrt{\Delta_{Ae}}t}|^2 - 1$. It does not decay for ω_A in the gap and decays completely to -1 for ω_A in the band.

With $G(s) = \alpha\sqrt{i(s+i\omega_e)})$, the final value theorem states that the steady state value is $\lim_{s\to 0} s\sigma_z(s) = \lim_{t\to\infty}\sigma_z(t)$.
Resonant case

$$\lim_{s\to 0} s\sigma_z(s) \;=\; \frac{-\alpha^2(\omega_e-\omega_A)}{\alpha^2(\omega_e-\omega_A)+2\epsilon^2} \tag{5.5}$$

For $\epsilon = 0$ this is the spontaneous decay solution.
In general there are four different cases:

- For ω_A in the band ($\omega_A > \omega_e$) and ω_L in the gap ($\omega_L < \omega_e$), $G_L(0) + G_L^*(0) = 0$, $G_A(0) + G_A^*(0) = 2G_A(0)$ and therefore

$$\lim_{s\to 0} s\sigma_z(s) = \frac{-2G_A(0)(i\delta + G_L^*(0))(-i\delta + G_L(0))}{2G_A(0)(i\delta + G_L^*(0))(-i\delta + G_L(0))} = -1 \tag{5.6}$$

- For ω_L in the band and ω_A in the gap:

$$\lim_{s\to 0} s\sigma_z(s) = \frac{0}{2\epsilon^2(G_L(0)+G_L^*(0))} = 0 \tag{5.7}$$

- For both ω_L and ω_A in the gap $G_L(0)+G_L^*(0) = 0$ and $G_A(0)+G_A^*(0) = 0$. L'Hôpital's rule can be used. The stationary state depends on the initial condition:

$$\lim_{s\to 0} s\sigma_z(s) = \frac{(\sigma_z(0) + \frac{\alpha}{\sqrt{\Delta_{eA}}})(\delta - \alpha\sqrt{\Delta_{eL}})^2}{(1+\frac{\alpha}{\sqrt{\Delta_{eA}}})(\delta-\alpha\sqrt{\Delta_{eL}})^2 + 2\epsilon^2(\frac{\alpha}{\sqrt{\Delta_{eL}}}+2)} \tag{5.8}$$

- For both ω_L and ω_A in the band:

$$\lim_{s\to 0} s\sigma_z(s) = -\frac{\sqrt{\Delta_{Ae}}(\delta^2+\alpha^2\Delta_{Ae})}{\sqrt{\Delta_{Ae}}(\delta^2+\alpha^2\Delta_{Ae}) + 2\epsilon^2\sqrt{\Delta_{Le}}} \tag{5.9}$$

Chapter 6

Fluctuation Dissipation Theorem

This chapter was published in [33]. Correlation functions of a driven two-level system embedded in a photonic crystal are analyzed. The equations of motion for two-time correlations are derived by two different methods, the quantum regression theorem and the fluctuation dissipation theorem, and found to be the same.

6.1 Introduction

In most theoretical treatments of open quantum systems the Markov approximation is used. That means it is assumed that quanta emitted from the system disappear in the reservoir. However, there are systems where this is not justified, e.g. for an emitter in a photonic crystal. The multiple Bragg reflections from the crystal planes can trap photons (band gap). But even in allowed bands, they create a significant memory of the photon bath that influences the system at later times. In the calculation of system correlations (Mollow spectrum), quantum regression approaches are used [34] that are justified in the Markov case.

However, the quantum regression "theorem" (QRT) ist not always applicable. A counter-example was provided by Ford and O'Connell [35]. We want to analyze here the QR approach for the case of a driven atom in a photonic crystal by comparing the equations of motion for correlations with those derived from linear response theory, as they are used in the fluctuation

dissipation theorem (FDT). The discussion highlights transient (or inhomogeneous) terms that are absent for one-time averages, but drive correlations – they provide a correction to the naive form of the QRT [36]. The same kind of transients also appears in the FDT, although technically for different reasons. The analysis shows that the two methods have to face the same challenge, namely to bring the non-Markovian equations of motion in a form that can be efficiently solved.

6.2 Quantum regression theorem

The quantum regression theorem states that the equations of motion are the same for one-time as for two-time correlation functions [1]. The time dependence for the expectation value $\langle A(t)\rangle$ and the correlation function $\langle A(t)B(0)\rangle$ of two system observables is

$$\begin{aligned} \langle A(t)\rangle &= \mathrm{tr}\{U^{-1}(t)A(0)U(t)\rho\} \\ &= \mathrm{tr}_S\{A(0)\,\mathrm{tr}_B\{U(t)\rho_S\rho_B U^{-1}(t)\}\} \qquad (6.1) \\ \langle A(t)B(0)\rangle &= \mathrm{tr}\{U^{-1}(t)A(0)U(t)B(0)\rho\} \\ &= \mathrm{tr}_S\{A(0)\,\mathrm{tr}_B\{U(t)[B(0)\rho_S]\rho_B U^{-1}(t)\}\} \qquad (6.2) \end{aligned}$$

If the density matrix is at $t = 0$ in a product state $\rho(0) = \rho_S(0) \otimes \rho_B(0)$, the time dependence for both quantities is the same. The Wiener Khinchine theorem requires a stationary state to calculate the spectrum, but the stationary state is in general entangled for non-Markovian reservoirs. In other words, for a stationary correlation $\langle A(t)B(t')\rangle$ with both $t, t' \to \infty$, the density matrix at time t' is neither in product form nor does it contain sufficient information to predict the evolution towards the time t. A solution to circumvent this problem is provided by linear response theory and the fluctuation-dissipation theorem, that does not require an initial product state and a Markov approximation.

6.3 Fluctuation dissipation theorem

Several relations are called fluctuation-dissipation theorem in the literature. In our case, we use one that is suitable for zero temperature, also called Kubo relation [37], [38]. The system described by H_0 is perturbed by an additional

term H_1

$$H = H_0 + H_1, \quad H_1 = Af(t) \tag{6.3}$$

A is a hermitian operator and $f(t)$ is a test function vanishing in the very far past ($t \leq 0$). The system state is then described by ρ_0, so $\langle B(t)\rangle_0 = tr\{\rho_0 B(t)\}$.

The density matrix in the interaction picture is

$$\rho_I(t) = \rho(0) + \frac{1}{i}\int_0^t [H_{1I}(t), \rho_I(t)] \tag{6.4}$$

For a small parameter in $H_{1I}(t)$ this may be iterated as follows:

$$\begin{aligned}\rho_I(t) &= \rho(0) + \frac{1}{i}\int_0^t dt_1 [H_{1I}(t_1), \rho(0)] \\ &\quad + \frac{1}{i^2}\int_0^t dt_1 \int_0^{t_1} dt_2 [H_{1I}(t_2), [H_{1I}(t_1), \rho_I(0)]] + \ldots \end{aligned} \tag{6.5}$$

We use this formula to calculate the expectation value

$$\begin{aligned}\langle B(t)\rangle &= tr\{B_I(t)\rho_I(t)\} \\ &= \langle B_I(t)\rangle_0 + \frac{1}{i}\int_0^t dt_1 \langle [B_I(t), H_{1I}(t_1)]\rangle_0 \\ &\quad + \frac{1}{i^2}\int_0^t dt_1 \int_0^{t_1} dt_2 \langle [H_{1I}(t_2)[H_{1I}(t_1), B_I(t)]]\rangle_0 + \ldots \end{aligned} \tag{6.6}$$

with $H_{1I}(t) = A_I(t)f(t)$. The linear response of the system to the perturbation is achieved by performing the functional derivative $\delta/\delta f(t')$ around $f = 0$:

$$\left.\frac{\delta\langle B(t)\rangle}{\delta f(t')}\right|_{f=0} = \frac{\delta}{\delta f(t')}\int_{-\infty}^{\infty} dt' \Phi(t,t') f(t') = \Phi(t,t') \tag{6.7}$$

with the response function

$$\Phi(t,t') = -i\langle [B_I(t), A_I(t')]\rangle_0 \Theta(t-t') \tag{6.8}$$

In contrast to the QRT, this version of the FDT provides us only with the commutator expectation value. To obtain the anticommutator and to compare it to the QRT, a thermal state and a temperature dependent factor is necessary [37] that is singular in the zero temperature case. In addition, the temperature is not well-defined here, since we deal with a driven system.

6.4 Resonance fluorescence with coloured bath

We are investigating a two-level atom with frequency ω_A coupled to a radiation field with annihilation operators a_λ and creation operators a_λ^+. The coupling constants are denoted g_λ, and a driving laser with frequency ω_L and Rabi frequency ϵ is applied. The Hamilton operator in the frame rotating at the laser frequency ω_L is, making the rotating wave approximation ($\hbar = 1$),

$$\begin{aligned} H &= \frac{1}{2}\Delta_{AL}\sigma_z + \sum_\lambda \Delta_{\lambda L} a_\lambda^+ a_\lambda + \epsilon(\sigma_+ + \sigma_-) \\ &\quad + i\sum_\lambda g_\lambda (a_\lambda^+ \sigma_- - \sigma_+ a_\lambda) \end{aligned} \tag{6.9}$$

where the detunings are $\Delta_{AL} = \omega_A - \omega_L$, $\Delta_{\lambda L} = \omega_\lambda - \omega_L$. The Heisenberg equations of motion are

$$\dot{\sigma}_-(t) = -i\Delta_{AL}\sigma_-(t) + i\epsilon\sigma_z(t) + \sum_\lambda g_\lambda \sigma_z(t) a_\lambda(t) \tag{6.10}$$

$$\begin{aligned} \dot{\sigma}_z(t) &= -2i\epsilon\sigma_+(t) + 2i\epsilon\sigma_-(t) \\ &\quad -2\sum_\lambda g_\lambda (a_\lambda^+(t)\sigma_-(t) + \sigma_+(t)a_\lambda(t)) \end{aligned} \tag{6.11}$$

$$\dot{a}_\lambda(t) = -i\Delta_{\lambda L} a_\lambda(t) + g_\lambda \sigma_-(t) \tag{6.12}$$

with an analogous equation for $\sigma_+(t)$. The last equation is solved formally and substituted in the first two equations

$$\begin{aligned}
\dot{\sigma}_-(t) &= -i\Delta_{AL}\sigma_-(t) + i\epsilon\sigma_z(t) \\
&\quad + \sum_\lambda \int_0^t dt_1\, g_\lambda^2 \sigma_z(t)\sigma_-(t_1) e^{-i\Delta_{\lambda L}(t-t_1)} \\
&\quad + \sum_\lambda g_\lambda \sigma_z(t) a_\lambda(0) e^{-i\Delta_{\lambda L}t} \qquad (6.13) \\
\dot{\sigma}_z(t) &= -2i\epsilon\sigma_+(t) + 2i\epsilon\sigma_-(t) \\
&\quad - 2\sum_\lambda \int_0^t dt_1\, g_\lambda^2 \sigma_+(t_1)\sigma_-(t) e^{i\Delta_{\lambda L}(t-t_1)} \\
&\quad - 2\sum_\lambda g_\lambda a_\lambda^+(0)\sigma_-(t) e^{i\Delta_{\lambda L}t} \\
&\quad - 2\sum_\lambda \int_0^t dt_1\, g_\lambda^2 \sigma_+(t)\sigma_-(t_1) e^{-i\Delta_{\lambda L}(t-t_1)} \\
&\quad - 2\sum_\lambda g_\lambda \sigma_+(t) a_\lambda(0) e^{-i\Delta_{\lambda L}t} \qquad (6.14)
\end{aligned}$$

Weak driving Born approximation

In the integral terms of the foregoing equations, we are faced with products of system operators at different times. This highlights the nonlinearity of the equations that should be removed to get a closed system of equations. In this section, we use the evolution of the system alone, neglecting the coupling to the bath and the driving for a weak coupling Born approximation

$$\text{TC0}: \sigma_z(t) \approx \sigma_z(t_1), \quad \sigma_-(t) \approx e^{-i\Delta_{AL}(t-t_1)}\sigma_-(t_1), \quad t > t_1 \qquad (6.15)$$

from later to earlier times to get a time convolution (TC) integral. We will call this the TC0 approximation. It is also possible to use the opposite evolution for a time convolutionless (TCL) version of the equations, see Sec.6.7.2 below. An improved approximation is discussed in Sec.6.8. Defining the bath response at shifted frequencies $G_L(\tau) := \sum_\lambda g_\lambda^2 e^{-i\Delta_{\lambda L}\tau}$ and $G_A(\tau) := \sum_\lambda g_\lambda^2 e^{-i\Delta_{\lambda A}\tau}$, the expectation values with the photonic bath in

the vacuum state are

$$\begin{aligned}\langle\dot{\sigma}_-(t)\rangle &= -i\Delta_{AL}\langle\sigma_-(t)\rangle + i\epsilon\langle\sigma_z(t)\rangle \\ &\quad - \int_0^t dt_1\, G_L(t-t_1)\langle\sigma_-(t_1)\rangle \qquad (6.16)\\ \langle\dot{\sigma}_z(t)\rangle &= -2i\epsilon\langle\sigma_+(t)\rangle + 2i\epsilon\langle\sigma_-(t)\rangle \\ &\quad - \int_0^t dt_1\, (G_A(t-t_1) + G_A^*(t-t_1))\langle 1+\sigma_z(t_1)\rangle \qquad (6.17)\end{aligned}$$

where we used $a_\lambda(0)|0\rangle = 0$. The solution of these equations was given in chapter 5.

6.5 Spectrum via quantum regression theorem

In accordance with the quantum regression formula, for $t' = 0$ the correlation function can be found from the equations

$$\begin{aligned}\frac{d}{dt}\langle\sigma_+(t)\sigma_-(0)\rangle &= +i\Delta_{AL}\langle\sigma_+(t)\sigma_-(0)\rangle - i\epsilon\langle\sigma_z(t)\sigma_-(0)\rangle \\ &\quad - \int_0^t dt_1\, G_L^*(t-t_1)\langle\sigma_+(t_1)\sigma_-(0)\rangle \qquad (6.18)\\ \frac{d}{dt}\langle\sigma_z(t)\sigma_-(0)\rangle &= -2i\epsilon\langle\sigma_+(t)\sigma_-(0)\rangle + 2i\epsilon\langle\sigma_-(t)\sigma_-(0)\rangle \\ &\quad - \int_0^t dt_1\, (G_A(t-t_1) + G_A^*(t-t_1))\langle(1+\sigma_z(t_1))\sigma_-(0)\rangle \qquad (6.19)\end{aligned}$$

plus a similar equation for $\langle\sigma_-(t)\sigma_-(0)\rangle$, so we get a closed system for $\langle\sigma_+(t)\sigma_-(0)\rangle$, $\langle\sigma_z(t)\sigma_-(0)\rangle$, and $\langle\sigma_-(t)\sigma_-(0)\rangle$.

Stationary limit

The spectrum is proportional to the Fourier transform of the normally ordered dipole correlation function $\langle\sigma_+(t)\sigma_-(t')\rangle$ with respect to $t-t'$ in the stationary limit (i.e., both t and $t' \to \infty$). It will be sufficient to consider $t > t'$ [see eqs.(6.57, 6.58) below]. The initial conditions for the correlation functions are then fixed by stationary state expectation values

$\langle\sigma_+(t')\sigma_-(t')\rangle = \frac{1}{2}\langle 1+\sigma_z(t')\rangle$, $\langle\sigma_z(t')\sigma_-(t')\rangle = -\langle\sigma_-(t')\rangle$, $\langle\sigma_-(t')\sigma_-(t')\rangle = 0$. Since we now have $t' \neq 0$, additional terms must be added to the regression equations (6.18, 6.19). These happen to be zero for the normally ordered correlation in the weak-drive Born approximation (TC0), and eq.(6.18) still holds with $\sigma_-(0)$ replaced by $\sigma_-(t')$ everywhere. This is no longer true in the next-order (TC1 approximation), see Sec.6.8.

But if we consider the anti-normally ordered correlation $\langle\sigma_-(t')\sigma_+(t)\rangle$, a triple average containing, e.g., $\langle\sigma_-(t')a^+_\lambda(0)\sigma_z(t)\rangle$ occurs. So the commutator $[\sigma_-(t'), a^+_\lambda(0)]$ is required. Using the formal solution for the bath operator to make the operator $a_\lambda(t')$ appear and using the TC0 approximation, we find :

$$\begin{aligned}[\sigma_-(t'), a^+_\lambda(0)] &= [\sigma_-(t'), a^+_\lambda(t')]\, e^{-i\Delta_{\lambda L}t'} \\ &\quad -g_\lambda \int_0^{t'} dt_1\, e^{-i\Delta_{\lambda L}t_1}\,[\sigma_-(t'), \sigma_+(t_1)] \\ &= g_\lambda e^{-i\Delta_{AL}t'} \int_0^{t'} dt_1\, e^{-i\Delta_{\lambda A}t_1}\sigma_z(t_1) \qquad (6.20)\end{aligned}$$

The equation of motion for $\langle\sigma_-(t')\sigma_+(t)\rangle$ is then

$$\begin{aligned}\frac{d}{dt}\langle\sigma_-(t')\sigma_+(t)\rangle &= i\Delta_{AL}\langle\sigma_-(t')\sigma_+(t)\rangle - i\epsilon\langle\sigma_-(t')\sigma_z(t)\rangle \\ &\quad - \int_0^t dt_1\, G^*_L(t-t_1)\langle\sigma_-(t')\sigma_+(t_1)\rangle \\ &\quad + \int_0^{t'} dt_1\, G^*_L(t-t_1)e^{-i\Delta_{AL}(t'-t_1)}\langle\sigma_z(t_1)\sigma_z(t)\rangle \qquad (6.21)\end{aligned}$$

Note that the argument $t - t_1$ of the response function is positive over the integration range of the last line; this term therefore vanishes in the strict Markov limit. It is a "transient" that decays in the limit $t - t' \to \infty$.

6.6 Spectrum via fluctuation dissipation theorem

Instead of comparing the results of the QRT and FDT equations of motion, we compare the equations themselves. For the FDT approach

$$H = H_0 + H_1(t), \qquad H_1(t) = f(t)\sigma_- + f^*(t)\sigma_- \qquad (6.22)$$

where H_0 is the full system Hamilton operator eq.(6.9) and $f(t)$ an arbitrary complex function that vanishes for $t < 0$. We calculate the equations of motion for H and get an additional term $-if(t)\sigma_z(t)$ in the equation for $\sigma_+(t)$ and $2i(f(t)\sigma_-(t) - f^*(t)\sigma_+(t))$ in the equation for σ_z.

The linear response is obtained by taking the variational derivative $\frac{\delta\sigma(t)}{\delta f(t')}$ around $f(t) \equiv 0$, using $\frac{d}{dt}\frac{\delta\sigma(t)}{\delta f(t')} = \frac{\delta\dot{\sigma}(t)}{\delta f(t')}$. When setting $f(t) = f^*(t) = 0$, the terms containing $f^*(t)$ drop out. In the following, we use the shorthand notation

$$\sigma_{+,f}(t,t') := \left.\frac{\delta\sigma_+(t)}{\delta f(t')}\right|_{f=0} \tag{6.23}$$

and consider only $t \geq t'$. The averages $\langle\cdots\rangle$ are taken in the non-perturbed state ($f = 0$).

Applying the same procedure (the TC0 approximation) as above to reduce multi-time correlations to single-time averages, we get the equations of motion

$$\begin{aligned}
\frac{d}{dt}\langle\sigma_{+,f}(t,t')\rangle &= i\Delta_{AL}\langle\sigma_{+,f}(t,t')\rangle - i\epsilon\langle\sigma_{z,f}(t,t')\rangle \\
&\quad -i\delta(t-t')\langle\sigma_z(t)\rangle \\
&\quad -\int_0^t dt_1\langle\sigma_{+,f}(t_1,t')\rangle G_L^*(t-t_1) \qquad (6.24)\\
\frac{d}{dt}\langle\sigma_{z,f}(t,t')\rangle &= -2i\epsilon(\langle\sigma_{+,f}(t,t')\rangle - \langle\sigma_{-,f}(t,t')\rangle) \\
&\quad +2i\delta(t-t')\langle\sigma_-(t)\rangle \\
&\quad -2\int_0^t dt_1\langle\sigma_{z,f}(t_1,t')\rangle(G_A^*(t-t_1) + G_A(t-t_1)) \qquad (6.25)
\end{aligned}$$

With the fluctuation dissipation theorem $\langle\sigma_{+,f}(t,t')\rangle = -i\langle[\sigma_+(t),\sigma_-(t')]\rangle$ at the time $t = t'$, the initial conditions are

$$\begin{aligned}
\langle\sigma_{+,f}(t',t')\rangle &= -i\langle[\sigma_+(t'),\sigma_-(t')]\rangle = -i\langle\sigma_z(t')\rangle \qquad (6.26)\\
\langle\sigma_{z,f}(t',t')\rangle &= -i\langle[\sigma_z(t'),\sigma_-(t')]\rangle = 2i\langle\sigma_-(t')\rangle \qquad (6.27)\\
\langle\sigma_{-,f}(t',t')\rangle &= -i\langle[\sigma_-(t'),\sigma_-(t')]\rangle = 0 \qquad (6.28)
\end{aligned}$$

The terms containing $\delta(t-t')$ in Eqs.(6.24, 6.25) produce a jump of the response functions. This jump is of the same amount as the initial condition (6.26–6.28). Since we assign the initial value right after the jump, this implies that the solution before the jump is zero. This is consistent with eq. (6.8).

Born approximation including perturbation

One could argue that in the FDT approach instead of eq. (14) one has to include the solution containing $f(t)$. The approximation to keep or discard the term is independent of the weak coupling approximation.

Let us take a careful look at the equation of motion including the perturbation $H_1(t) = f(t)\sigma_- + f^*(t)\sigma_+$. Recalling eq.(6.13), we have without any approximations

$$\begin{aligned}\dot{\sigma}_+(t) &= i\Delta_{AL}\sigma_-(t) - i\epsilon\sigma_z(t) - if(t)\sigma_z(t) \\ &\quad + \int_0^t dt_1\, G_L^*(t-t_1)\sigma_+(t_1)\sigma_z(t) \\ &\quad + \sum_\lambda g_\lambda a_\lambda^+(0)\sigma_z(t)e^{i\Delta_{\lambda L}t} \qquad (6.29)\end{aligned}$$

where the sum over the bath modes has been performed in the memory integral. The last term vanishes when taking the expectation value (initial vacuum state for the bath).

When we now "pull back" the operator $\sigma_z(t)$ under the integral to the earlier time t_1, we have to take into account the perturbation $H_1(t)$ in the equations of motion (weak-drive Born approximation)

$$\dot{\sigma}_-(t) \approx -i\Delta_{AL}\sigma_-(t) + if^*(t)\sigma_z(t) \qquad (6.30)$$

$$\dot{\sigma}_+(t) \approx i\Delta_{AL}\sigma_+(t) - if(t)\sigma_z(t) \qquad (6.31)$$

$$\dot{\sigma}_z(t) \approx 2i(f(t)\sigma_-(t) - f^*(t)\sigma_+(t)) \qquad (6.32)$$

with initial conditions at t_1. The solution is up to linear order in $f(t), f^*(t)$ is

$$\begin{aligned}\sigma_-(t) &\approx e^{-i\Delta_{AL}(t-t_1)}\sigma_-(t_1) \qquad (6.33)\\ &\quad + i\int_{t_1}^t dt'\, e^{-i\Delta_{AL}(t-t')}f^*(t')\sigma_z(t_1)\end{aligned}$$

$$\begin{aligned}\sigma_+(t) &\approx e^{i\Delta_{AL}(t-t_1)}\sigma_+(t_1) \\ &\quad - i\int_{t_1}^t dt'\, e^{i\Delta_{AL}(t-t')}f(t')\sigma_z(t_1) \qquad (6.34)\end{aligned}$$

$$\sigma_z(t) \approx \sigma_z(t_1) + 2i\int_{t_1}^t dt' f(t')\sigma_-(t_1)e^{i\Delta_{AL}(t'-t_1)} \qquad (6.35)$$

Inserting eq.(6.35) into the memory integral, we get

$$\begin{aligned}
&\int_0^t dt_1\, G_L^*(t-t_1)\sigma_+(t_1)\sigma_z(t) \\
&\approx \int_0^t dt_1\, G_L^*(t-t_1)\Big[-\sigma_+(t_1) \\
&\qquad\qquad +i\int_{t_1}^t dt_2 f(t_2)(1+\sigma_z(t_1))e^{-i\Delta_{AL}(t_2-t_1)}\Big] \qquad (6.36)
\end{aligned}$$

At this stage, we are ready for the functional derivative with respect to $f(t')$. Combining Eqs.(6.29, 6.36) yields for the response function the (approximate) equation of motion

$$\begin{aligned}
\frac{d}{dt}\langle\sigma_{+,f}(t,t')\rangle &= i\Delta_{AL}\langle\sigma_{-,f}(t,t')\rangle - i\epsilon\langle\sigma_{z,f}(t,t')\rangle \\
&\quad -i\delta(t-t')\langle\sigma_z(t')\rangle \\
&\quad -\int_{t'}^t dt_1\, G_L^*(t-t_1)\langle\sigma_{+,f}(t_1,t')\rangle \\
&\quad +i\int_0^{t'} dt_1\, G_L^*(t-t_1)e^{-i\Delta_{AL}(t'-t_1)}\langle 1+\sigma_z(t_1)\rangle
\end{aligned}$$

Note the lower limit of the first integral, the quantity $\langle\sigma_{+,f}(t_1,t')\rangle$ being zero for $t_1 < t'$. The second term is a transient that does not appear in eq.(6.16) for the one-time average. This integral covers again only $0 < t_1 < t'$ and the response function $G_L^*(t-t_1)$ makes it vanish for $t - t' \to \infty$.

The same argument can be worked out for the response of the other observables: with transient terms appearing in some places. We compare to the regression approach in the following Section.

6.7 Comparison of the different approaches

6.7.1 Regression vs FDT

We compare the equations of motion for correlation functions in the form of commutators as calculated in the previous sections. First of all, the homogenous parts of the equations are identical for the regression approach and in linear response, apart from the memory integrals that start at $t_1 = 0$ for

quantum regression [eq.(6.21)] at $t_1 = t'$ in linear response [eq.(6.37)]. In addition, the transient terms look different. The extra term from the regression formula eq.(6.21) yields

$$\begin{aligned}
&\frac{d}{dt}\langle[\sigma_+(t),\sigma_-(t')]\rangle\Big|_{\rm tr1} \\
&= -\int_0^{t'} dt_1\, G_L^*(t-t_1)e^{-i\Delta_{AL}(t'-t_1)}\langle\sigma_z(t_1)\sigma_z(t)\rangle
\end{aligned} \tag{6.37}$$

The memory term of the regression formula (6.18) may be split in two integrals below and above t'. This gives a second transient term to be added to eq.(6.37),

$$\begin{aligned}
&-\int_0^{t'} dt_1\, G_L^*(t-t_1)\langle[\sigma_+(t_1),\sigma_-(t')]\rangle \\
&\approx -\int_0^{t'} dt_1\, G_L^*(t-t_1)\, e^{-i\Delta_{AL}(t'-t_1)}\langle\sigma_z(t_1)\rangle
\end{aligned} \tag{6.38}$$

in the TC0 approximation. On the other hand from linear response eq.(6.37) we have

$$\begin{aligned}
&i\,\frac{d}{dt}\langle\sigma_{+,f}(t,t')\rangle\Big|_{\rm tr} \\
&= -\int_0^{t'} dt_1\, G_L^*(t-t_1)e^{-i\Delta_{AL}(t'-t_1)}\langle 1+\sigma_z(t_1)\rangle
\end{aligned} \tag{6.39}$$

Within the accuracy of the weak-drive approximation, it is consistent to shift the σ_z operators in time. Doing this with $\sigma_z(t)$, the sum of Eqs.(6.37, 6.38) simplifies to the linear response result eq.(6.39).

It is interesting to see that (i) the correction to the regression equations takes a similar form as for master equations with non-factorizing initial conditions (a transient forcing dependent on one-time averages that dies out after the first time argument t'), see, e.g., Ref.[39]. And (ii) that the transient terms come out in the same form from the linear response analysis although they arise technically in different places (FD: pull back under the memory integral, QR: non-commuting system and bath operators).

6.7.2 Convolutionless formulation

De Vega and Alonso treat a similar problem in [36, 40]. We compare their results with ours, in the $\epsilon = 0$ case for consistency with the TC0 approximation:

$$\begin{aligned}
\frac{d}{dt}\langle\sigma_+(t)\sigma_-(t')\rangle &= i\Delta_{AL}\langle\sigma_+(t)\sigma_-(t')\rangle \\
&\quad - \int_0^t dt_1 G_A^*(t-t_1)\langle\sigma_+(t)\sigma_-(t')\rangle \qquad (6.40)\\
\frac{d}{dt}\langle\sigma_-(t')\sigma_+(t)\rangle &= i\Delta_{AL}\langle\sigma_-(t')\sigma_+(t)\rangle \\
&\quad - \int_0^t dt_1 G_A^*(t-t_1)\langle\sigma_-(t')\sigma_+(t)\rangle \\
&\quad + \int_0^{t'} dt_1 G_L^*(t-t_1)e^{-i\Delta_{AL}(t'-t_1)}\langle\sigma_z(t')\sigma_z(t)\rangle \qquad (6.41)
\end{aligned}$$

Since these equations do not contain convolutions, it is more appropriate to compare them to the convolution-less version of the QR equations. The latter are derived by using in eq. (6.13) and eq. (6.14) the "forward pull" (this could be called TCL0 approximation)

$$\sigma_z(t_1) \approx \sigma_z(t), \quad \sigma_-(t_1) \approx e^{-i\Delta_{AL}(t_1-t)}\sigma_-(t), \quad t_1 < t \qquad (6.42)$$

instead of eqs. (6.15). We then find that equations (6.18, 6.19) of our approach yield eqs. (6.40, 6.41). The last term in eq.(6.41) is produced by the transient correction that was worked out before, due to the nonzero commutator $[a_\lambda^\dagger(0), \sigma_-(t')]$. The only difference is therefore whether the equations contain convolutions or are written in convolution-less form.

6.8 Beyond weak driving

The previous argument can be generalized to moderate driving where the Rabi frequency ϵ is not small. More precisely, instead of eqs. (6.15), we include the pumping laser and solve

$$\begin{aligned}
\dot\sigma_-(t) &\approx -i\Delta_{AL}\sigma_-(t) + i\epsilon\sigma_z(t) \qquad (6.43)\\
\dot\sigma_z(t) &\approx -2i\epsilon\sigma_+(t) + 2i\epsilon\sigma_-(t) \qquad (6.44)
\end{aligned}$$

for pulling back the system operators and removing the nonlinearity. The resulting Bloch equations contain the bath response at shifted frequencies $G_{\pm\Omega}(\tau) = G_L(\tau)\,\mathrm{e}^{\pm i\Omega\tau}$ where $\Omega = \sqrt{\Delta_{AL}^2 + 4\epsilon^2}$ is the generalized Rabi frequency. In this way, we take into account the change in the bath spectral density across the Mollow sidebands.

The programme of the previous sections can be carried out as before to calculate the equations of motion for correlation and response functions. Without entering into the details, we find that the homogeneous part of the regression equations (all except the last lines of eqs.(6.18, 6.19)) is equal to the result of the fluctuation dissipation theorem. The remaining parts (the transient terms) are discussed in more detail here.

6.8.1 Linear response

In linear response, eq.(6.29) for $\sigma_+(t)$ can serve again as a starting point. We handle the correlation $\sigma_+(t_1)\sigma_z(t)$ under the integral in the spirit of a time-convolution approach and pull back the operator $\sigma_z(t)$ to the earlier time t_1. With the approximation that the system Hamiltonian H_S alone is sufficient here, this pull-back map is linear and can be written in the form

$$\sigma_z(t) = \sum_a R_{za}(t, t_1; f)\sigma_a(t_1), \qquad a = \pm, z \tag{6.45}$$

where $R_{za}(t, t_1; f)$ is a reminder that this depends on the perturbation $f(t')$ for $t > t' > t_1$. With the shorthand

$$\sigma_{+a}(t_1) = \sigma_+(t_1)\sigma_a(t_1) \tag{6.46}$$

for the operator product, the functional derivative becomes

$$\begin{aligned}\frac{\delta}{\delta f(t')}\left[\sigma_+(t_1)\sigma_z(t)\right] &= R_{za}(t - t_1)\sigma_{+a,f}(t_1, t') \\ &\quad - i\sigma_+(t_1)[\sigma_z(t), \sigma_-(t')]\Theta(t > t' > t_1)\end{aligned} \tag{6.47}$$

where $R_{za}(t-t_1)$ corresponds to the non-perturbed time evolution, given by eqs.(6.43,6.44). Its solution with initial conditions at t_1,

$$\begin{aligned}\sigma_z(t) &= \frac{1}{\Omega^2}\Big[\left(\Delta_{AL}^2+2\epsilon^2\,e^{-i\Omega(t-t_1)}+2\epsilon^2\,e^{i\Omega(t-t_1)}\right)\sigma_z(t_1)\\ &+\epsilon\left(2\Delta_{AL}-(\Delta_{AL}-\Omega)\,e^{-i\Omega(t-t_1)}-(\Delta_{AL}+\Omega)\,e^{i\Omega(t-t_1)}\right)\sigma_+(t_1)\\ &+\epsilon\left(2\Delta_{AL}-(\Delta_{AL}+\Omega)\,e^{-i\Omega(t-t_1)}-(\Delta_{AL}-\Omega)\,e^{i\Omega(t-t_1)}\right)\sigma_-(t_1)\Big]\end{aligned} \tag{6.48}$$

yields the matrix elements $R_{za}(t-t_1)$. In the second term in eq.(6.47), we have used the Kubo formula (6.8) for the conservative system defined by H_S to evaluate the linear response $\delta R_{za}(t,t_1;f)/\delta f(t')|_{f=0}$. The notation $\Theta(t>t'>t_1)$ is a square function with value unity as long as the double inequality holds.

The first line of eq.(6.47) gives the memory integral of the homogeneous part in the equations of motion. The second line yields the transient term

$$\begin{aligned} & i\,\frac{d}{dt}\langle\sigma_{+,f}(t,t')\rangle\Big|_{\rm tr}\\ &= \int_0^{t'} dt_1 G_L^*(t-t_1)\langle\sigma_+(t_1)[\sigma_z(t),\sigma_-(t')]\rangle\end{aligned} \tag{6.49}$$

The commutator must be evaluated with the non-perturbed system dynamics, using $R_{za}(t-t')$ instead of the pull back map eq.(6.45).

6.8.2 Quantum regression

In the regression method, the operator pullback is based only on the matrix with elements $R_{za}(t-t_1)$. Considering the commutator $\langle[\sigma_+(t),\sigma_-(t')]\rangle$, the memory term in its equation of motion reads

$$\int_0^t dt_1 G_L^*(t-t_1)\sum_a R_{za}(t-t_1)\langle[\sigma_{+a}(t_1),\sigma_-(t')]\rangle. \tag{6.50}$$

Note that now the time 0 remains the lower integration limit.

The comparison to the transient term of the fluctuation-dissipation approach is easier if we do not perform explicitly the pullback. The integration

range $0 < t_1 < t'$ does not appear in the linear response equations and can therefore be identified as a transient. Restoring the operator $\sigma_z(t)$, this piece of eq.(6.50) gives

$$\begin{aligned} &\text{transient 1 :} \\ &\int_0^{t'} dt_1 G_L^*(t-t_1)\langle[\sigma_+(t_1)\sigma_z(t),\sigma_-(t')]\rangle \end{aligned} \tag{6.51}$$

Other transient terms arise from eq.(6.20), because of a nonzero commutator with the initial field operator $a_\lambda^\dagger(0)$. Putting the two together, we have

$$\begin{aligned} &\text{transient 1+2 :} \\ &\int_0^{t'} dt_1 G_L^*(t-t_1)\,\langle[\sigma_+(t_1)\sigma_z(t),\sigma_-(t')] + [\sigma_-(t'),\sigma_+(t_1)]\sigma_z(t)\rangle \end{aligned}$$

$$\frac{d}{dt}\langle[\sigma_+(t),\sigma_-(t')]\rangle\Big|_{\rm tr} = \int_0^{t'} dt_1 G_L^*(t-t_1)\,\langle\sigma_+(t_1)[\sigma_z(t),\sigma_-(t')]\rangle \tag{6.52}$$

This is precisely the transient term found in linear response, eq.(6.49).

For completeness, we discuss briefly the regression equations for normally ordered correlations. The memory integral for the correlation $\langle\sigma_+(t)\sigma_-(t')\rangle$ is given by eq.(6.50) with the commutator under the integral replaced by the operator product. In the TC1 approximation, the memory integral involves the Green functions $G_{\pm\Omega}(\tau)$ [defined after eq.(6.44)], as can be seen from eq.(6.48). The correlation function is coupled to $\langle\sigma_a(t)\sigma_-(t')\rangle$ $(a = z, -)$ whose equation of motion contains additional, transient terms. These arise from the commutator $[a_\lambda(0),\sigma_-(t')]$ which becomes, by analogy to eq.(6.20)

$$\begin{aligned} &[a_\lambda(0),\sigma_-(t')] = \\ &-g_\lambda\int_0^{t'} dt_1\, e^{i\Delta_{\lambda L}t_1}\,\{2R_{-z}(t'-t_1)\sigma_-(t_1) - R_{-+}(t'-t_1)\sigma_z(t_1)\} \end{aligned} \tag{6.53}$$

This is written in the spirit of a convolution integral, the matrix elements $R_{-a}(t'-t_1)$ $(a = z, +)$ providing the pullback of the operator $\sigma_-(t')$ to the earlier time t_1. As an example, we give here one equation of motion that

features transient terms in the TC1 approximation

$$\begin{aligned}\frac{d}{dt}\langle\sigma_z(t)\sigma_-(t')\rangle &= -2i\epsilon\left(\langle\sigma_+(t)\sigma_-(t')\rangle - \langle\sigma_-(t)\sigma_-(t')\rangle\right) \\ &\quad -\frac{1}{2\Omega^2}\int_0^t dt_1\Bigg[\Big(\tfrac{1}{2}(\Delta_{AL}+\Omega)^2\left(G_\Omega(t-t_1)+G^*_\Omega(t-t_1)\right) \\ &\quad +4\epsilon^2\left(G_L(t-t_1)+G^*_L(t-t_1)\right) \\ &\quad +\tfrac{1}{2}(\Delta_{AL}-\Omega)^2\left(G_{-\Omega}(t-t_1)+G^*_{-\Omega}(t-t_1)\right)\Big) \\ &\quad \tfrac{1}{2}\langle(1+\sigma_z(t_1))\,\sigma_-(t')\rangle \\ &\quad -2\epsilon\Big((-\Delta_{AL}-\Omega)G^*_\Omega(t-t_1)+2\Delta_{AL}G^*_L(t-t_1) \\ &\quad +(-\Delta_{AL}+\Omega)G^*_{-\Omega}(t-t_1)\Big)\langle\sigma_+(t_1)\sigma_-(t')\rangle \\ &\quad -2\epsilon\Big((-\Delta_{AL}-\Omega)G_\Omega(t-t_1)+2\Delta_{AL}G_L(t-t_1) \\ &\quad +(-\Delta_{AL}+\Omega)G_{-\Omega}(t-t_1)\Big)\langle\sigma_-(t_1)\sigma_-(t')\rangle\Bigg] \\ &\quad +\int_0^{t'} dt_1 G_L(t-t_1)\langle(1+\sigma_z(t_1))\sigma_-(t')\rangle \end{aligned} \tag{6.54}$$

Compared to the TC0 version eq.(6.19), this equation contains the Green function at shifted frequencies and a transient term.

6.9 Numerical results

6.9.1 Emission spectrum

The spectrum of the atomic dipole is defined as the Fourier transform of the normally ordered dipole autocorrelation

$$S_d(\omega) = \lim_{t'\to\infty}\int_{-\infty}^{\infty} \mathrm{d}\tau\langle\sigma_+(t'+\tau)\sigma_-(t')\rangle\,\mathrm{e}^{-\mathrm{i}\omega\tau} \tag{6.55}$$

Assuming that the correlation function becomes stationary, we have

$$\langle\sigma_+(t'-\tau)\sigma_-(t')\rangle = \langle\sigma_+(t')\sigma_-(t'+\tau)\rangle = \langle\sigma_+(t'+\tau)\sigma_-(t')\rangle^* \tag{6.56}$$

so that eq.(6.55) assumes the form of a Laplace transform

$$S_d(\omega) = 2\,\mathrm{Re}\,\sigma_{+-}(s \to i\omega) \tag{6.57}$$

$$\sigma_{+-}(s) = \lim_{t'\to\infty} \int_0^\infty \mathrm{d}\tau\, \mathrm{e}^{-s\tau} \langle \sigma_+(t'+\tau)\sigma_-(t')\rangle \tag{6.58}$$

One can show that this definition must be multiplied with the photonic mode density to get the photon emission rate at frequency ω [41]. This definition is used in Fig.6.1. Note that the Laplace variable s approaches the imaginary axis from the right half-plane (positive real part).

6.9.2 Laplace transformation

The equations can be solved by a Laplace transformation when the transient terms are neglected. The bath correlation functions $G_L(\tau)$, $G_L^*(\tau)$, have Laplace transforms (denoted with square bracket around the argument)

$$G_L[s] = \alpha\sqrt{is - \Delta_{eL}}, \qquad G_L^*[s] = -i\alpha\sqrt{is + \Delta_{eL}} \tag{6.59}$$

for a photonic crystal with a three-dimensional anisotropic dispersion relation and a band edge frequency $\omega_e = \omega_L + \Delta_{eL}$ [42]. The strength of the coupling to the photonic band is parametrized by α with dimension [frequency]$^{1/2}$.

When the equations for the two-time correlation functions are solved by a Laplace transformation, the initial conditions should be imposed at equal times $t = t'$ in equilibrium, but not at $t = 0$, where the bath is in the vacuum state. As an example, we consider the following equation (from the TC0 approximation):

$$\begin{aligned}\frac{d}{dt}\langle \sigma_+(t)\sigma_-(t')\rangle &= +i\Delta_{AL}\langle \sigma_+(t)\sigma_-(t')\rangle - i\epsilon\langle \sigma_z(t)\sigma_-(t')\rangle \\ &\quad - \int_0^t dt_1\, G_L^*(t-t_1)\langle \sigma_+(t_1)\sigma_-(t')\rangle \end{aligned} \tag{6.60}$$

We neglect the lower integration range $0 < t_1 < t'$ and change to the time difference $\tau = t_1 - t'$:

$$\begin{aligned}&\int_0^t dt_1\, G_L^*(t-t_1)\langle \sigma_+(t_1)\sigma_-(t')\rangle \\ &\approx \int_0^{t-t'} d\tau\, G_L^*(t-t'-\tau)\langle \sigma_+(t'+\tau)\sigma_-(t')\rangle \end{aligned} \tag{6.61}$$

which is a convolution integral. Furthermore

$$\frac{d}{dt}\langle\sigma_+(t)\sigma_-(t')\rangle = \frac{d}{d\tau}\langle\sigma_+(t'+\tau)\sigma_-(t')\rangle \tag{6.62}$$

Applying the Laplace transformation $\int_0^\infty d\tau\, e^{-s\tau}$ yields

$$\begin{aligned} & s\,\sigma_{+-}(s) - \langle\sigma_+(t')\sigma_-(t')\rangle|_{t'\to\infty} \\ & = i\Delta_{AL}\sigma_{+-}(s) - i\epsilon\,\sigma_{z-}(s) - G_L^*[s]\sigma_{+-}(s) \end{aligned} \tag{6.63}$$

where the notation $\sigma_{a-}(s)$ $(a = \pm, z)$ is a defined by generalizing eq.(6.58). Similar algebraic equations are obtained for $\sigma_{z-}(s)$ and $\sigma_{--}(s)$. The analytic continuation of $\sigma_{+-}(s)$ to $s = i\omega$ gives the dipole spectrum (6.57).

In the TC1 approximation, the memory terms are more involved compared to eq.(6.60), see eq.(6.54) in Sec.6.8.2. The transient terms arising there must be neglected to apply the Laplace technique.

In Fig.6.1, the parameters are chosen such that the left peak lies close to the band edge. It is suppressed relative to the central and right peaks only in the low-order approximation TC0, however. In the following order, the symmetry of the spectrum is nearly fully restored.

The response function of the driven two-level system is illustrated in Fig.6.2 where the imaginary part of its Fourier transform $\Phi(\omega)$ is plotted for different laser frequencies. The absorption on the red sideband for blue detuning and on the blue sideband for red detuning can be explained from the dressed levels and happens already for a flat continuum (thin gray lines). The TC1 approximation gives less absorption on the red sideband (more on the blue one), compared to a flat band (light gray lines) because of the asymmetric spectral density. We note that the linear absorption spectrum is more regular than the normally ordered emission spectrum within the TC1 approximation: the latter would diverge and be negative at the detuning corresponding to the lower thick spectrum in Fig.6.2.

6.10 Remarks

We have seen that the limited validity of the quantum regression formula can be healed by considering transient terms that appear from a careful treatment of the operator ordering. The same transient terms are also provided by the fluctuation dissipation theorem. De Vega and Alonso [36, 40] treat the

problem with a coherent state approach. The time-convolutionless version of our equations is identical to their modified version of the quantum regression approach.

Lee and Lai use a Fourier transformation approach for the problem [43]. They do not adress the operator ordering problem that delivered the transient terms in our derivation of the QRT equations. These extra terms also appear in the correlations of a Brownian particle (damped oscillator), see the book [6]. To bring the nonlinear Bloch equations into linear form, Lee and Lai work in the low-order approximation only (called TC0 here). Fig.6.1 illustrates that this can lead to qualitative differences in the symmetry of the spectrum compared to the next order TC1.

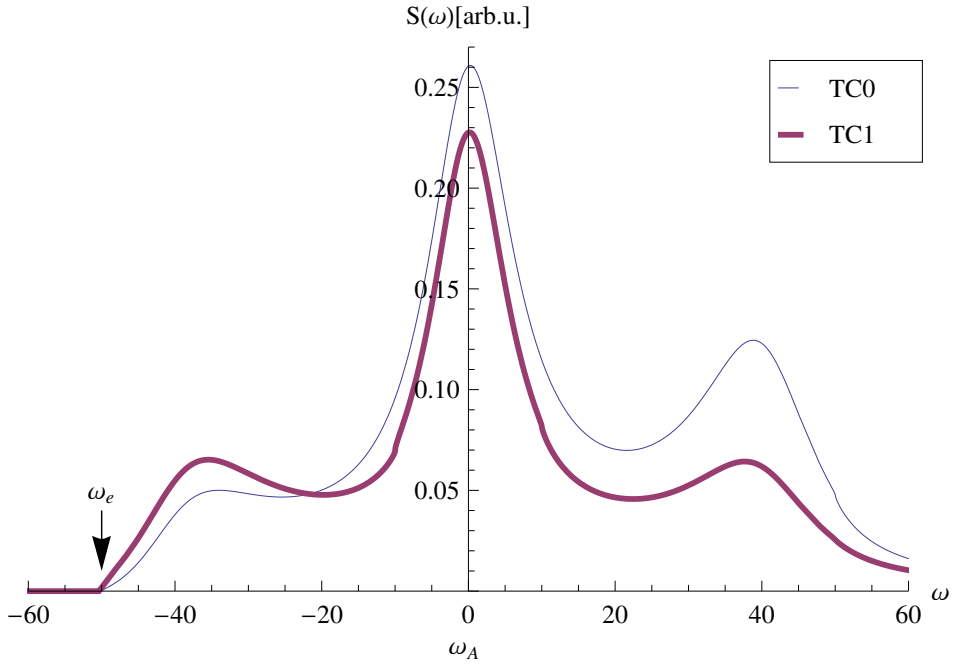

Figure 6.1: Mollow spectrum for resonant driving. Thin line: weak-drive approximation (called TC0 in the main text); thick line: approximation TC1. We plot the spectrum defined in eq.(6.57) multiplied with the spectral density: $S(\omega) = S_d(\omega)\,\mathrm{Re}\,G_L^*[i\omega]$, as appropriate for the photon emission rate per unit bandwidth.
Parameters: $\Delta_{AL} = 0$ and $\omega_A - \omega_e = 50\,\alpha^2$, $\epsilon = 20\,\alpha^2$. Fermi's Golden Rule predicts a linewidth in the TC0 approximation of $\mathrm{Re}\,G_L[s \to 0] = \alpha\sqrt{\omega_A - \omega_e} = \sqrt{50}\,\alpha^2 = \mathrm{Re}\,G_A[s \to 0]$. Applying TC1, the asymmetry of the spectral density appears already at the level of the Golden Rule: carrier linewidth $\mathrm{Re}\,G_L[s \to 0] = \sqrt{50}\,\alpha^2$, sidebands $\mathrm{Re}\,G_{\pm\Omega}[s \to 0] = \alpha\,\mathrm{Re}\sqrt{\pm\Omega + \omega_A - \omega_e} = \{\sqrt{90}, \sqrt{10}\}\alpha^2$.

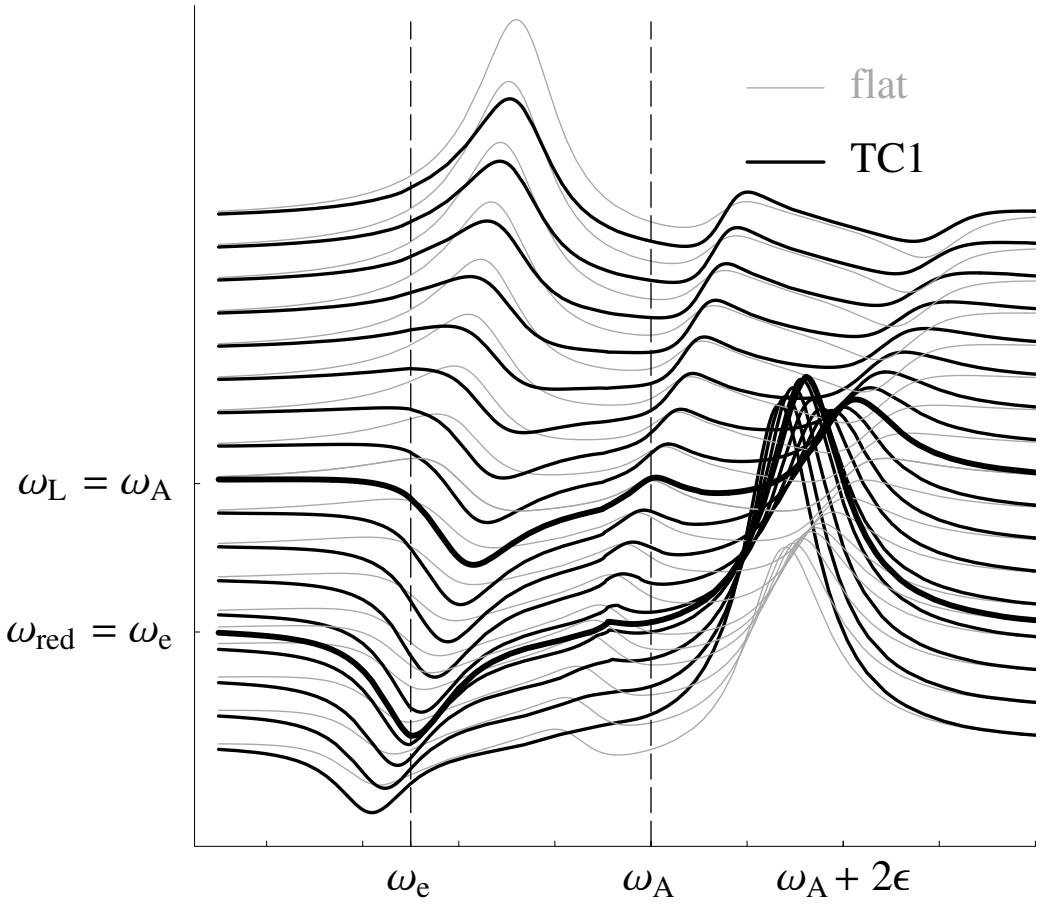

Figure 6.2: Linear absorption spectrum calculated from the commutator $-\mathrm{i}[\sigma^\dagger(t'), \sigma(t)]$ ($t \geq t'$, response function), for different laser frequencies. The spectra are shifted vertically for better viewing. The upper thick line corresponds to resonant driving ($\omega_L = \omega_A$); for the lower one, $\omega_L = \omega_A - 0.45\,\epsilon$: the red sideband in the Mollow triplet is located at the band edge, $\omega_L - \Omega = \omega_e$. Parameters: as in Fig.6.1; from bottom to top, the laser frequency ω_L increases in steps of $0.1\,\epsilon$ from $\omega_A - 0.8\,\epsilon$ to $\omega_A + 0.8\,\epsilon$. Thin gray lines: flat spectral density, fixed to the value at ω_A, thick black lines: photonic band with lower edge $\omega_e = \omega_A - 2.5\,\epsilon$, calculated with the TC1 approximation. On resonance, the decay rate is $\mathrm{Re}\, G_A[0] = (1/\sqrt{8})\,\epsilon \approx 0.35\,\epsilon$.

6.11 Dependence on the parameters - numerical examples

On the following pages we present some illustrative examples of the spectrum $S(\omega) = S_d(\omega)\,\mathrm{Re}\,G_L^*[i\omega]$ with different parameter values. Each example is calculated for the TC0 as well as for the TC1 approximation. The thin, blue line is the result for TC0, the thick, purple line for TC1.

Distance from bandgap $\omega_A - \omega_e$

If the bandgap is far away and the atom frequency deep in the band, the density of states becomes nearly flat and the spectrum looks similar to the Mollow triplet.

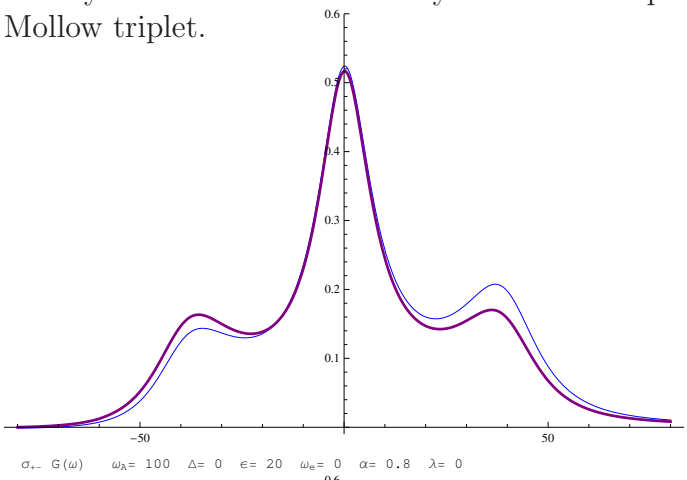

Figure 6.3: $S(\omega)$, $\omega_A = \omega_L = 100$, $\omega_e = 0$, $\epsilon = 20$,$\alpha = 0.8$, $\lambda = 0$

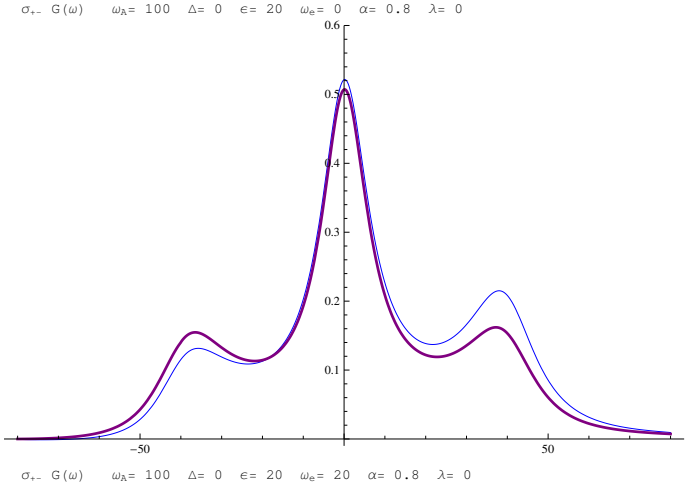

Figure 6.4: $S(\omega)$, $\omega_A = \omega_L = 100$, $\omega_e = 20$, $\epsilon = 20$,$\alpha = 0.8$, $\lambda = 0$

With decreasing distance $\omega_A - \omega_e$, the left peak becomes more supressed. This effect is stronger for TC0 than for TC1.

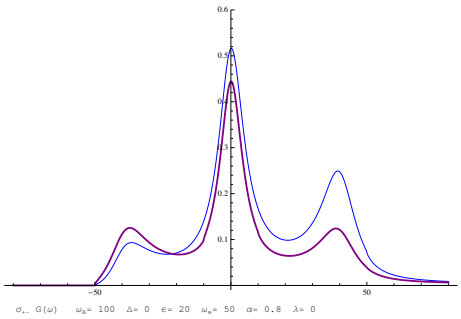

Figure 6.5: $S(\omega)$, $\omega_A = \omega_L = 100$, $\omega_e = 50$, $\epsilon = 20$, $\alpha = 0.8$, $\lambda = 0$

With one sideband in the gap, even negative peaks appear in the TC1 solution. That may be a signal that the parameters are out of the range of validity of the performed approximations.

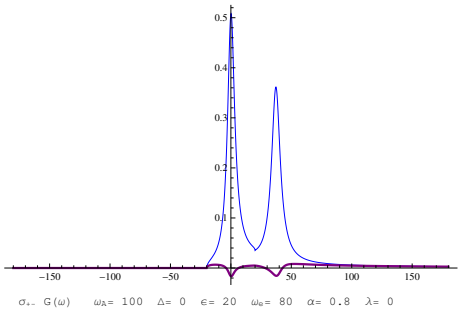

Figure 6.6: $S(\omega)$, $\omega_A = \omega_L = 100$, $\omega_e = 80$, $\epsilon = 20$, $\alpha = 0.8$, $\lambda = 0$

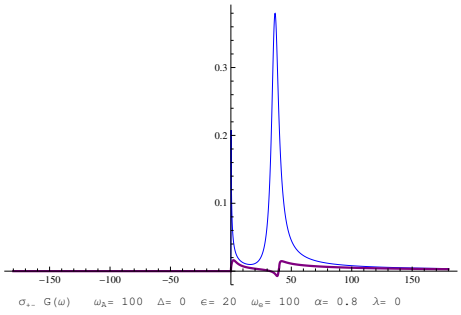

Figure 6.7: $S(\omega)$, $\omega_A = \omega_L = 100$, $\omega_e = 100$, $\epsilon = 20$, $\alpha = 0.8$, $\lambda = 0$

For ω_A in the bandgap, in TC0 the steady state values of the one-time expectation values are not independent of the initial values. In contrast to this, in TC1 there is a unique stationary state.

Changing the Rabi frequency ϵ

Stronger driving causes the side peaks to move apart.

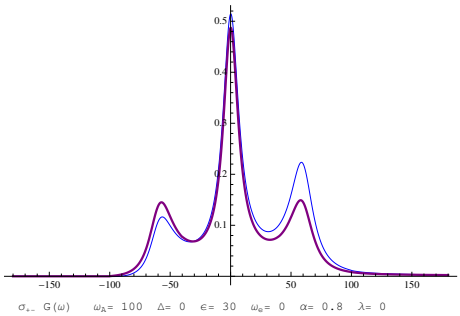

Figure 6.8: $S(\omega)$, $\omega_A = \omega_L = 100$, $\omega_e = 0$, $\epsilon = 30$, $\alpha = 0.8$, $\lambda = 0$

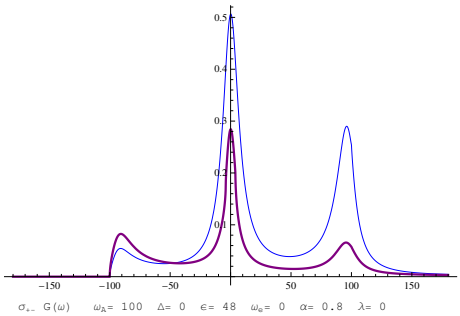

Figure 6.9: $S(\omega)$, $\omega_A = \omega_L = 100$, $\omega_e = 0$, $\epsilon = 48$, $\alpha = 0.8$, $\lambda = 0$

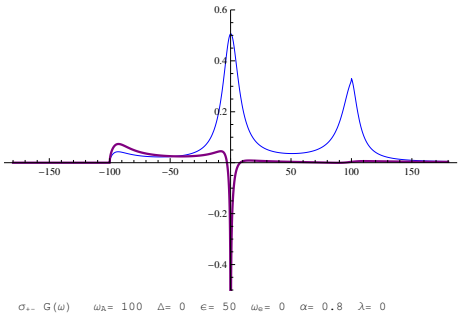

Figure 6.10: $S(\omega)$, $\omega_A = \omega_L = 100$, $\omega_e = 0$, $\epsilon = 50$, $\alpha = 0.8$, $\lambda = 0$

When the side peak is in the gap, similar effects occur like for making smaller $\omega_A - \omega_e$. For stronger Rabi frequency, the TC0 solution appears to be more physical than the TC1 solution, that has a negative middle peak.

Cut-off parameter

Not only the density of states at the band-edge is relevant. Indeed, the cut-off parameter plays an important role. We use a cut-off function $e^{-\lambda(\omega-\omega_e)^2}$. For increasing cut-off parameter, the right peak disappears for the TC0 solution. For the TC1 solution, the intensity is lowered on all three peaks.

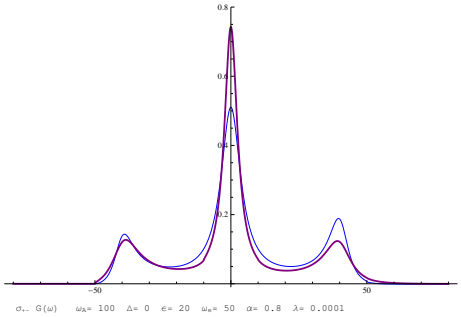

Figure 6.11: $S(\omega)$, $\omega_A = \omega_L = 100$, $\omega_e = 50$, $\epsilon = 20$, $\alpha = 0.8$, $\lambda = 0.0001$

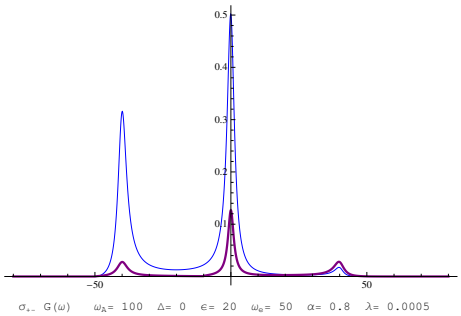

Figure 6.12: $S(\omega)$, $\omega_A = \omega_L = 100$, $\omega_e = 50$, $\epsilon = 20$, $\alpha = 0.8$, $\lambda = 0.0005$

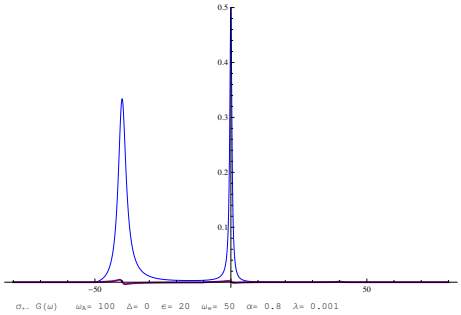

Figure 6.13: $S(\omega)$, $\omega_A = \omega_L = 100$, $\omega_e = 50$, $\epsilon = 20$, $\alpha = 0.8$, $\lambda = 0.001$

Increasing coupling constant α

Decreasing the coupling constant sharpens the peak. For small α, the result is quite similar for TC0 and TC1.

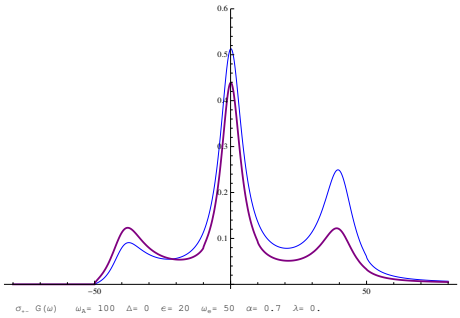

Figure 6.14: $S(\omega)$, $\omega_A = \omega_L = 100$, $\omega_e = 50$, $\epsilon = 20$, $\alpha = 0.7$, $\lambda = 0$

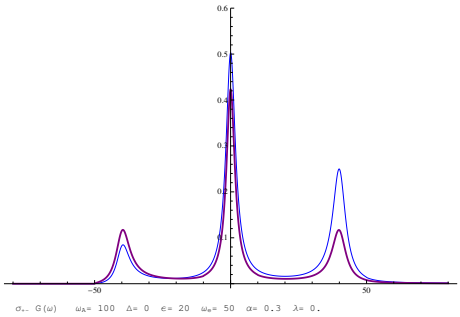

Figure 6.15: $S(\omega)$, $\omega_A = \omega_L = 100$, $\omega_e = 50$, $\epsilon = 20$, $\alpha = 0.3$, $\lambda = 0$

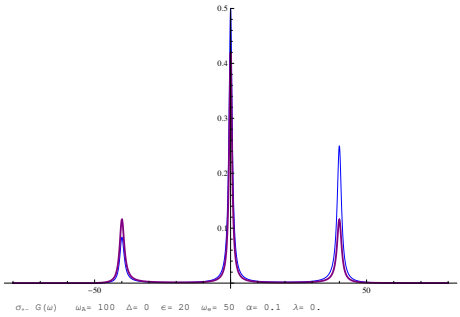

Figure 6.16: $S(\omega)$, $\omega_A = \omega_L = 100$, $\omega_e = 50$, $\epsilon = 20$, $\alpha = 0.1$, $\lambda = 0$

Detuning $\omega_A - \omega_L$

Even for small detunings, the peaks are strongly suppressed in TC1.

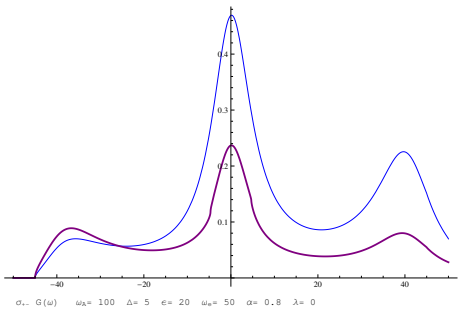

Figure 6.17: $S(\omega)$, $\omega_A - \omega_L = 5$, $\omega_e = 50$, $\epsilon = 20$, $\alpha = 0.8$, $\lambda = 0$

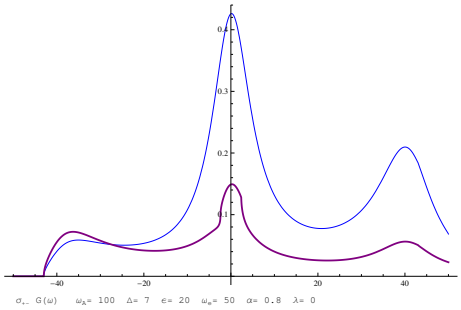

Figure 6.18: $S(\omega)$, $\omega_A - \omega_L = 7$, $\omega_e = 50$, $\epsilon = 20$, $\alpha = 0.8$, $\lambda = 0$

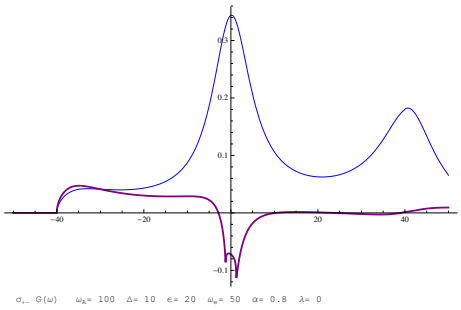

Figure 6.19: $S(\omega)$, $\omega_A - \omega_L = 10$, $\omega_e = 50$, $\epsilon = 20$, $\alpha = 0.8$, $\lambda = 0$

In the last plot, the detuning is too strong for the TC1 approximation.

6.12 Squeezing

The squeezing phenomenon appears already in the case of the Mollow spectrum [44]. It was discussed for the case of a photonic crystal density of states by Lee and Lai [45]. We treat this topic in the framework of the preceding section.

The dipole operator can be resolved into quadratures

$$\sigma_-(t) = \frac{x_\theta(t) + ip_\theta(t)}{\sqrt{2}} e^{-i\theta} \tag{6.64}$$

The squeezing spectrum is

$$\begin{aligned} S_\theta(\omega) &= 2\,\mathrm{Re}\int_0^\infty \langle \delta x_\theta(t)\delta x_\theta(t-\tau)\rangle e^{i\omega\tau} d\tau & (6.65)\\ &= \mathrm{Re}\int_0^\infty e^{-2i\theta}\langle \sigma_-(t)\sigma_-(t+\tau)\rangle + e^{2i\theta}\langle \sigma_+(t)\sigma_+(t+\tau)\rangle \\ &\quad +\langle \sigma_+(t)\sigma_-(t+\tau)\rangle + \langle \sigma_-(t)\sigma_+(t+\tau)\rangle d\tau & (6.66)\end{aligned}$$

The four appearing correlation spectra are calculated in TC0 (thin blue line) and TC1 (thick purple line) approximation.

6.12.1 Numerical examples

For later comparison, we first show the squeezing spectra in free space (Mollow triplet) for $\theta = 0$ (left) and $\theta = \pi/2$ (right).

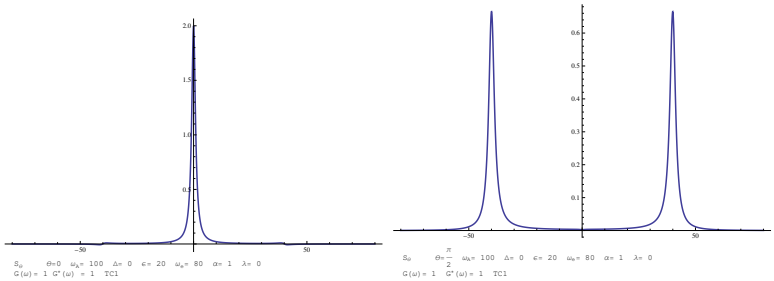

In the next plot, the squeezing spectrum is plotted as a function of the angle θ for the left, the middle and the right peak respectively.

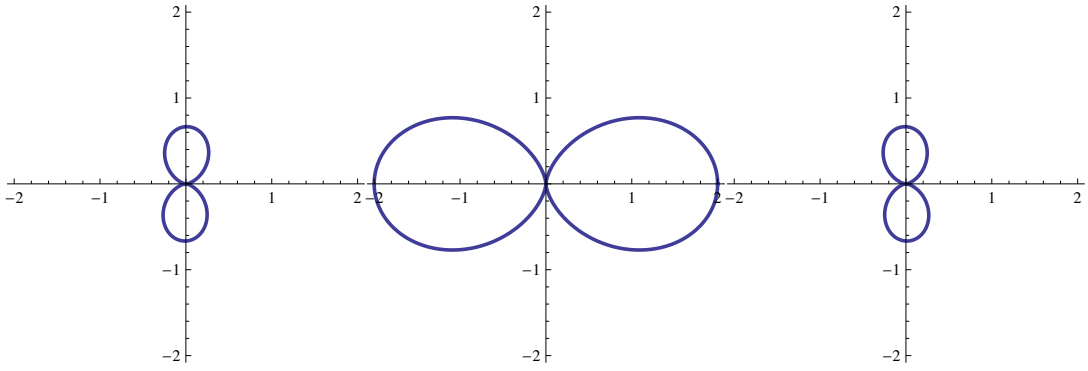

$\omega_1 = -39.9687$ $\omega_2 = 0$ $\omega_3 = 39.9687$ $\omega_A = 100$ $\Delta = 0$ $\epsilon = 20$ $\omega_e = 80$ $\alpha = 1$ $\lambda = 0$ $G(\omega) = 1$ $G^*(\omega) = 1$ TC1

We plot the spectra for ten different squeezing angles. The squeezing angle varies from 0 to π. For $\theta = 0$, the middle peak contributes the biggest part to the squeezing, whereas for $\theta = \pi/2$, the main contribution comes from the side peaks.

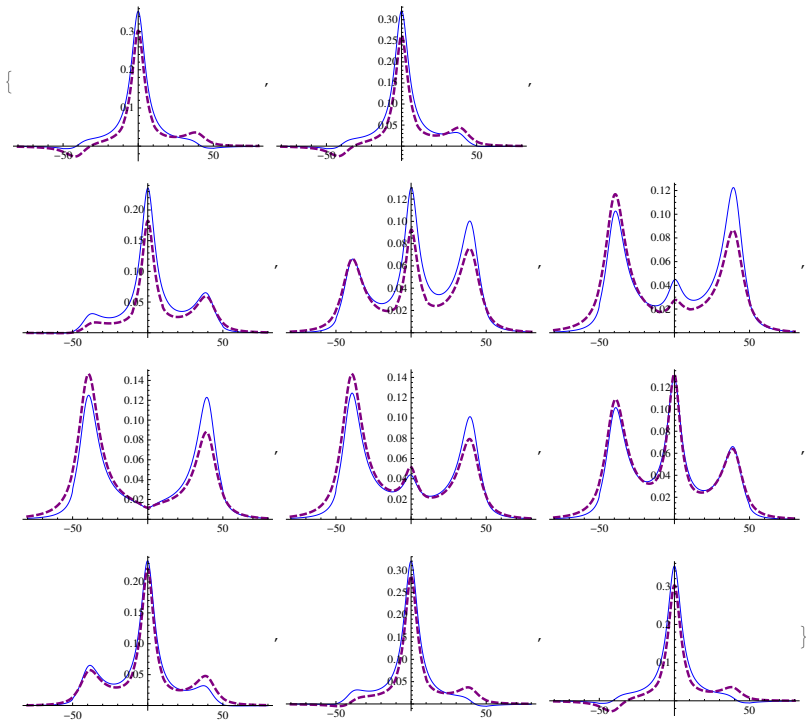

S_θ $\omega_A = 100$ $\Delta = 0$ $\epsilon = 20$ $\omega_e = 50$ $\alpha = 0.8$ $\lambda = 0$ $G(\omega) = e^{-\lambda\,(\omega-\omega_e+\omega_L)^2}\,\alpha\sqrt{\omega-\omega_e+\omega_L}$ $G^*(\omega) = -i\,e^{-\lambda\,(\omega+\omega_e-\omega_L)^2}\,\alpha\sqrt{\omega+\omega_e-\omega_L}$

In the next plot the squeezing of them is shown for each of the three peaks as a function of the angle θ.

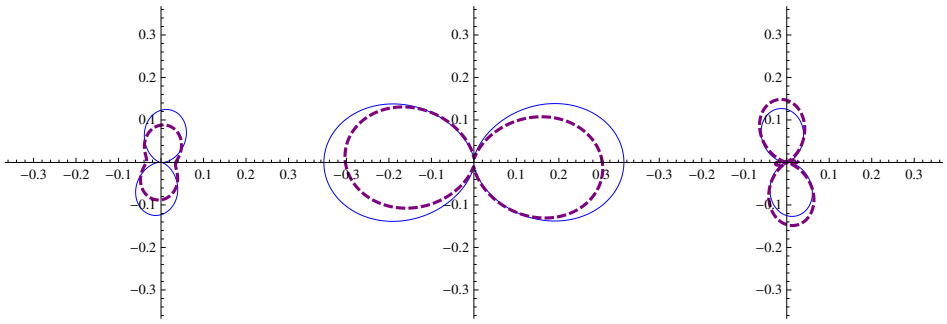

ω_{10}= -39.3126 ω_{20}= 0 ω_{30}= 39.284 ω_{11}= -39.4282 ω_{21}= 0 ω_{31}= 39.0072 ω_{A}= 100 Δ= 0 ϵ= 20 ω_{e}= 50 α= 0.8 λ= 0

$G(\omega) = e^{-\lambda\,(\omega-\omega_e+\omega_L)^2}\,\alpha\,\sqrt{\omega-\omega_e+\omega_L}$ $G^*(\omega) = -i\,e^{-\lambda\,(\omega+\omega_e-\omega_L)^2}\,\alpha\,\sqrt{\omega+\omega_e-\omega_L}$

For some parameters, the results for TC0 and TC1 differ considerably.

In the next plot, the left peak is in the gap due to high ϵ. The left peak shows no squeezing in TC1, but in TC0.

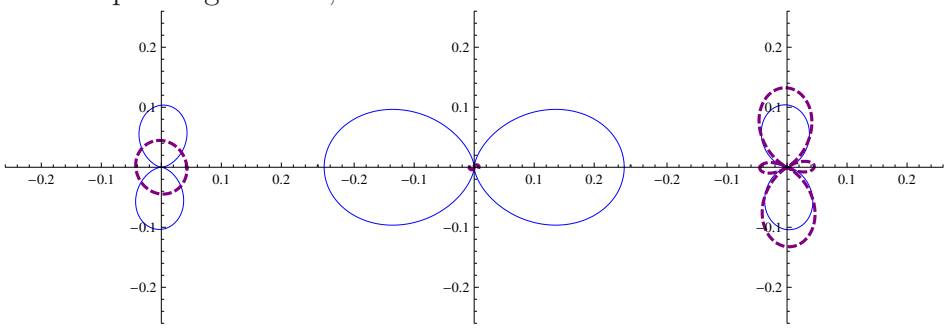

ω_{10}= -154.982 ω_{20}= 0 ω_{30}= 154.989 ω_{11}= -158.256 ω_{21}= 0 ω_{31}= 157.941 ω_A= 100 Δ= 0 ϵ= 80 ω_e= 0 α= 0.8 λ= 0

$G(\omega) = e^{-\lambda(\omega-\omega_e+\omega_L)^2}\,\alpha\sqrt{\omega-\omega_e+\omega_L}$ $G^*(\omega) = -i\,e^{-\lambda(\omega+\omega_e-\omega_L)^2}\,\alpha\sqrt{\omega+\omega_e-\omega_L}$

For finite cut-off parameter, the right peak shows no squeezing in TC1.

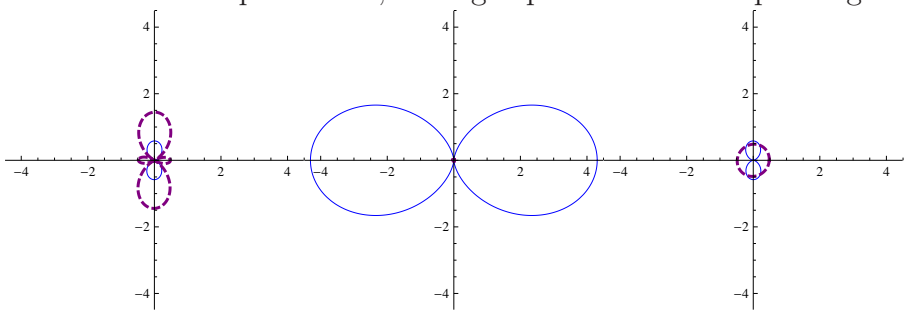

ω_{10}= -40.0019 ω_{20}= 0 ω_{30}= 40.0019 ω_{11}= -39.9841 ω_{21}= 0 ω_{31}= 39.9979 ω_A= 100 Δ= 0 ϵ= 20 ω_e= 50 α= 0.8 λ= 0.001

$G(\omega) = e^{-\lambda(\omega-\omega_e+\omega_L)^2}\,\alpha\sqrt{\omega-\omega_e+\omega_L}$ $G^*(\omega) = -i\,e^{-\lambda(\omega+\omega_e-\omega_L)^2}\,\alpha\sqrt{\omega+\omega_e-\omega_L}$

Another possibility to change the squeezing is to change the detuning.

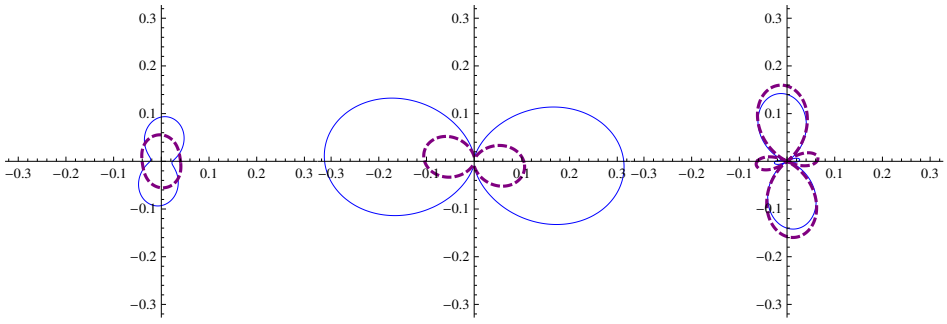

ω_{10}= -39.928 ω_{20}= 0 ω_{30}= 39.7646 ω_{11}= -40.2342 ω_{21}= 0 ω_{31}= 39.6291 ω_A= 100 Δ= 7 ϵ= 20 ω_e= 50 α= 0.8 λ= 0

$G(\omega) = e^{-\lambda(\omega-\omega_e+\omega_L)^2}\,\alpha\sqrt{\omega-\omega_e+\omega_L}$ $G^*(\omega) = -i\,e^{-\lambda(\omega+\omega_e-\omega_L)^2}\,\alpha\sqrt{\omega+\omega_e-\omega_L}$

Chapter 7

Projection operator method

7.1 General method

In chapter 5 and 6, we used the Wigner Weisskopf procedure to derive the Heisenberg equations of motion for the TC0 equations. For the TC1 equations we extendended this approach by including not only the atom part of the Bloch equations, but also the driving in the memory integral. However there are several other methods to derive Heisenberg equations of motion for expectation values of the system variables. In this chapter we use the projection operator formalism of [46], see also [47, 48]. It works also for a time-dependent Hamilton operator. With this method, higher orders are calculated systematically.

7.1.1 Basic relations

This section recalls some standard quantum relations and fixes the notation to be used in the following sections.

Starting point is the Liouville von Neumann equation for the system and bath density matrix

$$\dot{\rho}(t) = -iL(t)\rho(t) \tag{7.1}$$

with the Liouville operator

$$L(t)\cdot = [H(t), \cdot] \tag{7.2}$$

$H(t)$ consists of a time-independent part and H_0 and a time-dependent part $H_1(t)$. Accordingly

$$L(t)\cdot = (L_0 + L_1(t))\cdot \tag{7.3}$$

Eq. (7.1) is formally solved:

$$\rho(t) = U_+(t,t_0)\rho(t_0) \tag{7.4}$$

where $U_+(t,t_0)$ is defined as $U_+(t,t_0) = T_+[e^{-\int_{t_0}^{t} dt' iL(t')}]$.

The expectation value of an operator A is

$$\langle A\rangle_t = \mathrm{tr}\{A\rho(t)\} = \mathrm{tr}\{A(t)\rho\} \tag{7.5}$$

where $A(t) = U_-(t,t_0)A$ and $U_-(t,t_0) := T_-[\exp(i\int_{t_0}^{t} dt' L(t'))]$; T_- stands for increasing time ordering from left to right. In interaction picture:

$$\hat{U}_-(t,t_0) = T_-[\exp(i\int_{t_0}^{t} dt' \hat{L}_1(t'))] \tag{7.6}$$

$$\hat{L}_1(t) = e^{iL_0(t-t_0)} L_1(t) e^{-iL_0(t-t_0)} \tag{7.7}$$

The time-dependence of $\hat{U}_-(t,t_0)$ is

$$\frac{\partial}{\partial t}\hat{U}_-(t,t_0) = \hat{U}_-(t,t_0) i\hat{L}_1(t) \tag{7.8}$$

A projection operator P, $P^2 = P$, $Q = 1 - P$ is used.
We apply P and Q on the right of eq.(7.8)

$$\frac{d}{dt}\hat{V}_-(t) = \hat{V}_-(t) i\hat{L}_1(t)P + \hat{W}_-(t) i\hat{L}_1(t)P \tag{7.9}$$

$$\frac{d}{dt}\hat{W}_-(t) = \hat{V}_-(t) i\hat{L}_1(t)Q + \hat{W}_-(t) i\hat{L}_1(t)Q \tag{7.10}$$

with

$$\hat{V}_-(t) = \hat{U}_-(t,t_0)P \tag{7.11}$$

$$\hat{W}_-(t) = \hat{U}_-(t,t_0)Q \tag{7.12}$$

7.1.2 Time convolution decomposition

Eq. (7.10) is solved as

$$\hat{W}_-(t) = Q\hat{u}_-(t,t_0) + \int_{t_0}^{t} d\tau \hat{V}_-(\tau) i\hat{L}_1(\tau) Q\hat{u}_-(t,\tau) \tag{7.13}$$

where

$$\hat{u}_-(t,\tau) = T_-[\exp(\int_\tau^t d\tau' i\hat{L}_1(\tau')Q)] \tag{7.14}$$

Eq. (7.13) in eq. (7.9) results

$$\begin{aligned}\frac{d}{dt}\hat{V}_-(t) &= \hat{V}_-(t)i\hat{L}_1(t)P + \int_{t_0}^t d\tau \hat{V}_-(\tau)i\hat{L}_1(\tau)Q\hat{u}_-(t,\tau)i\hat{L}_1(t)P \\ &\quad +Q\hat{u}_-(t,t_0)i\hat{L}_1(t)P \end{aligned}\tag{7.15}$$

Usually $PA = A$, hence

$$\hat{V}_-(t)A = \hat{U}_-(t,t_0)PA = \hat{A}(t) \tag{7.16}$$

The result is then

$$\begin{aligned}\frac{d}{dt}\hat{A}(t) &= \hat{V}_-(t)i\hat{L}_1(t)A + \int_{t_0}^t d\tau \hat{V}_-(\tau)i\hat{L}_1(\tau)Q\hat{u}_-(t,\tau)i\hat{L}_1(t)A \\ &\quad +Q\hat{u}_-(t,t_0)i\hat{L}_1(t)A \end{aligned}\tag{7.17}$$

7.1.3 Expansion formulas: time convolution decomposition

The integral kernel as well as the inhomogenous term of eq.(7.17) are expanded in powers of the Liouville operator.

$$\frac{d}{dt}\hat{A}(t) = \hat{U}_-(t,t_0)i\hat{L}_1(t)A + \int_{t_0}^t d\tau \hat{K}_-(t,\tau)A + \hat{I}_-(t) \tag{7.18}$$

$$\hat{K}_-(t,\tau) := \hat{U}_-(\tau,t_0)Pi\hat{L}_1(\tau)Q\hat{u}_-(t,\tau) \tag{7.19}$$

$$\hat{I}_-(t) := Q\hat{u}_-(t,t_0)i\hat{L}_1(t)A \tag{7.20}$$

Expansion of the kernel (expansion of $\hat{u}_-(t,\tau)$)

$$\begin{aligned}\int_{t_0}^t d\tau \hat{K}_-(t,\tau) &= \int_{t_0}^t dt_1 \hat{U}_-(t_1,t_0)P\hat{\Phi}_{-,2}(t,t_1) \\ &\quad +\sum_{n=3}^\infty \int_{t_0}^t dt_1 \int_{t_0}^{t_1} dt_2 ... \int_{t_0}^{t_n-2} dt_{n-1} \\ &\quad \hat{U}_-(t_{n-1},t_0)P\hat{\Phi}_{-,n}(t,t_1,....t_{n-2},t_{n-1}) \end{aligned}\tag{7.21}$$

where

$$\hat{\Phi}_{-,2}(t,t_1) = i\hat{L}_1(t_1)Qi\hat{L}_1(t) \tag{7.22}$$

$$\hat{\Phi}_{-,n}(t,t_1,....t_{n-2},t_{n-1}) = i\hat{L}_1(t_{n-1})Qi\hat{L}_1(t_{n-2})...Qi\hat{L}_1(t_1)QiL_1(t) \tag{7.23}$$

$$P\hat{\Phi}_{-,n}(t,t_1,....t_{n-2},t_{n-1}) =: \langle i\hat{L}_1(t_{n-1})i\hat{L}_1(t_{n-2})...iL_1(t)\rangle_{APC} \tag{7.24}$$

Where we defined the "antipartial cumulants". Explicitly:

$$\begin{aligned}\langle i\hat{L}_1(t_1)iL_1(t)\rangle_{APC} &= Pi\hat{L}_1(t_1)Qi\hat{L}_1(t) &(7.25)\\ &= \langle\langle i\hat{L}_1(t_1)i\hat{L}_1(t)\rangle\rangle - \langle\langle i\hat{L}_1(t_1)\rangle\rangle\langle\langle i\hat{L}_1(t)\rangle\rangle &(7.26)\end{aligned}$$

With $P. = \langle\langle . \rangle\rangle$. For the next order:

$$\begin{aligned}\langle i\hat{L}_1(t_2)i\hat{L}_1(t_1)iL_1(t)\rangle_{APC} &= Pi\hat{L}_1(t_2)Qi\hat{L}_1(t_1)Qi\hat{L}_1(t)\\ &= \langle\langle i\hat{L}_1(t_2)i\hat{L}_1(t_1)i\hat{L}_1(t)\rangle\rangle\\ &\quad -\langle\langle i\hat{L}_1(t_2)i\hat{L}_1(t_1)\rangle\rangle\langle\langle i\hat{L}_1(t)\rangle\rangle\\ &\quad -\langle\langle i\hat{L}_1(t_2)\rangle\rangle\langle\langle i\hat{L}_1(t_1)i\hat{L}_1(t)\rangle\rangle\\ &\quad +\langle\langle i\hat{L}_1(t_2)\rangle\rangle\langle\langle i\hat{L}_1(t_1)\rangle\rangle\langle\langle i\hat{L}_1(t)\rangle\rangle &(7.27)\end{aligned}$$

For the last term of eq.(7.18), a similar expansion applies:

$$\begin{aligned}I_-(t) &= (Qi\hat{L}_1(t) + \int_0^t dt_1 Q\hat{\Phi}_{-2}(t,t_1)\\ &\quad + \sum_{n=3}^{\infty}\int_0^t dt_1\int_0^{t_1} dt_2 ...\int_0^{t_{n-2}} dt_{n-1} Q\Phi_{-,n}(t,t_1,.....,t_{n-2},t_{n-1}))A\end{aligned} \tag{7.28}$$

7.1.4 Time convolutionless decomposition

The equation of motion of the last section involves a convolution integral with the time dependent operator and an integral kernel. By arranging the basic equations in a different way, this convolution integral can be avoided and the equations may be solved more easily. Using

$$\begin{aligned}\hat{V}_-(\tau) &= \hat{U}_-(\tau,t_0)P = \hat{U}_-(t,t_0)(P+Q)\hat{U}_+(t,\tau)P\\ &= \hat{V}_-(t)\hat{U}_+(t,\tau)P + \hat{W}_-(t)\hat{U}_+(t,\tau)P\end{aligned} \tag{7.29}$$

and eq.(7.14), eq.(7.10) is solved as

$$\begin{aligned}\hat{W}_-(t) &= Q\hat{u}_-(t,t_0) \\ &\quad +(\hat{V}_-(t)+\hat{W}_-(t))\int_{t_0}^{t} d\tau \hat{U}_+(t,\tau)Pi\hat{L}_1(\tau)Q\hat{u}_-(t,\tau) \quad (7.30)\end{aligned}$$

We solve this equation for $\hat{W}_-(t)$:

$$\hat{W}_-(t) = [Q\hat{u}_-(t,t_0) - \hat{V}_-(t)(\hat{\Theta}_-(t)^{-1}-1)]\hat{\Theta}_-(t) \quad (7.31)$$

with

$$\begin{aligned}\hat{\Theta}_-(t) &= \Big(1-\int_{t_0}^{t} d\tau \hat{U}_+(t,\tau)Pi\hat{L}_1(\tau)Q\hat{u}_-(t,\tau)\Big)^{-1} \\ &=: \Big(1-\hat{S}_-(t)\Big)^{-1} \quad (7.32)\end{aligned}$$

From eq.(7.9) and eq.(7.31) we get

$$\begin{aligned}\frac{d}{dt}\hat{V}_-(t) &= \hat{V}_-(t)i\hat{L}_1(t)P - \hat{V}_-(t)(1-\Theta_-(t))i\hat{L}_1(t)P \\ &\quad +Q\hat{u}_-(t,t_0)\Theta_-(t)i\hat{L}_1(t)P \quad (7.33)\end{aligned}$$

So for $\hat{A}(t)$:

$$\begin{aligned}\frac{d}{dt}\hat{A}(t) &= \hat{V}_-(t)i\hat{L}_1(t)A - \hat{V}_-(t)(1-\Theta_-(t))i\hat{L}_1(t)A \\ &\quad +Q\hat{u}_-(t,t_0)\Theta_-(t)i\hat{L}_1(t)A \quad (7.34)\end{aligned}$$

7.1.5 Expansion formulas: time convolutionless decomposition

Working out on eq. (7.34)

$$\frac{d}{dt}\hat{A}(t) = \hat{\Psi}_-(t)A + \hat{J}_-(t) \quad (7.35)$$

with

$$\hat{\Psi}_-(t) = \hat{U}_-(t,t_0)P\hat{\Theta}_-(t)i\hat{L}_1(t) \quad (7.36)$$

$$\hat{J}_-(t) = Q\hat{u}_-(t,t_0)\hat{\Theta}_-(t)i\hat{L}_1(t)A \quad (7.37)$$

$\hat{\Psi}_-(t)$ has the form

$$\hat{\Psi}_-(t) = \hat{U}_-(t,t_0)\sum_{n=0}^{\infty} P(\hat{S}(t))^n i\hat{L}_1(t) \tag{7.38}$$

$$=: \hat{U}_-(t,t_0)\sum_{n=1} P\hat{\Psi}_{-,n}(t) \tag{7.39}$$

We expand the exponentials in $\hat{U}_+(t,\tau)$ and $\hat{u}_-(t,\tau)$.
The first terms of the expansion are with $P. = \langle\langle . \rangle\rangle$

$$\hat{\Psi}_{-,1}(t) = Pi\hat{L}_1(t) \tag{7.40}$$

$$\begin{aligned}\hat{\Psi}_{-,2}(t) &= \int_{t_0}^{t} dt_1 Pi\hat{L}_1(t_1)Qi\hat{L}_1(t) \\ &= \int_{t_0}^{t} dt_1 \langle\langle i\hat{L}_1(t_1)(1-P)i\hat{L}_1(t)\rangle\rangle) \\ &= \int_{t_0}^{t} dt_1 \Big(\langle\langle i\hat{L}_1(t_1)i\hat{L}_1(t)\rangle\rangle - \langle\langle i\hat{L}_1(t_1)\rangle\rangle\langle\langle i\hat{L}_1(t)\rangle\rangle\Big)\end{aligned} \tag{7.41}$$

$$\begin{aligned}\hat{\Psi}_{-,3}(t) &= \int_{t_0}^{t} dt_1 \int_{t_0}^{t_1} dt_2 \Big\{ Pi\hat{L}_1(t_2)Qi\hat{L}_1(t_1)Qi\hat{L}_1(t) \\ &\quad -Pi\hat{L}_1(t_1)Pi\hat{L}_1(t_2)Qi\hat{L}_1(t)\Big\} \\ &= \int_{t_0}^{t} dt_1 \int_{t_0}^{t_1} dt_2 \Big\{ \langle\langle i\hat{L}_1(t_2)i\hat{L}_1(t_1)i\hat{L}_1(t)\rangle\rangle - \langle\langle i\hat{L}_1(t_2)i\hat{L}_1(t_1)\rangle\rangle\langle\langle i\hat{L}_1(t)\rangle\rangle \\ &\quad -\langle\langle i\hat{L}_1(t_2)\rangle\rangle\langle\langle i\hat{L}_1(t_1)i\hat{L}_1(t)\rangle\rangle - \langle\langle i\hat{L}_1(t_1)\rangle\rangle\langle\langle i\hat{L}_1(t_2)i\hat{L}_1(t)\rangle\rangle \\ &\quad +\langle\langle i\hat{L}_1(t_2)\rangle\rangle\langle\langle i\hat{L}_1(t_1)\rangle\rangle\langle\langle i\hat{L}_1(t)\rangle\rangle \\ &\quad +\langle\langle i\hat{L}_1(t_1)\rangle\rangle\langle\langle i\hat{L}_1(t_2)\rangle\rangle\langle\langle i\hat{L}_1(t)\rangle\rangle\end{aligned}$$

These cumulants are called anti-ordered cumulants

$$\hat{\Psi}_{-,1}(t) = \langle i\hat{L}_1(t)\rangle_{AOC} \tag{7.42}$$

$$\hat{\Psi}_{-,2}(t) = \int_{t_0}^{t} dt_1 \langle i\hat{L}_1(t_1)i\hat{L}_1(t)\rangle_{AOC} \tag{7.43}$$

$$\hat{\Psi}_{-,n}(t) = \int_{t_0}^{t} dt_1 ... \int_{t_0}^{t_{n-2}} dt_{n-1} \langle i\hat{L}_1(t_{n-1})...i\hat{L}_1(t)\rangle_{AOC} \tag{7.44}$$

$$\tag{7.45}$$

$$\begin{aligned}\hat{J}_-(t) &= Q\hat{u}_-(t,t_0)\sum_{n=0}^{\infty}(\hat{S}(t))^n i\hat{L}_1(t)A \\ &= \sum_{n=1}^{\infty}\hat{J}_{-,n}(t) \qquad (7.46)\end{aligned}$$

$$\hat{J}_{-,1}(t) = Q\hat{L}_1(t)A \qquad (7.47)$$

$$\hat{J}_{-,2}(t) = Q\int_{t_0}^{t} dt_1 i\hat{L}_1(t_1)Qi\hat{L}_1(t)A \qquad (7.48)$$

7.2 Application to PhC Resonance Fluorescence

7.2.1 Hamilton operator

The general form of the Hamilton operator for the projection method is

$$H = H_0 + H_1(t) \qquad (7.49)$$

We choose the following partitioning into H_0 and H_1

$$\begin{aligned}H_0 &= \frac{1}{2}\omega_A\sigma_z + \sum_\lambda \omega_\lambda a_\lambda^+ a_\lambda \\ H_1(t) &= \epsilon(\sigma_+ e^{-i\omega_L t} + \sigma_- e^{i\omega_L t}) + i\sum_\lambda g_\lambda(a_\lambda^+\sigma_- - a_\lambda\sigma_+) \qquad (7.50) \\ &= H_{1L}(t) + H_{1I}(t) \qquad (7.51)\end{aligned}$$

The time dependent operators (in the sense of the interaction picture) are

$$\begin{aligned}e^{iH_0t}H_{1L}(t)e^{-iH_0t} &= \epsilon e^{-i\omega_L t}e^{i\omega_A t}\sigma_+ + \epsilon e^{i\omega_L t}e^{-i\omega_A t}\sigma_- \\ &= \tilde{\epsilon}(t)\sigma_+ + \tilde{\epsilon}^*(t)\sigma_- \\ e^{iH_0t}H_{1I}(t)e^{-iH_0t} &= i\sum_\lambda g_\lambda(a_\lambda^+\sigma_- e^{i\omega_\lambda t - i\omega_A t} + a_\lambda\sigma_+ e^{-i\omega_\lambda t + i\omega_A t}) \\ &= b^+(t)\sigma_- + b^-(t)\sigma_+\end{aligned}$$

7.2.2 2nd and 3rd order TCL expansion

We apply the expansion in 7.1.5 to our problem.
and use the projection operator

$$PA = \mathrm{tr}_B\{\rho_B A\} \tag{7.52}$$

The first order $\hat{\Psi}_-(t)$, eq.(7.40):

$$\begin{aligned}\hat{\Psi}_{-,1}(t)\sigma_+ &= Pi\hat{L}_1(t)\sigma_+ \\ &= Pi(b^+ + \tilde{\epsilon}^*(t))(-\sigma_z) \\ &= -i\langle b^+ + \tilde{\epsilon}^*(t)\rangle_B\sigma_z \\ &= -i\tilde{\epsilon}^*(t)\sigma_z\end{aligned}$$

$$\hat{U}(t,t_0)\hat{\Psi}_{-,1}(t)\sigma_+ = -i\tilde{\epsilon}^*(t)\hat{\sigma}_z(t)$$

Define $B^+ := (b^+(t) + \tilde{\epsilon}^*(t))$, $B^- := (b^-(t) + \tilde{\epsilon}(t))$. Second order $\hat{\Psi}_-(t)$ eq.(7.41):

$$\begin{aligned}\hat{\Psi}_{-,2}(t)\sigma_+ &= \int_{t_0}^t dt_1\Big(\langle\langle i\hat{L}_1(t_1)i\hat{L}_1(t)\rangle\rangle - \langle\langle i\hat{L}_1(t_1)\rangle\rangle\langle\langle i\hat{L}_1(t)\rangle\rangle\Big)\sigma_+ \\ &= -\int_{t_0}^t dt_1\Big\{\Big(\langle\langle B^-(t_1)B^+(t)\rangle\rangle + \langle\langle B^+(t)B^-(t_1)\rangle\rangle\Big)\sigma_+ \\ &\quad -\Big(\langle\langle B^+(t)B^+(t_1)\rangle\rangle - \langle\langle B^+(t_1)B^+(t)\rangle\rangle\Big)\sigma_- \\ &\quad -\Big(\langle\langle B^-(t_1)\rangle\rangle\langle\langle B^+(t)\rangle\rangle + \langle\langle B^+(t)\rangle\rangle\langle\langle B^-(t_1)\rangle\rangle\Big)\sigma_+ \\ &\quad +\Big(\langle\langle B^+(t)\rangle\rangle\langle\langle B^+(t_1)\rangle\rangle - \langle\langle B^+(t_1)\rangle\rangle\langle\langle B^+(t)\rangle\rangle\Big)\sigma_-\Big\}\end{aligned} \tag{7.53}$$

The appearing one- and two-time correlation functions are for example:

$$\langle\langle B^+(t)\rangle\rangle = \tilde{\epsilon}^*(t) \tag{7.54}$$

$$\langle\langle B^-(t_1)B^+(t)\rangle\rangle = \langle b^-(t_1)b^+(t)\rangle_B + \tilde{\epsilon}(t_1)\tilde{\epsilon}^*(t) \tag{7.55}$$

Since many of the correlations vanish, the result is

$$\hat{\Psi}_{-,2}(t)\sigma_+ = -\int_{t_0}^t dt_1\langle b^-(t_1)b^+(t)\rangle_B\sigma_+ \tag{7.56}$$

$$\hat{U}_-(t,t_0)\hat{\Psi}_{-,2}(t)\sigma_+ = -\int_{t_0}^{t} dt_1 \langle b^-(t_1)b^+(t)\rangle_B \hat{\sigma}_+(t) \tag{7.57}$$

In order to determine $\hat{\Psi}_{-,3}(t)$ we first note:

$$\begin{aligned}\langle\langle B^-(t_2)B^+(t_1)B^+(t)\rangle\rangle &= +\langle b^-(t_2)b^+(t_1)\rangle_B \tilde{\epsilon}^*(t) + \langle b^-(t_2)b^+(t)\rangle_B \tilde{\epsilon}^*(t_1) \\ &\quad +\tilde{\epsilon}(t_2)\tilde{\epsilon}^*(t_1)\tilde{\epsilon}^*(t)\end{aligned} \tag{7.58}$$

$$\begin{aligned}\langle B^-(t_2)B^+(t_1)B^+(t)\rangle_{AOC} &= \langle\langle B^-(t_2)B^+(t_1)B^+(t)\rangle\rangle - \langle\langle B^-(t_2)B^+(t_1)\rangle\rangle\langle\langle B^+(t)\rangle\rangle \\ &\quad -\langle\langle B^-(t_2)\rangle\rangle\langle\langle B^+(t_1)B^+(t)\rangle\rangle \\ &\quad -\langle\langle B^+(t_1)\rangle\rangle\langle\langle B^-(t_2)B^+(t)\rangle\rangle \\ &\quad +\langle\langle B^-(t_2)\rangle\rangle\langle\langle B^+(t_1)\rangle\rangle\langle\langle B^+(t)\rangle\rangle \\ &\quad +\langle\langle B^+(t_1)\rangle\rangle\langle\langle B^-(t_2)\rangle\rangle\rangle\langle\langle B^+(t)\rangle\rangle\rangle \\ &= 0\end{aligned} \tag{7.59}$$

$$\hat{\Psi}_{-,3}(t) = \int_{t_0}^{t} dt_1 \int_{t_0}^{t_1} dt_2 \langle i\hat{L}_1(t_2) i\hat{L}_1(t_1) i\hat{L}_1(t)\rangle_{AOC} = 0 \tag{7.60}$$

$$\begin{aligned}\hat{J}_{-,1} &= Q i\hat{L}_1(t)A \\ &= i\hat{L}_1(t)A - i\langle\hat{L}_1(t)\rangle_B A \\ &= iB^+(t)(\sigma_{-+} - \sigma_{+-}) - i\langle B^+(t)\rangle_B(\sigma_{-+} - \sigma_{+-})\end{aligned} \tag{7.61}$$

$$\begin{aligned}\hat{J}_{-,2} = \int_{t_0}^{t} dt_1 \; &\Big(i\hat{L}_1(t_1) i\hat{L}_1(t) - i\hat{L}_1(t_1)\langle i\hat{L}_1(t)\rangle_B \\ &-\langle i\hat{L}_1(t_1) i\hat{L}_1(t)\rangle_B + \langle i\hat{L}_1(t_1)\rangle_B \langle i\hat{L}_1(t)\rangle_B \Big) A\end{aligned} \tag{7.62}$$

These terms will disappear after taking the trace.

7.2.3 2nd and 3rd order TCL equations of motion

Collecting the results of the preceding paragraph, we arrive at the equations of motion:

$$\begin{aligned}
\frac{d}{dt}\langle\sigma_+(t)\rangle &= i\tilde{\epsilon}(t)\langle\sigma_{-+}(t)-\sigma_{+-}(t)\rangle - \int_0^t dt_1 G(t_1-t)\langle\sigma_+(t)\rangle \\
\frac{d}{dt}\langle\sigma_-(t)\rangle &= i\tilde{\epsilon}^*(t)\langle\sigma_{+-}(t)-\sigma_{-+}(t)\rangle - \int_0^t dt_1 G(t-t_1)\langle\sigma_-(t)\rangle \\
\frac{d}{dt}\langle\sigma_{+-}(t)\rangle &= i\tilde{\epsilon}(t)\langle\sigma_-(t)\rangle - i\tilde{\epsilon}^*(t)\langle\sigma_+(t)\rangle \\
&\quad - \int_0^t dt_1 G(t_1-t) + G(t-t_1)\langle\sigma_{+-}(t)\rangle \\
\frac{d}{dt}\langle\sigma_{-+}(t)\rangle &= -i\tilde{\epsilon}(t)\langle\sigma_-(t)\rangle + i\tilde{\epsilon}^*(t)\langle\sigma_+(t)\rangle \\
&\quad + \int_0^t dt_1 G(t_1-t) + G(t-t_1)\langle\sigma_{+-}(t)\rangle
\end{aligned}$$

with $\sigma_{+-} := \sigma_+\sigma_-$
The 3rd order terms are zero.
With the definitions $\xi(t) = \int_0^t dt_1\langle b^-(t_1)b^+(t)\rangle$, and the rotating frame quantities $\tilde{\sigma}_+(t) = e^{-i(\omega_A-\omega_L)t}\sigma_+(t)$, $\tilde{\sigma}_-(t) = e^{i(\omega_A-\omega_L)t}\sigma_-(t)$, $\tilde{\xi}(t) = \xi(t)e^{i(\omega_A-\omega_L)t}$, $\tilde{\xi}^*(t) = \xi^*(t)e^{-i(\omega_A-\omega_L)t}$ and using $\sigma_z = \sigma_{+-} - \sigma_{-+}$ we arrive at

$$\frac{d}{dt}\langle\tilde{\sigma}_+(t)\rangle = -i\epsilon\langle\sigma_z(t)\rangle - [\tilde{\xi}(t) + i(\omega_A-\omega_L)]\langle\tilde{\sigma}_+(t)\rangle \tag{7.63}$$

$$\frac{d}{dt}\langle\tilde{\sigma}_-(t)\rangle = i\epsilon\langle\sigma_z(t)\rangle - [\tilde{\xi}^*(t) - i(\omega_A-\omega_L)]\langle\tilde{\sigma}_-(t)\rangle \tag{7.64}$$

$$\frac{d}{dt}\langle\sigma_z(t)\rangle = 2i\epsilon\langle\tilde{\sigma}_-(t)\rangle - 2i\epsilon\langle\tilde{\sigma}_+(t)\rangle - (\xi(t)+\xi^*(t))\langle 1\rangle - (\xi(t)+\xi^*(t))\langle\sigma_z(t)\rangle \tag{7.65}$$

These equations are identical to the TCL equations of chapter 6. That means, those equations are correct to 3rd order.

The equivalent master-equation in Lindblad form with time dependent coefficients is

$$\dot{\rho} = i[H_S,\rho] + \xi(t)[\sigma_-\rho\sigma_+ - \sigma_+\sigma_-\rho] + h.c. \tag{7.66}$$

with

$$H_S = \epsilon(\sigma_+ + \sigma_-) + \frac{1}{2}(\omega_A - \omega_L)\sigma_z \tag{7.67}$$

$$\tag{7.68}$$

$\xi(t)$ must be positive to ensure that the equation is trace-preserving and completely positive. A master equation in Lindblad form with constant coefficients describes a Markovian open quantum system. The time dependence of the coefficients reflects the non-Markovianity of the problem. Such master equations were discussed in e.g. [49].

7.2.4 Environment functions

The first integral of the response function $\xi(t) = \int_0^t dt' G(t'-t)$ with

$$G(t'-t) = \alpha \int_{\omega_e}^{\infty} d\omega e^{i(\omega-\omega_A)(t'-t)} \frac{\sqrt{\omega-\omega_e}}{\omega} \tag{7.69}$$

We did not perform the approximation $\omega \approx \omega_e$ in the denominator like in eq.(3.19) for the reason of convergence. In the band we get:

$$\begin{aligned} \xi(t) &= \int_0^t dt' G(t'-t) \\ &= \frac{\alpha\pi}{\omega_A}(-\sqrt{\Delta_{Ae}}\mathrm{erf}((-1)^{3/4}\sqrt{\Delta_{Ae}t}) \\ &\quad +i\sqrt{\omega_e}(-1-e^{it\omega_A}(-1+\mathrm{erf}((-1)^{1/4}\sqrt{t\omega_e})))) \end{aligned} \tag{7.70}$$

In the gap:

$$\begin{aligned} \xi(t) &= \frac{i\alpha\pi}{\omega_A}(\sqrt{-\Delta_{Ae}}\mathrm{erf}((-1)^{1/4}\sqrt{-\Delta_{Ae}t}) \\ &\quad +\sqrt{\omega_e}(-1-e^{it\omega_A}(-1+\mathrm{erfc}((-1)^{1/4}\sqrt{t\omega_e})))) \end{aligned} \tag{7.71}$$

In the long time limit in the gap:

$$\lim_{t\to\infty}\int_0^t dt'\xi(t') = -i\frac{\pi\alpha(\omega_A - 2\omega_e + 2\sqrt{-\omega_e\Delta_{Ae}})}{2\omega_A^2\sqrt{-\Delta_{Ae}}} + i\frac{\pi\alpha(-\sqrt{\omega_e}+\sqrt{-\Delta_{Ae}})}{\omega_A}t \tag{7.72}$$

in the band

$$\lim_{t\to\infty}\int_0^t dt'\xi(t') = -i\frac{\pi\alpha(-\omega_e+\sqrt{\omega_e\Delta_{Ae}})}{2\omega_A^2\sqrt{\Delta_{Ae}}}+\frac{\pi\alpha(-i\sqrt{\omega_e}-\sqrt{\Delta_{Ae}})}{\omega_A}t \tag{7.73}$$

7.2.5 Special cases

Spontaneous decay In the case without driving, we see directly from eq.(7.65) that the equations decouple

$$\frac{d}{dt}\langle\sigma_z(t)\rangle = -(\xi(t)+\xi^*(t))\langle\sigma_z(t)\rangle-(\xi(t)+\xi^*(t)) \tag{7.74}$$

$$\frac{d}{dt}\langle\tilde{\sigma}_+(t)\rangle = -[\tilde{\xi}(t)+i(\omega_A-\omega_L)]\langle\tilde{\sigma}_+(t)\rangle \tag{7.75}$$

The population inversion is therefore

$$\langle\sigma_z(t)\rangle = (\langle\sigma_z(0)\rangle+1)e^{\int_0^t dt'(\xi(t')+\xi^*(t'))}-1 \tag{7.76}$$

Resonance fluorescence in free space With the free space response function eq.(4.53), $\xi(t)=\xi^*(t)\propto\beta$ the free space equations eqs.(4.54) are recovered for $\breve{\sigma}_+(t)=e^{-i\omega_A t}\sigma_+(t)$. (Without noise terms).

7.2.6 Numerical examples

The equations (7.65) can be solved numerically with Mathematica (see uchi8a.nb). We give some examples for $\langle\sigma_z\rangle$
Spontaneous decay $\epsilon=0$ in the gap and in the band:

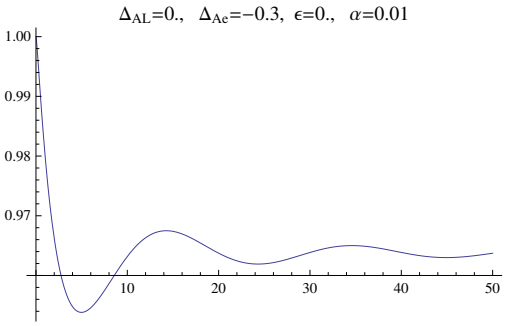

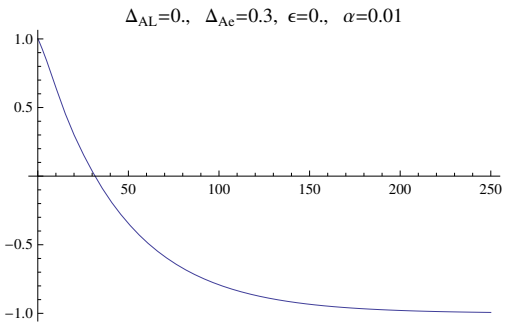

Atom frequency in the gap, smaller and bigger Rabi frequency:

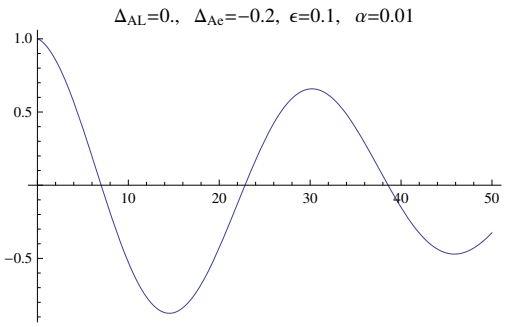

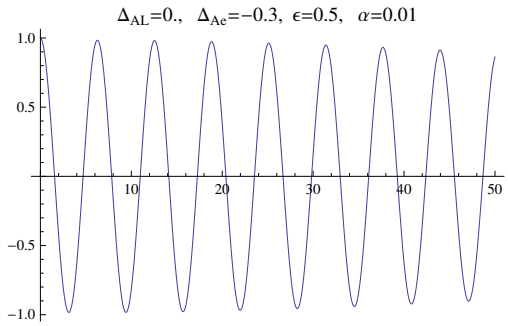

For larger coupling in the gap, a revival phenomenon appears.

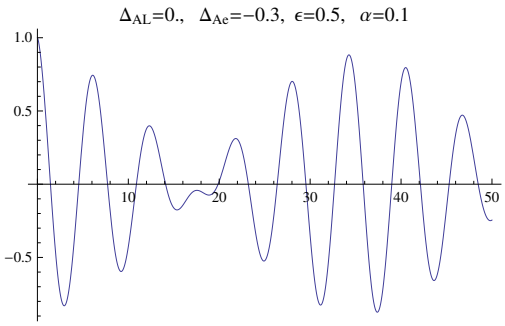

In the band, with different couplings:

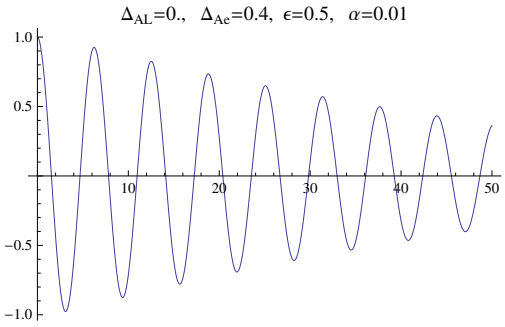

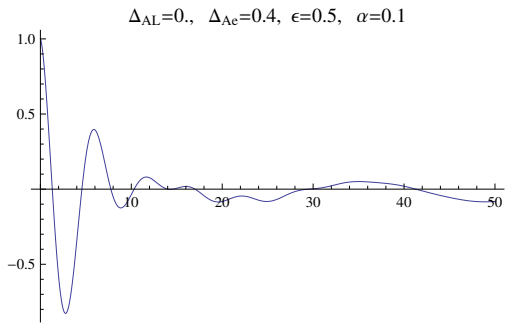

For larger couplings the approximation is not appropriate and the solution becomes unphysical. A physical solution should stay inside the Bloch sphere with $|\langle\sigma_z\rangle| \leq 1$.

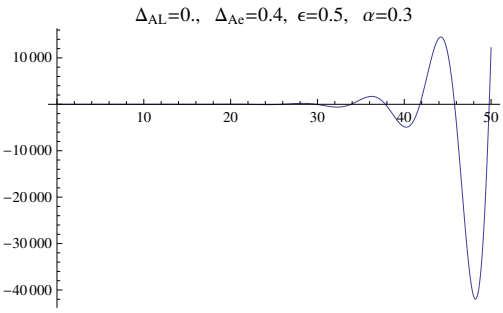

7.2.7 TC 3rd order

In this section we apply the results of section 7.1.2 to our problem to get the time convolution version of the equations. The first term of the right hand side of eq.(7.18) for $A = \sigma_+$ up to 3rd order is

$$\hat{U}_-(t,t_0)Pi\hat{L}_1(t)A = i\tilde{\epsilon}^*(t)(\sigma_{-+}(t) - \sigma_{+-}(t)) \tag{7.77}$$

The 2nd term is

$$\begin{aligned}\int_{t_0}^{t} d\tau \hat{K}_-(t,\tau)A &= \int_{t_0}^{t} dt_1 \hat{U}_-(t_1,t_0)\langle i\hat{L}_1(t_1)i\hat{L}_1(t)\rangle_{APC}\sigma_+ \\ &+ \int_{t_0}^{t} dt_1 \int_{t_0}^{t_1} dt_2 \\ &\hat{U}_-(t_2,t_0)\langle i\hat{L}_1(t_2)i\hat{L}_1(t_1)i\hat{L}_1(t)\rangle_{APC}\sigma_+ \end{aligned} \tag{7.78}$$

Since for 2nd order $\langle . \rangle_{APC} = \langle . \rangle_{AOC}$

$$\langle i\hat{L}_1(t_1)i\hat{L}_1(t)\rangle_{APC}\sigma_+ = -\int_{t_0}^{t} dt_1 \langle b^-(t_1)b^+(t)\rangle\sigma_+(t_1) \tag{7.79}$$

For the 3rd order we first calculate

$$\begin{aligned}\hat{L}_1(t_2)\hat{L}_1(t_1)\hat{L}_1(t)\sigma_+ &= -B^-(t_2)B^+(t_1)B^+(t)\sigma_{+-} - B^-(t_2)B^+(t)B^+(t_1)\sigma_{+-} \\ &+B^+(t_1)B^+(t)B^-(t_2)\sigma_{-+} + B^+(t)B^+(t_1)B^-(t_2)\sigma_{-+} \\ &+B^+(t_2)B^-(t_1)B^+(t)\sigma_{-+} + B^+(t_2)B^+(t)B^-(t_1)\sigma_{-+} \\ &-B^-(t_1)B^+(t)B^+(t_2)\sigma_{+-} - B^+(t)B^-(t_1)B^+(t_2)\sigma_{+-}\end{aligned} \tag{7.80}$$

The 3rd order cumulants are

$$\begin{aligned}\langle B^-(t_2)B^+(t_1)B^+(t)\rangle_{APC} &= \langle\langle B^-(t_2)B^+(t_1)B^+(t)\rangle\rangle \\ &\quad -\langle\langle B^-(t_2)B^+(t_1)\rangle\rangle\langle\langle B^+(t)\rangle\rangle \\ &\quad -\langle\langle B^-(t_2)\rangle\rangle\langle\langle B^+(t_1)B^+(t)\rangle\rangle \\ &\quad +\langle\langle B^-(t_2)\rangle\rangle\langle\langle B^+(t_1)\rangle\rangle\langle\langle B^+(t)\rangle\rangle \quad (7.81)\end{aligned}$$

In contrast to the TCL equations, not all the 3rd order cumulants are zero:

$$\begin{aligned}\langle B^-(t_2)B^+(t_1)B^+(t))\rangle_{APC} &= \langle b^-(t_2)b^+(t)\rangle\epsilon^*(t_1) \\ \langle B^-(t_2)B^+(t)B^+(t_1)\rangle_{APC} &= \langle b^-(t_2)b^+(t_1)\rangle\epsilon^*(t) \\ \langle B^+(t_1)B^+(t)B^-(t_2)\rangle_{APC} &= 0 \\ \langle B^+(t)B^+(t_1)B^-(t_2)\rangle_{APC} &= 0 \\ \langle B^+(t_2)B^-(t_1)B^+(t)\rangle_{APC} &= 0 \\ \langle B^+(t_2)B^+(t)B^-(t_1)\rangle_{APC} &= 0 \\ \langle B^-(t_1)B^+(t)B^+(t_2)\rangle_{APC} &= \langle b^-(t_1)b^+(t_2)\rangle\epsilon^*(t) \\ \langle B^+(t)B^-(t_1)B^+(t_2)\rangle_{APC} &= 0 \quad (7.82)\end{aligned}$$

The 3rd term of eq.(7.18)

$$\begin{aligned}I_-(t) &= Qi\hat{L}_1(t) + \int_0^t dt_1 Q\hat{\Phi}_{-2}(t,t_1) \\ &\quad + \int_0^t dt_1 \int_0^{t_1} dt_2 Q\Phi_{-,3}(t,t_1,t_2))\sigma_+ \quad (7.83)\end{aligned}$$

The first term of $I_-(t)$

$$Qi\hat{L}_1(t)\sigma_+ = b^+(\sigma_{-+} - \sigma_{+-}) \quad (7.84)$$

disappears ofter averaging as well as the others.

7.2.8 TC equations of motion

Collecting the results of the preceding section, we arrive at the time convolution equations of motion up to 2nd order

$$\begin{aligned}
\frac{d}{dt}\langle\sigma_+(t)\rangle &= -i\tilde{\epsilon}^*(t)\langle\sigma_z(t)\rangle - \int_0^t dt_1 G(t_1-t)\langle\sigma_+(t_1)\rangle \\
\frac{d}{dt}\langle\sigma_-(t)\rangle &= i\tilde{\epsilon}(t)\langle\sigma_z(t)\rangle - \int_0^t dt_1 G(t-t_1)\langle\sigma_-(t_1)\rangle \\
\frac{d}{dt}\langle\sigma_z(t)\rangle &= 2i\tilde{\epsilon}^*(t)\langle\sigma_-(t)\rangle - 2i\tilde{\epsilon}(t)\langle\sigma_+(t)\rangle \\
&\quad - \int_0^t dt_1 (G(t_1-t)+G(t-t_1))(\langle\sigma_z(t_1)\rangle + 1)
\end{aligned} \tag{7.85}$$

The 3rd order equations are

$$\begin{aligned}
\frac{d}{dt}\langle\sigma_+(t)\rangle &= -i\tilde{\epsilon}^*(t)\langle\sigma_z(t)\rangle - \int_0^t dt_1 G(t_1-t)\langle\sigma_+(t_1)\rangle \\
&\quad + i\int_0^t dt_1 \int_0^{t_1} dt_2 \Big[G(t_2-t)\epsilon^*(t_1) \\
&\quad + G(t_2-t_1)\epsilon^*(t) + G(t_1-t_2)\epsilon^*(t)\Big]\frac{1}{2}(\langle\sigma_z(t_2)\rangle + 1) \\
\frac{d}{dt}\langle\sigma_-(t)\rangle &= i\tilde{\epsilon}(t)\langle\sigma_z(t)\rangle - \int_0^t dt_1 G(t-t_1)\langle\sigma_-(t_1)\rangle \\
&\quad - i\int_0^t dt_1 \int_0^{t_1} dt_2 \Big[G(t-t_2)\epsilon(t_1) \\
&\quad + G(t_1-t_2)\epsilon(t) + G(t_2-t_1)\epsilon(t)\Big]\frac{1}{2}(\langle\sigma_z(t_2)\rangle + 1) \\
\frac{d}{dt}\langle\sigma_z(t)\rangle &= 2i\tilde{\epsilon}^*(t)\langle\sigma_-(t)\rangle - 2i\tilde{\epsilon}(t)\langle\sigma_+(t)\rangle \\
&\quad - \int_0^t dt_1 (G(t_1-t)+G(t-t_1))(\langle\sigma_z(t_1)\rangle + 1)
\end{aligned} \tag{7.86}$$

7.2.9 Numerical solution: time-evolution of TC2 and TC3

For the solution of this system of integro-differential equations we use a iterative method. It is suitable even for higher orders. Its limitations are the long computation time for longer system time.

Iterative variational method

Following [50], we consider a general nonlinear system:

$$D[\sigma(t)] + F[\sigma(t)] = g(t) \tag{7.87}$$

with a differential operator D and a operator F and a given function $g(t)$. For the iterative method, where σ_n is the nth iteration, the following correction functional is considered:

$$\sigma_{n+1}(t) = \sigma_n(t) + \int_0^t \lambda(s)[\sigma'(s) + \tilde{F}[\sigma_n(s)]]ds \tag{7.88}$$

$\tilde{F}[\sigma_n(s)]$ is a restricted variation i.e. $\delta\tilde{F}[\sigma_n(s)] = 0$. λ is a Lagrange multiplier that is chosen using a variational method.

$$\begin{aligned} \delta\sigma_{n+1}(t) &= \delta\sigma_n(t) + \delta\int_0^t \lambda(s)[\sigma_n'(s) + \tilde{F}[\sigma_n(s)]]ds & (7.89)\\ &= \delta\sigma_n(t) + \lambda(s)\delta\sigma_n(s)|_{s=t} - \int_0^t \lambda'(s)\delta\sigma_n(s)ds & (7.90)\end{aligned}$$

The conditions for λ are

$$\begin{aligned} \lambda'(s) &= 0 & (7.91)\\ 1 + \lambda(t) &= 0 & (7.92)\end{aligned}$$

Therefore the Langrange multiplier is $\lambda(t) = -1$.
In our problem, D ist the time derivative left side of the equation system, F is the homogenous part of the right side and g is the inhomogeeous part.

Plots

We present the numerical solution for TC 2nd order and TC 3rd order. The first plot is the solution using the method of chapter 5 for comparison.

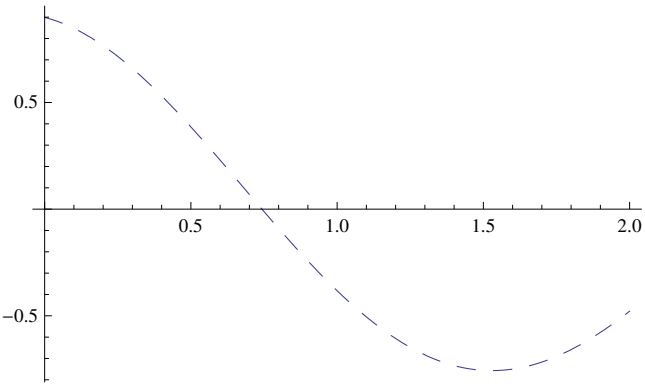

$\sigma_z(t)$
$\omega_A = \omega_L, \omega_A - \omega_e = 1, \epsilon = 1, \alpha = 0.1$

2nd order:

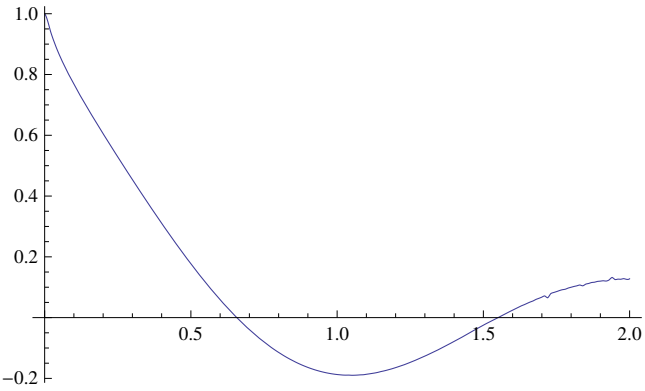

$\sigma_z(t)$
$\omega_A = \omega_L, \omega_A - \omega_e = 1, \epsilon = 1, \alpha = 0.1, \omega_c = 200$

3rd order:

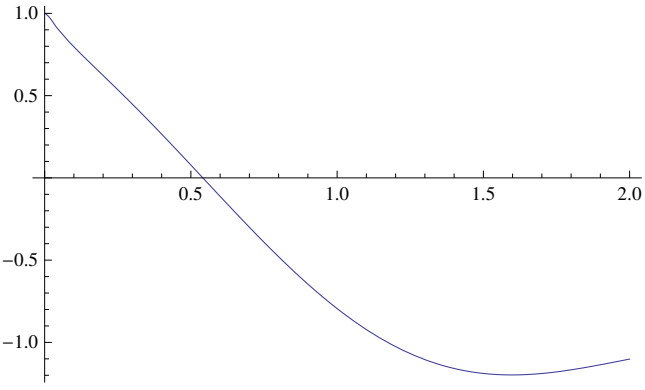

$\sigma_z(t)$
$\omega_A = \omega_L, \omega_A - \omega_e = 1, \epsilon = 1, \alpha = 0.1, \omega_c = 100$

7.2.10 Correlations

To get the equations for the correlations we use the quantum regression theorem without the transient terms for simplicity. We use a Laplace transform in order to calculate the spectrum.

$$f(i\omega) := \int_0^\infty dt f(t) e^{i\omega t} \tag{7.93}$$

$$\begin{aligned}
&\int_0^t dt_1 \int_0^{t_1} dt_2 G(t_2 - t) e^{i\Delta t_1} \sigma(t_2) \\
&= \int_0^t dt_2 \int_{t_2}^t dt_1 G^*(t - t_2) e^{i\Delta t_1} \sigma(t_2) \quad \longrightarrow \quad \frac{1}{i\Delta}[G^*(\omega + \Delta)\sigma(\omega + \Delta) + G^*(\omega)\sigma(\omega + \Delta) \\
&\int_0^t dt_1 \int_0^{t_1} dt_2 G(t_2 - t_1) e^{i\Delta t} \sigma(t_2) \quad \longrightarrow \quad \frac{1}{-i\omega - i\Delta} G^*(\omega + \Delta)\sigma(\omega + \Delta)
\end{aligned}$$

here $G(t) = G_A(t)$.
For second order the Laplace-Fourier transform is,

$$\begin{aligned}
-\sigma_{+-}(0) - i\omega\sigma_{+-}(\omega) &= -i\epsilon\sigma_{z-}(\omega - \Delta) - G^*(\omega)\sigma_{+-}(\omega) \\
-\sigma_{--}(0) - i\omega\sigma_{-}(\omega) &= i\epsilon\sigma_{z-}(\omega + \Delta) - G(\omega)\sigma_{--}(\omega) \\
-\sigma_{z-}(0) - i\omega\sigma_{z-}(\omega) &= 2i\epsilon\sigma_{--}(\omega - \Delta) - 2i\epsilon\sigma_{+-}(\omega + \Delta) \\
&\quad -(G(-i\omega) + G(i\omega))(\sigma_{z-}(i\omega) + \frac{\sigma_-}{-i\omega})
\end{aligned} \tag{7.94}$$

Frequency shift of the first two equations results in a closed linear system:

$$\begin{aligned}
-\sigma_{+-}(0) - i(\omega + \Delta)\sigma_{+-}(\omega + \Delta) &= -i\epsilon\sigma_{z-}(\omega) - G^*(\omega + \Delta)\sigma_{+-}(\omega + \Delta) \\
-\sigma_{--}(0) - i(\omega - \Delta)\sigma_{-}(\omega - \Delta) &= i\epsilon\sigma_{z-}(\omega) - G(\omega - \Delta)\sigma_{--}(\omega - \Delta) \\
-\sigma_{z-}(0) - i\omega\sigma_{z-}(\omega) &= 2i\epsilon\sigma_{--}(\omega - \Delta) - 2i\epsilon\sigma_{+-}(\omega + \Delta) \\
&\quad -(G^*(\omega) + G(\omega))(\sigma_{z-}(\omega) + \frac{\sigma_-}{-i\omega})
\end{aligned} \tag{7.95}$$

These equations are identical to the TC0 equations of chapter 6.

Including all terms up to 3rd order and shifted:

$$
\begin{aligned}
-\sigma_{+-} - i(\omega+\Delta)\sigma_{+-}(\omega+\Delta) &= -i\epsilon\sigma_{z-}(\omega) - G^*(\omega+\Delta)\sigma_{+-}(\omega+\Delta) \\
&\quad -\frac{\epsilon}{\Delta}\Big((G^*(\omega)+G^*(\omega+\Delta))[\sigma_{z-}(\omega)+\frac{\sigma_-(0)}{-i\omega}] \\
&\quad -\frac{\epsilon}{\omega}(G(\omega)+G^*(\omega))[\sigma_{z-}(\omega)+\frac{\sigma_-(0)}{-i\omega}] \\
-\sigma_{--} - i(\omega-\Delta)\sigma_{-}(\omega-\Delta) &= i\epsilon\sigma_{z-}(\omega) - G(\omega-\Delta)\sigma_{--}(\omega-\Delta) \\
&\quad -\frac{\epsilon}{\Delta}\Big((G(\omega)+G(\omega-\Delta))[\sigma_{z-}(\omega)+\frac{\sigma_-(0)}{-i\omega}] \\
&\quad +\frac{\epsilon}{\omega}(G(\omega)+G^*(\omega))[\sigma_{z-}(\omega)+\frac{\sigma_-(0)}{-i\omega}] \\
-\sigma_{z-} - i\omega\sigma_{z-}(\omega) &= 2i\epsilon\sigma_{--}(\omega-\Delta) - 2i\epsilon\sigma_{+-}(\omega+\Delta) \\
&\quad -(G^*(\omega)+G(\omega))(\sigma_{z-}(\omega)+\frac{\sigma_-}{-i\omega})
\end{aligned}
\tag{7.96}
$$

In the resonant case $\Delta = 0$ the Laplace transformed equations (7.86) of 3rd order are

$$
\begin{aligned}
-\sigma_{+-}(0) - i\omega\sigma_{+-}(\omega) &= -i\epsilon\sigma_{z-}(\omega) - G^*(\omega)\sigma_{+-}(\omega) \\
&\quad +i\epsilon\mathcal{L}[tG^*(t)](\omega)(\sigma_{z-}(\omega)+\frac{1}{-i\omega}) \\
&\quad -\frac{\epsilon}{\omega}(G(\omega)+G^*(\omega))(\sigma_{z-}(\omega)+\frac{1}{-i\omega}) \\
-\sigma_{--}(0) - i\omega\sigma_{--}(\omega) &= i\epsilon\sigma_{z-}(\omega) - G(\omega)\sigma_{--}(\omega) \\
&\quad -i\epsilon\mathcal{L}[tG(t)](\omega)(\sigma_{z-}(\omega)+\frac{1}{-i\omega}) \\
&\quad +\frac{\epsilon}{\omega}(G(\omega)+G^*(\omega))(\sigma_{z-}(\omega)+\frac{1}{-i\omega}) \\
-\sigma_{z-}(0) - i\omega\sigma_{z-}(i\omega) &= 2i\epsilon\sigma_{--}(\omega) - 2i\epsilon\sigma_{+-}(\omega) \\
&\quad -(G^*(\omega)+G(\omega))(\sigma_{z-}(\omega)+\frac{1}{-i\omega})
\end{aligned}
\tag{7.97}
$$

$\mathcal{L}[tG(t)]$ is the Laplace transformation of $tG(t)$.

7.2.11 Results

We want to compare the numerical results with our former solutions of the spectrum

In the following figures, the blue, dotted curve is the TC0 solution, identical to the 2nd order of ch. 6. The dashed, magenta curve is the TC1 solution of chapter 6. The purple curve is the 3rd order solution of eqns.(7.96,7.97) .

The first first plot is qualitatively similar for the different solutions, however the height of the peaks differ.

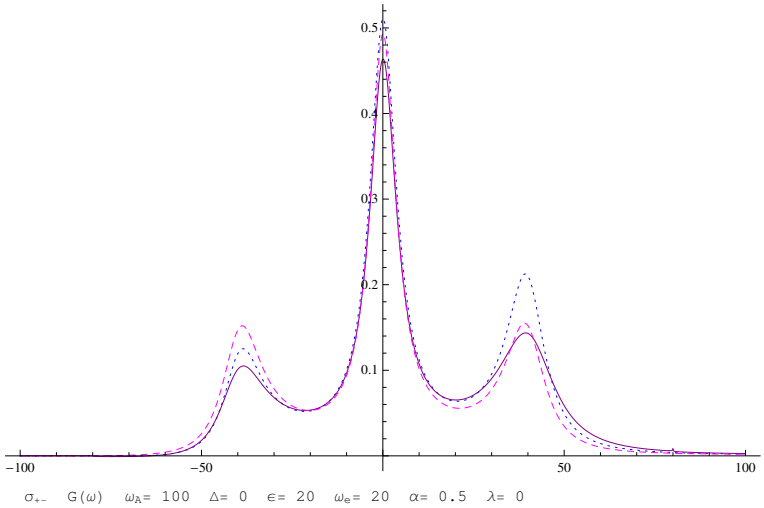

With a larger system-bath coupling the peaks broaden, the middle peak is considerably smaller for the 3rd order solution:

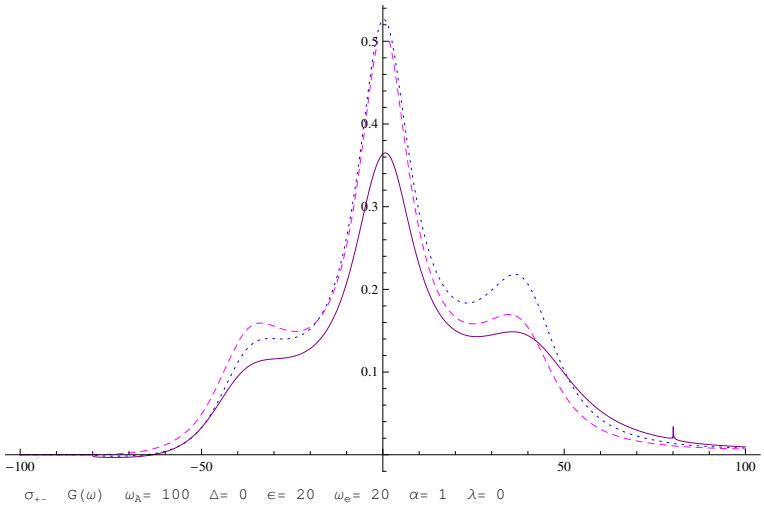

For a bigger band edge frequency,the right peak is split in two parts. The results are very different for the TC1 and the 3rd order solution.

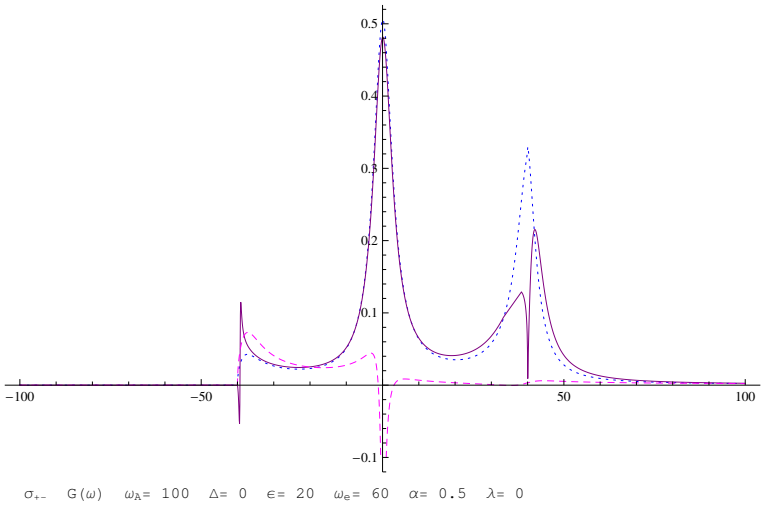

For a considerable atom-laser detuning, the middle peak is negative in the 3rd order solution.

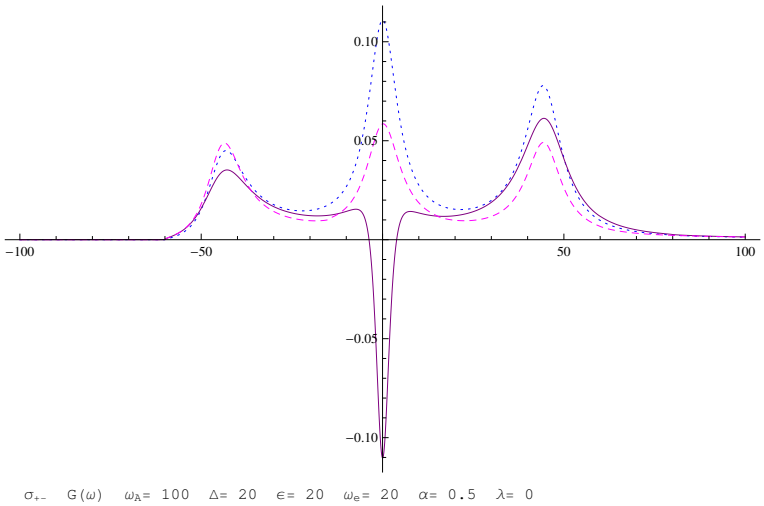

Bibliography

[1] M. O. Scully, M. S. Zubairy, *Quantum Optics*. Cambridge University Press (1997).

[2] L. Mandel, E. Wolf, *Optical Coherence and Quantum Optics*. Cambridge Univerity Press, Cambridge (1995).

[3] S. Pironio, et al., 'Random numbers certified by bell's theorem', *Nature* **464**, 1021 (2010).

[4] M. Woldeyohannes, S. John, 'Coherent control of spontaneous emission near a photonic band edge', *Journal of Optics B* **5**, R43 (2003).

[5] P. Lodahl, et al., 'Controlling the dynamics of spontaneous emission from quantum dots by photonic crystals', *Nature* **430**(5), 654 (2004).

[6] H.-P. Breuer, F. Petruccione, *The Theory of Open Quantum Systems*. Oxford University Press, Oxford (2002).

[7] G. Lindblad, 'On the generators of quantum dynamical semigroups', *Commun. math. Phys.* **48**, 119 (1976).

[8] R. Alicki, K. Lendi, *Quantum Dynamical Semigroups and Applications*. Springer-Verlag (1987).

[9] P. Pechukas, 'Reduced dynamics need not be completely positive', *Phys. Rev. Lett.* **73**(8), 1060 (1994).

[10] A. Imamoglu, 'Stochastic wave-function approach to non-markovian systems', *Phys. Rev. A* **50**, 3650 (1994).

[11] H.-P. Breuer, 'The non-markovian quantum behaviour of open systems: An exact monte carlo method employing stochastic product states', *Eur. Phys. J. D* **29**, 105 (2004).

[12] U. Weiss, *Quantum Dissipative Systems*. World Scientific, Singapore (1999).

[13] A. J. Leggett, et al., 'Dynamics of the dissipative two-state system', *Rev. Mod. Phys.* **59**, 1 (1987).

[14] K. Busch, S. Lölkes, R. B. Wehrspohn, H. Föll, *Photonic Crystals*. John Wiley & Sons (2006).

[15] C. Henkel, G. Boedecker, M. Wilkens, 'Local fields in a soft matter bubble', *Appl. Phys. B* **93**, 217 (2008).

[16] G. Boedecker, C. Henkel, 'All-frequency effective medium theory of a photonic crystal', *Opt. Exp.* **11**, 1590 (2003).

[17] D. W. L. Sprung, H. Wu, J. Martorell, 'Scattering by a finite periodic potential', *Am.J.Phys.* **61**, 1118 (1993).

[18] E. Merzbacher, *Quantum Mechanics*. Wiley & Sons, Hoboken, NJ (1998).

[19] J. M. Bendickson, J. P. Dowling, 'Analytic expressions for the electromagnetic mode density in finite, one-dimensional, photonic band-gap structures', *Phys. Rev. E* **53**(4), 4107 (1996).

[20] K. Sakoda, K. Ohtaka, T. Ueta, 'Low-threshold laser oscillation due to group-velocity anomaly peculiar to two- and three-dimensional photonic crystals', *Opt. Express* **4**, 481 (1999).

[21] M. Wubs, A. Lagendijk, 'Local optical density of states in finite crystals of plane scatterers', *Phys. Rev. E* **65**, 046612 (2002).

[22] M. Born, E. Wolf, *Principles of Optics*. Cambridge University Press, Cambridge (1999).

[23] D.-Y. Jeong, Y. H. Ye, Q. M. Zhang, 'Effective optical properties associated with wave propagation in photonic crystals of finite length along the propagation direction', *J. Appl. Phys.* **92**(8), 4194 (2002).

[24] P. Lambropoulos, G. M. Nikolopoulos, T. R. Nielsen, S. Bay, 'Fundamental quantum optics in structured reservoirs', *Rep. Prog. Phys.* **63**, 455 (2000).

[25] A. Moroz, 'Minima and maxima of the local density of states for one-dimensional periodic systems', *Europhys. Lett.* **46**(4), 419 (1999).

[26] A. Tip, A. Moroz, J. M. Combes, 'Band structure of absorptive photonic crystals', *J. Phys. A: Math. Gen.* **33**, 6223 (2000).

[27] J. B. Pendry, 'Photonic band structures', *J. mod. Optics* **41**, 209 (1994).

[28] S. Foteinopoulou, E. N. Economou, C. M. Soukoulis, 'Refraction at media with negative refractive index', *Phys. Rev. Lett.* **90**, 107402 (2003).

[29] K. Sakoda, *Optical Properties of Photonic Crystals*. Springer (2001).

[30] M. Florescu, S. John, 'Single-atom switching in photonic crystals', *Phys. Rev. A* **64**, 033801 (2001).

[31] G. M. Palma, K. A. Suominen, A. K. Ekert, 'Quantum computers and dissipation', *Proc. Roy. Soc. Lond. A* **452**, 567 (1996).

[32] G. Boedecker, C. Henkel, C. Hermann, O. Hess, *Photonic Crystals*, chap. 2. Spontaneous emission in photonic structures: Theory and simulation, in Busch et al.[14] (2006).

[33] G. Boedecker, C. Henkel, 'Validity of the quantum regression theorem for resonance fluorescence in a photonic crystal', *Annalen der Physik* **524**, 805 (2012).

[34] H. J. Kimble, L. Mandel, 'Theory of resonance fluorescence', *Phys. Rev. A* **13**, 2123 (1976).

[35] G. W. Ford, R. F. O'Connel, 'There is no quantum regression theorem', *Phys. Rev. Lett.* **77**, 798 (1996).

[36] I. de Vega, D. Alonso, 'Non-markovian reduced propagator, multiple-time correlation functions, and master equations with general initial conditions in the weak-coupling limit', *Phys. Rev. A* **73**, 022102 (2006).

[37] K. M. Case, 'On fluctuation-dissipation theorems', *Transport Theory and statistical physics* **2**(2), 129 (1972).

[38] R. Kubo, 'The fluctuation-dissipation theorem', *Rep. Progr. Phys.* **29**, 255 (1966).

[39] E. Pollak, J. Shao, D. H. Zhang, 'Effects of initial correlations on the dynamics of dissipative systems', *Phys. Rev. E* **77**, 021107 (2008).

[40] I. de Vega, D. Alonso, 'Emission spectra of atoms with non-markovian interaction: Fluorescence in a photonic crystal', *Phys. Rev. A* **77**, 043836 (2007).

[41] M. Orszag, *Quantum Optics – Including Noise Reduction, Trapped Ions, Quantum Trajectories and Decoherence*. Springer, Berlin (2000).

[42] S. John, T. Quang, 'Spontaneous emission near the edge of a photonic band gap', *Phys. Rev. A* **50**(2), 1764 (1994).

[43] R.-K. Lee, Y. Lai, 'Fluorescence squeezing spectra near a photonic bandgap', *J. Opt. B: Quantum Semicl. Opt.* **6**, S715 (2004).

[44] D. F. Walls, P. Zoller, 'Reduced quantum fluctuations in resonance fluorescence', *Phys. Rev. Lett.* **47**, 709 (1981).

[45] R.-K. Lee, Y. Lai, 'Resonance fluorescence squeezing spectra from photonic bandgap crystals', quant-ph/0308100.

[46] C. Uchiyama, F. Shibata, 'Unified projection operator formalism in nonequilibrium statistical mechanics', *Phys. Rev. E* **60**, 2636 (1999).

[47] C. Uchiyama, F. Shibata, 'A systematic projection operator formalism in nonequilibrium statistical mechanics', *J. Phys. Soc. Jap.* **65**, 887 (1996).

[48] C. Uchiyama, F. Shibata, 'Theory of spin relaxation in a quantum environment: strongly coupled spin-boson system', *Phys. Lett. A* **267**, 7 (2000).

[49] B. L. Hu, J. P. Paz, Y. Zhang, 'Quantum brownian motion in a general environment: Exact master equation with nonlocal dissipation and colored noise', *Phys. Rev. D* **45**, 2843 (1992).

[50] S.-Q. Wang, J.-H. He, 'Variational iteration method for solving integro-differential equations', *Phys. Lett. A* **367**, 188 (2007).